

BioPol ehf.
Marine Biotechnology
545 Skagaströnd
Iceland
<http://biopol.is>



Optimising yield of antioxidants and sunscreens in Icelandic marine microalgae for sustainable biosynthesis of ingredients for cosmetic products

Final Report AVS 2016, 2018-2020

Grant number: R 16 007-16

Dr. Bettina Scholz
Prof. Dr. Ulf Karsten
Dr. Gissur Örlygsson



Universität
Rostock



Traditio et Innovatio



Report Summary

<i>Title</i>	Optimising yield of antioxidants and sunscreens in Icelandic marine microalgae for sustainable biosynthesis of ingredients for cosmetic products	
<i>Authors</i>	Scholz, B.; Karsten, U.; Örylgsson, G.	
<i>Report nr.</i>	ISBN-XXXX	Date 21.09.2020
<i>Funding:</i>	AVS grant number: R 16 007-16	
<i>Summary:</i>	<p>Antioxidants and sunscreen metabolites either synthetic or natural both are important in cosmeceutical market. Nowadays markets are more oriented towards natural or herbal based cosmeceuticals and there is a tremendous economic potential in the production of such metabolites.</p> <p>Assuming that microalgae and cyanobacteria inhabiting northern Icelandic coastal areas, have evolved to cope to intense sunlight and high UV radiation levels, typical in this region particularly during the summer months, may be rich sources of photoprotectants. Consequently, the present study focused on the induction of typical sun screening compounds such as mycosporine-like amino acids (MAAs), scytonemin and sulfated polysaccharides (SPS) by exposure of initially 50 selected microalgae and cyanobacteria, isolated from Icelandic coastal areas, to a defined broad band UV illumination. In addition, enzymatic and non-enzymatic components of the antioxidative defense systems as well as scavenging activities were also analysed. The results obtained from this first screening revealed the presence of all tested compounds and activities in four cyanobacteria strains, although in the case of MAAs only traces were detected. These strains were then used in a further induction experiment in which two UV broad band sets under variation of the exposure time were tested. In total, 10 MAAs were detected by HPLC analysis in samples obtained from this induction survey in which 22 samples were analysed out of 48 assays, showing distinctive strain specific differences. Three of the MAAs were not further identifiable and were therefore dedicated as M-328, M-329 and M-341. The attempt to isolate and characterise these MAAs at a later stage was not successful. The remaining seven identified MAAs such as asterina-330, shinorine and palythinol are common in cyanobacteria and are most discussed in literature as natural antioxidants. Two of the tested cyanobacteria strains were subjected to tests of different flocculants (sodium hydroxide (NaOH), Iron (III) chloride (FeCl₃), and chitosan (poly-(D)glucosamine)) as alternative harvest methods as well as effects of drying temperatures and storage lengths, revealing the alkaline flocculation as best alternative harvest method and a relative high temperature stability of the MAAs. Comparing effects of up-scale cultivations under different nutrient scenarios on growth, the presence and concentrations of photoprotective compounds, components of the non-enzymatic antioxidative defense system and antioxidant power of <i>Synechococcus</i> I and II, two distinct semi-continuous culture conditions (exchange of 30 L medium, , and addition of nutrients for 30 L medium both in weekly intervals) versus batch culture as well as urea as NaNO₃ replacement were tested under two UV illumination sets in 100 L conventional bubble column photobioreactors (PBRs). The results showed best yields in the weekly addition assay with NaNO₃ as N source. In order to optimize the UV-light penetration in comparison to the conventional PBR system an annular PBR design with internal illumination was chosen, using <i>Synechococcus</i> II as model organism in combination with the culture and UV illumination optimizations from the former experiments.</p> <p>In principle, the enhancement of photoprotective compounds in response to UV stress was successful, although for example the MAA concentrations obtained initially were low and only in the range of natural occurring ones found in phytoplankton communities according to literature. Even in the final experiment under optimised conditions MAA concentrations obtained were only up to 61% higher than in the first induction experiment and were still low compared to values reached for instance in the red seaweed <i>Porphyra</i> sp. Nevertheless, the overall richness of the tested cyanobacteria in photoprotectants (MAAs, scytonemin, SPS) and components of the enzymatic and non-enzymatic antioxidative defense systems such as polyphenols (flavonoids), superoxide dismutase (SOD), catalase (CAT), ascorbate peroxidase (APX) and glutathione reductase (GR), might point to future opportunities to utilize these valuable metabolites in cosmetic products by application of a biorefinery approach.</p>	
<i>Keywords:</i>	<i>cultivation, biochemical composition, inducement of MAAs</i>	

Contents

1.	Introduction.....	1
1.1	Impacts of Ultraviolet Radiation (UVR) on Human Skin.....	1
1.2	Conventional Skin Care Products with UV-Screening Properties.....	5
1.2.1	Organic UV Filters.....	7
1.2.2	Inorganic UV Filters.....	7
1.2.3	Hybrid UV Filters (Organic/Inorganic Compounds)	8
1.2.4	Hazards of Conventional Sunscreen Compounds.....	8
1.3	Photoprotection in Marine Microalgae.....	10
1.3.1	Photoprotective Substances.....	11
1.3.1.1	Mycosporine-like Amino Acids.....	11
1.3.1.2	Scytonemin.....	13
1.3.1.3	Sporopollenin.....	16
1.3.1.4	Sulfated Polysaccharides.....	16
1.3.2	Antioxidant Defence Strategies	18
1.3.2.1	Non- Enzymatic Constituents.....	19
1.3.2.1.1	Ascorbate.....	19
1.3.2.1.2	Flavonoids.....	19
1.3.2.1.3	Carotenoids	20
1.3.2.1.4	Glutathione.....	22
1.3.2.1.5	Tocopherols.....	22
1.3.2.1.6	Phenolic Compounds.....	22
1.3.2.2	Antioxidant Enzymes.....	24
1.3.2.2.1	Superoxide Dismutase.....	24
1.3.2.2.2	Catalase.....	24
1.3.2.2.3	Ascorbate Peroxidase.....	24
1.3.2.2.4	Glutathione Reductase and Glutathione Peroxidase.....	24
2.	Objectives and Aims of the Study.....	25
3.	Material and Methods.....	26
3.1	Algal Strains and Culture Conditions.....	26
3.1.1	Algal Species.....	26
3.1.2	Cultivation.....	27
3.2	Experimental Designs.....	28
3.2.1	First Screening for Photoprotective Compounds and Scavenging Activities.....	28
3.2.2	Induction of Photoprotective Compounds and Antioxidative Defenses.....	30
3.2.3	Photoprotective Compound Stability.....	31
3.2.3.1	Alternative Harvest Methods.....	31
3.2.3.2	Effects of Drying Temperatures and Storage lengths	33
3.2.4	Experiments in 100 L Photobioreactors (PBRs).....	33
3.2.4.1	Conventional Bubble Column PBRs.....	33
3.2.4.2	Internally Illuminated Bubble Column PBR.....	35
3.3	Determination of Growth.....	35
3.4	Harvest and Processing.....	36
3.5	Biochemical Analysis.....	36
3.5.1	Sunscreen Compounds.....	36
3.5.1.1	Mycosporine-like Amino Acids (MAAs).....	36
3.5.1.1.1	LC-Analysis.....	36
3.5.1.1.2	Spectrophotometric Analysis.....	37
3.5.1.2	Scytonemin.....	37

3.5.1.3	Sporopollenin.....	37
3.5.1.4	Sulfated Polysaccharides.....	38
3.5.2	Antioxidant Defense Strategies	38
3.5.2.1	Non- Enzymatic Constituents.....	38
3.5.2.1.1	Ascorbate.....	38
3.5.2.1.2	Flavonoids.....	38
3.5.2.1.3	Carotenoids	38
3.5.2.1.4	Glutathione.....	39
3.5.2.1.5	Tocopherols.....	39
3.5.2.1.6	Phenolic Compounds.....	39
3.5.2.2	Antioxidant Enzymes.....	39
3.5.2.2.1	Superoxide Dismutase (SOD, EC 1.15.1.1).....	39
3.5.2.2.2	Catalase (EC 1.11.1.6).....	39
3.5.2.2.3	Ascorbate Peroxidase (AP, EC 1.11.1.1).....	39
3.5.2.2.4	Glutathione Reductase (GR, EC 1.6.4.2).....	40
3.5.3	Scavenging Activity Assays.....	40
3.5.3.1	2,2-Diphenyl-1-picrylhydrazyl-free-radical-scavenging activity (DPPH).....	40
3.5.3.2	Superoxide-anion-scavenging assay (SAS).....	40
3.5.3.3	Hydrogen-peroxide-scavenging activity (HPS).....	40
3.5.3.4	Ferric-reducing antioxidant power assay (FRAP).....	41
3.5.4	Screening for Compound Classes.....	41
3.5.5	Gross Compositions.....	41
3.5.5.1	Chlorophyll <i>a</i>	41
3.5.5.2	Proteins.....	41
3.6	Statistical Analysis.....	42
4.	Results	43
4.1	First Screening for Photoprotective Compounds and Scavenging Activities.....	43
4.2	Induction of Photoprotective Compounds and Antioxidative Defenses.....	46
4.3	Photoprotective Compound Stability.....	53
4.3.1	Alternative Harvest Methods.....	53
4.3.2	Effects of Drying Temperatures and Storage Lengths	55
4.4	Experiments in 100 L Photobioreactors (PBRs).....	57
4.4.1	Conventional Bubble Column PBRs.....	57
4.4.2	Internally Illuminated Bubble Column PBR.....	60
5.	Discussion.....	64
5.1	Sun Protective Compounds from Selected Cyanobacteria and their Induction.....	64
5.2	The Induction of Components of the Antioxidative Defense System and Scavenging Activities.....	65
5.3	Processing of the Biomasses <i>versus</i> Compound Stability.....	68
5.4	Conventional Bubble Column PBR <i>versus</i> Internally Illuminated PBR.....	69
6.	Conclusions and Future Perspectives.....	40
7.	Acknowledgements.....	70
8.	References.....	70
9.	Appendix.....	88

1. Introduction

1.1 Impacts of Ultraviolet Radiation (UVR) on Human Skin

Comprising roughly 16% of body mass, the skin is the largest organ of the body. Skin is organized into two primary layers, epidermis, and dermis, which together are made up of epithelial, mesenchymal, glandular and neurovascular components. The epidermis, of ectodermal origin, is the outermost layer and serves as the body's point of contact with the environment. As such, epidermal biological and physical characteristics play an enormous role in resistance to environmental stressors such as infectious pathogens, chemical agents, and ultraviolet radiation (UVR) (e.g. Lowe 2006, Slominski et al. 2012, Ngoc et al. 2019).

Being a component of the electromagnetic spectrum, UV photons fall between the wavelengths of visible light and gamma radiation. UV energy can be subdivided into UV-A, -B and -C components based on electro physical properties, with UV-C photons having the shortest wavelengths (100–280 nm) and highest energy, UV-A having the longest (315–400 nm) but least energetic photons and UV-B falling in between (Fig. 1). Each component of UV can exert a variety of effects on cells, tissues, and molecules.

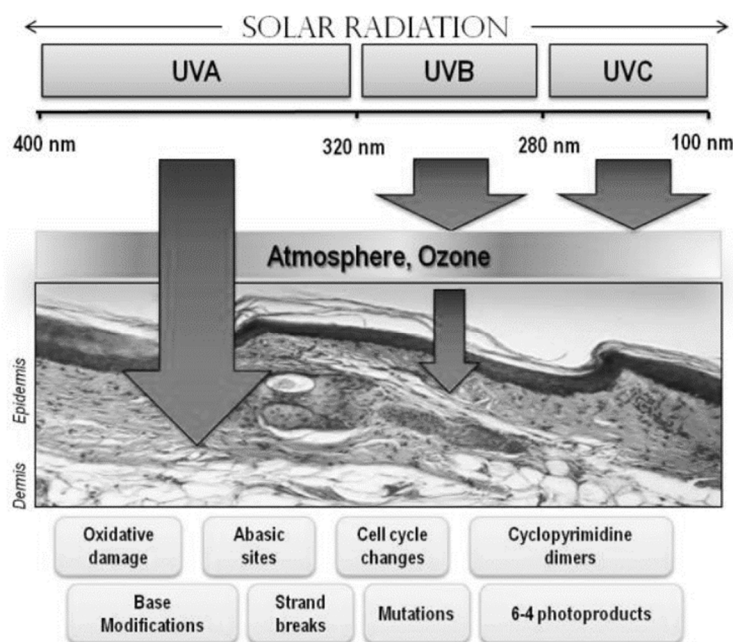


Figure 1. Electromagnetic spectrum of visible and UV radiation and biologic effects on the skin. Solar UV radiation can be subdivided into UVA, UVB and UVC components, however because of atmospheric ozone that absorbs UVC, ambient sunlight is predominantly UVA (90%–95%) and UVB (5%–10%). UV penetrates the skin in a wavelength dependent manner. Longer wavelength UVA penetrates deeply into the dermis reaching well into the dermis. In contrast, UVB is almost completely absorbed by the epidermis, with comparatively little reaching the dermis. UVA is efficient at generating reactive oxygen species that can damage DNA via indirect photosensitizing reactions. UVB is directly absorbed by DNA which causes molecular rearrangements forming the specific photoproducts such as cyclobutene dimers and 6-4 photoproducts. Mutations and cancer can result from many of these modifications to DNA (Ngoc et al. 2019).

UV has many effects on skin physiology, with some consequences occurring acutely and others in a delayed manner. One of the most obvious acute effects of UV on the skin is the induction of inflammation. UVB induces a cascade of cytokines, vasoactive and neuroactive mediators in the skin that together result in an inflammatory response and causes “sunburn” (e.g. Slominski et al. 2012, Skobowiat et al. 2013). If the dose of UV exceeds a threshold damage response, keratinocytes activate apoptotic pathways and die. Such apoptotic keratinocytes can be identified by their pyknotic nuclei and are known as “sunburn cells” (Bayerl et al. 1995). UV also leads to an increase in epidermal thickness, termed hyperkeratosis. By causing cell injury, UV induces damage response pathways in keratinocytes. Damage signals such as p53 activation profoundly alter keratinocyte physiology, mediating cell cycle arrest, activating DNA repair and inducing apoptosis if the damage is sufficiently great. Several h after UV exposure, however, and damage response signals abate, epidermal keratinocytes proliferate robustly (Coelho et al. 2009), mediated by a variety of epidermal growth factors. Increased keratinocyte cell division after UV exposure leads to accumulation of epidermal keratinocytes which increases epidermal thickness. Epidermal hyperplasia protects the skin better against UV penetration (Scott et al. 2012).

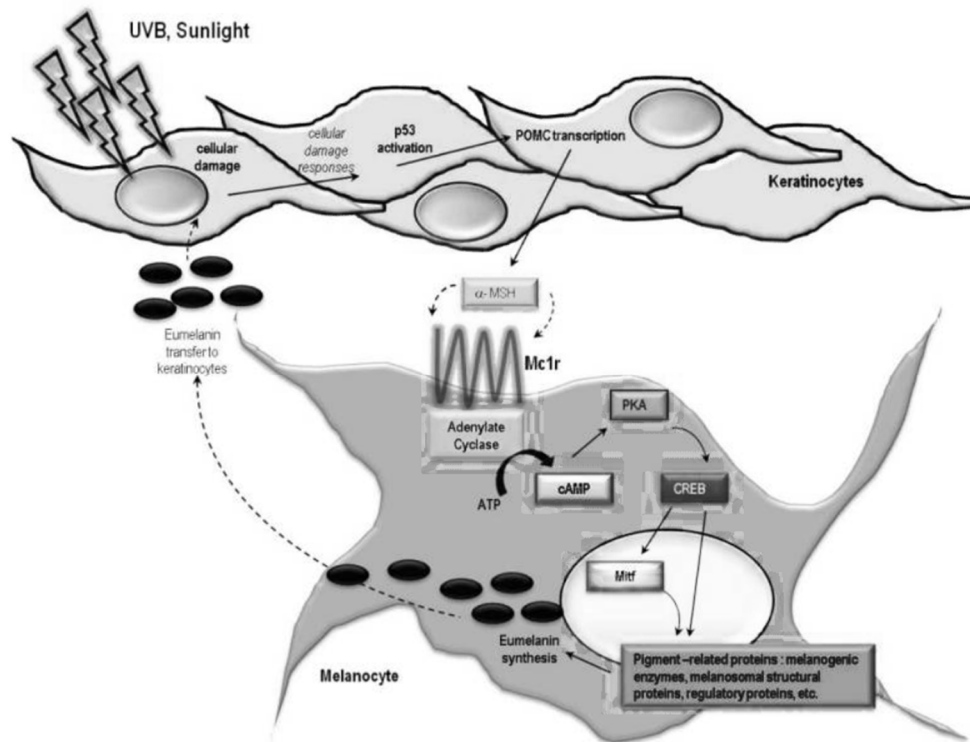


Figure 2. Mechanisms of the physiologic tanning response. Hormonal interactions between epidermal keratinocytes and melanocytes mediate much of the cutaneous melanisation response. DNA and cellular damage in keratinocytes up-regulates transcription of the pro-opiomelanocortin (POMC) gene which encodes production and secretion of melanocyte stimulating hormone (α -MSH). α -MSH binding to melanocortin 1 receptor (MC1R) on melanocytes in the basal epidermis generates the second messenger cAMP via interactions between MC1R and adenylyl cyclase and leads to activation of protein kinase A and the cAMP responsive binding element (CREB) and microphthalmia (Mitf) transcription factors. CREB and Mitf directly enhance melanin production by raising levels of tyrosinase and other melanin biosynthetic enzymes. Thus, MSH-MC1R signalling leads to enhanced pigment synthesis by melanocytes and accumulation of melanin by epidermal keratinocytes. By this mechanism, the skin is better protected against UV insults. Of note, UV-induced pigmentation may also occur through other signalling pathways as well as direct effects of UV on melanocytes, and there is some disagreement in the field over the role of epidermal MSH in the adaptive pigmentary response (D’Orazio et al. 2013).

Coupled with epidermal hyperkeratosis is adaptive melanisation of the skin, also known as tanning (e.g. D’Orazio et al. 2006, Cui et al. 2007). UV up-regulates production and epidermal accumulation of melanin pigment in the skin (e.g. Mitra & Fisher 2009). This important physiologic response protects the skin against subsequent UV damage, and defects in this pathway are linked with cancer susceptibility. UV-mediated skin darkening is biphasic, with initial skin darkening occurring from redistribution and/or molecular changes to existing epidermal melanin pigments. Delayed increases in skin darkening, mediated by actual up-regulation in melanin synthesis and transfer to keratinocytes, begin several h to days after UV exposure (Beattie et al. 2005). Adaptive melanisation is likely a complex physiologic response (Slominski et al. 2001) involving multiple skin cell types interacting in a variety of ways (Fig. 2) (e.g. Slominski et al. 2007 a, b). UV has many other effects on the skin, including induction of an immune-tolerant or immunosuppressive state (e.g. Schade et al. 2005, De Gruijl 2008) and production of vitamin D by direct conversion of 7-dehydrocholesterol into vitamin D₃ (cholecalciferol) (Holick 2002). Ambient sunlight, for the most part, is a mixture of UVA and UVB, yet each UV component may exert different and distinct effects on the skin (Polefka & Meyer 2012). UVB, for example, is a potent stimulator of inflammation and the formation of DNA photolesions (such as mutagenic thymine dimers) (Sklar et al. 2013), whereas UVA is much less active in these measures but instead is a potent driver of oxidative free radical damage to DNA and other macromolecules (Sander et al. 2004). Thus, each may contribute to carcinogenesis through different mechanisms (Sage et al. 2012). The influence of UVA and UVB on skin physiology is an active area of investigation.

Besides promoting formation of photodimers in the genome, UV causes mutations by generating reactive oxygen species (ROS) such as superoxide anion, hydrogen peroxide and the hydroxyl radical (Meyskens et al. 2001) (Fig. 3). Nucleotides are highly susceptible to free radical injury. Oxidation of nucleotide bases promotes mispairing outside of normal Watson-Crick parameters, causing mutagenesis (Schulz et al. 2000). The transversion guanine→ thymine, for example, is a well-characterized mutation caused by ROS by oxidizing guanine at the 8th position to produce 8-hydroxy-2'-deoxyguanine (8-OHdG) (Kunisada et al. 2005). 8-OHdG tends to pair with an adenine instead of cytosine and therefore this oxidative change mutates a G/C pair into an A/T pair. Such mutations can be found in tumours isolated from the skin, suggesting that oxidative injury can be carcinogenic (Agar et al. 2004). Cellular maintenance pathways exist to inactivate oxidative species as well as to repair the DNA damage they cause. The base excision repair pathway (BER) is the main molecular means by which cells reverse free radical damage in DNA to avoid oxidative mutagenesis. This pathway is initiated by damage-specific glycosylases that scan DNA for specific alterations including deaminated, alkylated or oxidized bases. After altered or inappropriate bases are recognized by a lesion-specific glycosylase, the enzyme cleaves the nucleotide base from the sugar and phosphodiesterase backbone by lysis of the *N*-glycosylic bond between the base and the deoxyribose. This step forms an abasic or apurinic /apyrimidinic (AP) site in the DNA, which is then processed and repaired using the complementary strand as a template to ensure fidelity.

Cells also have a complex and robust network of antioxidant molecules that detoxify reactive species to prevent free radical changes to DNA and other macromolecules. Glutathione (GSH) is an oligopeptide made up of three amino acids- cysteine, glycine and glutamine and is among the most important cellular antioxidant molecules. By donating electrons to otherwise reactive molecules, GSH functions as a reducing agent to neutralize reactivity of free radicals. In the process, glutathione itself becomes oxidized but can be reduced to its basal state by glutathione reductase using NADPH as an

electron donor and be recycled. In any cell, therefore, glutathione can be found in both its reduced and oxidized forms and abnormalities in the ratio of reduced to oxidized glutathione can indicate oxidative stress. Catalase is another major antioxidant enzyme that detoxifies hydrogen peroxide (e.g. Kadekaro et al. 2012), whereas superoxide dismutases (SOD's) inactivate superoxide anions (Krol et al. 2000).

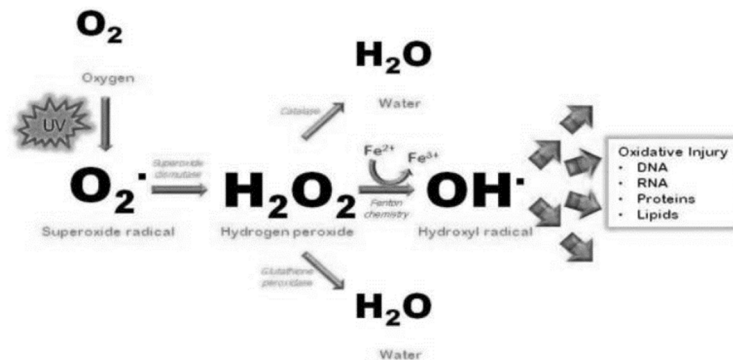


Figure 3. UV generates oxidative free radicals. UV photons interact with atomic oxygen to promote formation of free radical derivatives such as superoxide, hydrogen peroxide and the highly reactive hydroxyl radical. Free radicals avidly attack macromolecules such as protein, lipid, RNA and DNA, altering their structure and interfering with their function. Detoxifying and protective enzymes such as superoxide dismutase, catalase and glutathione peroxidase detoxify and reduce levels of oxidative species in the cell (D’Orazio et al. 2013).

Besides free radical formation, UV directly affects nucleotide base pairing in DNA (Cleaver & Crowley 2002). Pyrimidine bases are particularly vulnerable to chemical alteration by absorption of UV energy. Shorter-wavelength UV photons, particularly UV-B and UV-C, cleave internal 5–6 double bonds of pyrimidines. When this occurs between adjacent pyrimidines, abnormal covalent bonds may form and alter the three-dimensional structure of the double helix. Two major photolesions- cyclobutene pyrimidine dimers or (6,4)- photoproducts- predictably form in this way after UV exposure, and both are highly mutagenic (Sarasin 1999). It is estimated that one day’s worth of sun exposure results in up to 10^5 UV-induced photolesions in every skin cell (Hoeijmakers 2009). UV-induced photolesions impair transcription, block DNA replication and base pair abnormally. They cause characteristic transition mutations known as “UV signature mutations”. The abundance of UV signature mutations in cancer-regulatory genes among many primary skin cancer isolates strongly supports UV as a cancer-causing agent (e.g. Hodis et al. 2012).

Skin cancers are by far the most common malignancies of humans, with well over a million cases diagnosed each year (Rogers et al. 2010). Like many other cancers contributed to by environmental etiologies (in this case UV), skin cancer incidence increases markedly with age presumably reflecting the long latency between carcinogen exposure and cancer formation. Skin cancers are commonly grouped into two main categories, melanoma, and non-melanoma skin cancers (NMSC), based on cell of origin and clinical behaviour. Risk of skin cancer is heavily influenced by UV exposure and by skin pigmentation (Narayanan et al. 2010).

1.2 Conventional Skin Care Products with UV-Screening Properties

It has been proved that photoprotectors, especially sunscreens, play a critical role in reducing the incidence of human skin disorders (pigment symptoms and skin aging) induced by UVR. Sunscreen was first commercialized in the United States in 1928 and has been expanded worldwide as an integral part of the photoprotection strategy (Sambandan & Ratner 2011). It has been found to prevent and minimize the negative effects of UV light based on its ability to absorb, reflect, and scatter solar rays (Palm & O'Donoghue 2007, Donglikar & Deore 2016). Over the decades of development, sunscreens have been improved step-by-step, accompanying the innovation of photoprotective agents (Singer et al. 2019). Certainly, recent sunscreens are found to not only address UV effects, but also protect the skin from other risks (e.g., IR, blue light, and pollution) (Lee 2018). Indeed, while UV radiation is commonly implicated in skin disorder development, it is crucial to note the potential role of these considerable harmful factors (Mistry 2017). It has been suggested that these factors can worsen disorders of dyspigmentation, accelerating aging, and eliciting genetic mutations (Schieke 2003, Ngoc et al. 2019).

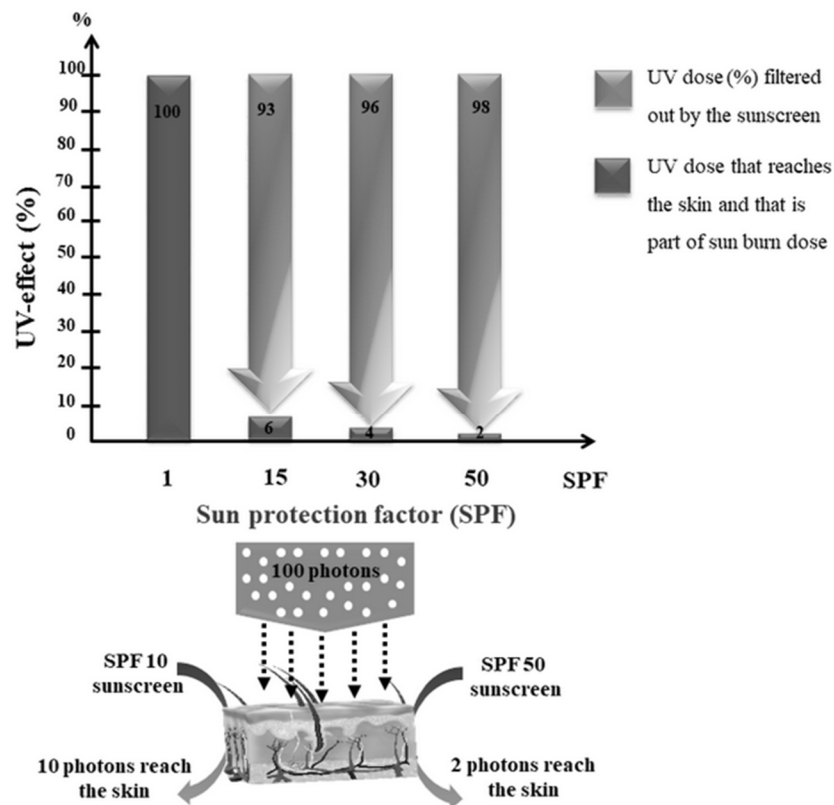


Figure 4. Illustration of the sun protection factor (SPF) definitions, including filtered and transmitted UV radiation (Osterwalder & Herzog 2009).

The photoprotective efficiency of sunscreens is determined through sun protection factor (SPF) and the protection grade of UVA (PA) values. According to Food and Drug Administration (FDA) regulations, commercial products must be labelled with SPF values that indicate how long they will protect the user from UV radiation and must show the effectiveness of protection (Schalka & Reis 2011). The SPF values are generally in the range of 6–10, 15–25, 30–50, and 50+, corresponding to low, medium, high, and extremely high protection, respectively. Nevertheless, there are some

fundamental controversial regarding the SPF. Some argument is that an SPF 15 sunscreen can absorb 93% of the erythemogenic UV radiations, while an SPF 30 product can block 96%, which is just over 3% more (Fig. 4) (Osterwalder & Herzog 2009). The argument may be correct when evaluating sun protection capacity but is not sufficient in assessing the amount of UV radiation entering the skin. In other words, half as much UV radiation will penetrate the skin when applying an SPF 30 product compared to an SPF 15 product. This is also illustrated by comparing SPF 10 with SPF 50 sunscreen. Ten and two photons transmit (%) through sunscreen film and enter the skin when applying SPF 10 and SPF 50 products, respectively, as a difference factor of five it is expected (Osterwalder & Herzog 2009). On the other hand, in 1996, the Japan Cosmetic Industry Association (JCIA) developed an in vivo persistent pigment darkening (PPD) method to evaluate UVA efficacy of sunscreen (Moyal 2010). Sunscreens are labelled with PA+, PA++, PA+++, and PA++++, corresponding to the level of protection grade of UVA (PA) obtained from the PPD test (Wang et al. 2008). Sunscreens labelled as PA+ express low protection, mainly contributed by between two and four UVA filters. Sunscreens containing four to eight sunscreen agents show moderate levels of UVA blocking and are labelled as PA++. In contrast, the PA+++ and PA++++ symbols represent products that are composed of more than eight UVA filters and provide a high sunscreen efficacy (e.g. Wang et al. 2008).

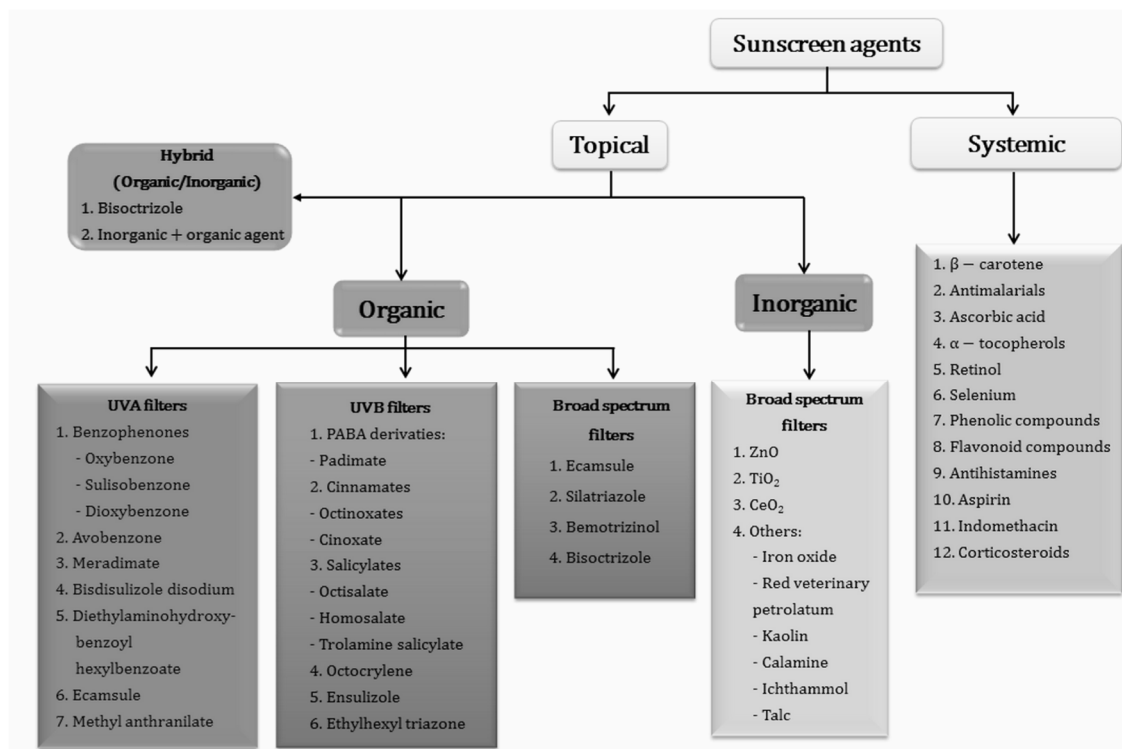


Figure 5. Sunscreen compound classification (Latha et al. 2013).

Sunscreen compounds are basically categorized into inorganic and organic UV filters which have specific mechanisms of action upon exposure to sunlight (Fig. 5). Inorganic agents reflect and scatter light, while organic blockers absorb high-energy UV radiation (Vergou et al. 2011). Recently, hybrid materials combining properties of both, organic and inorganic compounds, have attracted the attention of scientists as a promising sunscreen agent. In addition, botanical agents, which contain large amounts of antioxidant compounds, can be used as inactive ingredients to protect the skin against adverse effects (e.g., photoaging, wrinkles, and pigment).

1.2.1 Organic UV Filters

Organic blockers are classified into either UVA (anthranilates, dibenzoylmethanes, and benzophenones) or UVB filters (salicylates, cinnamates, para-aminobenzoic acid (PABA) derivatives, and camphor derivative), which play an important role in absorption activity of sunscreen (Fig. 5) (Serpone et al. 2007). These agents show outstanding properties, including stability, non-irritant, non-volatile, non-photosensitizing, and non-staining to human skin, compared to inorganic UV filters (Pathak 1982). They are mostly used in combination at levels currently allowed by the FDA to provide broad-spectrum absorption, as well as increased SPF values (U.F.A.D. 2000). Nevertheless, the combination is limited in selecting the appropriate UVA/UVB filters to avoid possible negative interactions between the combining agents (Pathak 1982). Particularly, some organic filters (e.g., PABA, PABA derivatives, and benzophenones) show considerable negative effects, including eczematous dermatitis and increased risk of skin cancer (Serpone et al. 2007). Therefore, sunscreens have recently minimized or avoided the use of these compounds to protect consumers from undesirable effects. In addition, some photo unstable filters (e.g., avobenzene and dibenzoylmethane) show a number of photoreactive results in the formation of photoproducts that can absorb in different UV regions, therefore reducing their photoprotective efficacy (e.g. Paris 2019). Particularly, these photodegradation products can come in direct contact with the skin, thus promoting phototoxic, photosensitizing, and photoallergic contact dermatitis on the skin (Gaspar & Maia Campos 2006).

1.2.2 Inorganic UV Filters

Inorganic blockers have been approved to protect human skin from direct contact with sunlight by reflecting or scattering UV radiation over a broad spectra (Sambandan & Ratner 2011). The current agents are ZnO, TiO₂, Fe_xO_y, calamine, ichthammol, talc, and red veterinary petrolatum (Fig. 5). Although they are generally less toxic, more stable, and safer for human than those of organic ingredients, they are visible due to white pigment residues left on the skin and can stain clothes (Palm & O'Donoghue 2007). Since the early 1990s, these metal oxides have been synthesized in the form of micro and nanoscale particles (10–50 nm), which can reduce the reflection of visible light and make them appear transparent throughout the skin (Palm & O'Donoghue 2007). For instance, micro-size TiO₂ and ZnO have been replaced nano-size TiO₂ and ZnO in sunscreen, eliminating undesired opaqueness and improve SPF value (Smijs & Pavel 2011).

Moreover, the main disadvantage of utilization of nanoparticles (NPs) is that sunscreens tend to block shorter wavelength from UVAII to UVB rather than long radiation (visible and UVA range). Most NPs can produce ROS radicals and are small enough to penetrate the stratum corneum, thus causing severe skin effects with prolonged exposure, such as photoallergic contact dermatitis and skin aging (Giacomoni 2001). Therefore, in order to improve natural appearance as well as reduce side effects on the skin, these cosmetics using nanoparticles need to be controlled by numerous factors, including particles size and distribution, agglomeration and aggregation, and morphology and structure of the NPs (Paris 2019). For instance, the utilization of TiO₂ and ZnO NP-coated silicon or doped elements (Al₂O₃ and Zr) can minimize ROS production and prevent negative effects as mentioned above (Jacobs et al. 2010).

1.2.3 Hybrid UV Filters (Organic/Inorganic Compounds)

According to the literature, hybrid materials are two half-blended materials intended to create desirable functionalities and properties (Mistry 2017). They are constituted of organic components (molecule or organic polymer) mixed with inorganic components (metal oxides, carbonates, phosphates, chalcogenides, and allied derivatives) at the molecular or nanoscale (Gonzalez et al. 2002). The combination creates ideal materials with a large spectrum and high chemical, electrochemical, optical transparency, magnetic, and electronic properties (Mistry 2017). Furthermore, some less toxic and biocompatible hybrid materials have been utilized as active ingredients in cosmetics due to their ability to absorb or deliver organic substances into the hair cuticle and skin layers, thereby improving the care effect (Gonzalez et al. 2002).

1.2.4 Hazards of Conventional Sunscreen Compounds

Sunscreen use has significantly expanded in the last decades as consequence of the perception that sun exposure may be the main cause for the development of skin cancer and the photo aging process (Maier & Korting 2005). Further reports have shown that, in the last 20 years, the incidence of non-melanoma skin cancer (NMSC) has increased significantly (Halpern & Kopp 2005). Daily application of sunscreen products is highly recommended by health care professionals and it has been suggested that the incidence of NMSC can be drastically reduced (or even prevented) by avoidance of excessive exposure to UV radiation and by using sunscreen (Halpern & Kopp 2005).

According to the literature, sunscreen agents should be safe, nontoxic, chemically inert, non-irritating, and fully protect against broad spectrum that can prevent photo-carcinogenesis and photoaging (FDA 2012). However, there have been also negative effects reported, including contact sensitivity, photoallergic dermatitis, and risk of vitamin D deficiency (e.g. Holick 2003, Gorham et al. 2007, Kerr & Ferguson 2010, Faurschou et al. 2012).

Recent research has given the evidence of the harmful effects (radicals' generation, risks of skin cancer and estrogen like-effects) of the available chemical sunscreens in the market and their regular application to the skin (Bhatia & Kim 2011). These chemical agents were proven as primary causative agents for increasing the cancer risk by virtue of their abundant free radical generating properties and oestrogen-like effects. These effects are similar to many banned chemicals such as dichloro-diphenyl trichloroethane (DDT), dioxin, and polychlorinated biphenyls (PCBs), but they are still present in the market due to profit gaining purpose of the chemical industries. Most of the chemical sunscreens contain 2–5% of UVA and UVB blockers as the active ingredients. Most of these UV-blocker compounds are cancer causing elements, e.g. Benzophenone (and similar compounds) and Avobenzone (powerful free radical generators), Padimate-O or other *p*-aminobenzoic acid (PABA) derivatives (DNA damaging effects), and Triethanolamine (formation of cancer-causing nitrosamines). Most of the sunscreen compounds are either UVA or UVB protective and are usually combined with other sunscreen chemicals to produce a "broad-spectrum" product. Furthermore, in sunlight, some show instability after a particular period of time. In addition, widespread use of cosmetics has led to a ubiquitous presence of some ingredients in the aquatic environment which can cause hormonal effects on aquatic organisms and insects (Christen et al. 2011, Ozáez et al. 2013). For example, the use of the two most popular organic filters, octinoxate (ethylhexyl methoxycinnamate) and oxybenzone, has recently been restricted in Hawaii because of their negative effect on the coral reefs (Siller et al.

2018). Furthermore, in early 2020, the National Oceanic and Atmospheric Administration (NOAA) issued a warning that following chemicals in sunscreens may have harmful and partly lethal effects on marine life: Oxybenzone, Benzophenone-1, Benzophenone-8, OD-PABA, 4-Methylbenzylidene camphor, 3-Benzylidene camphor, nano-Titanium dioxide, nano-Zinc oxide (Fig. 6) (Downs et al. 2014, 2016, NOAA 2020). Considering the manifold interactions of up to now untested man-made chemicals and aquatic organisms the list of harmful compounds might be far more comprehensive than at this point is known.

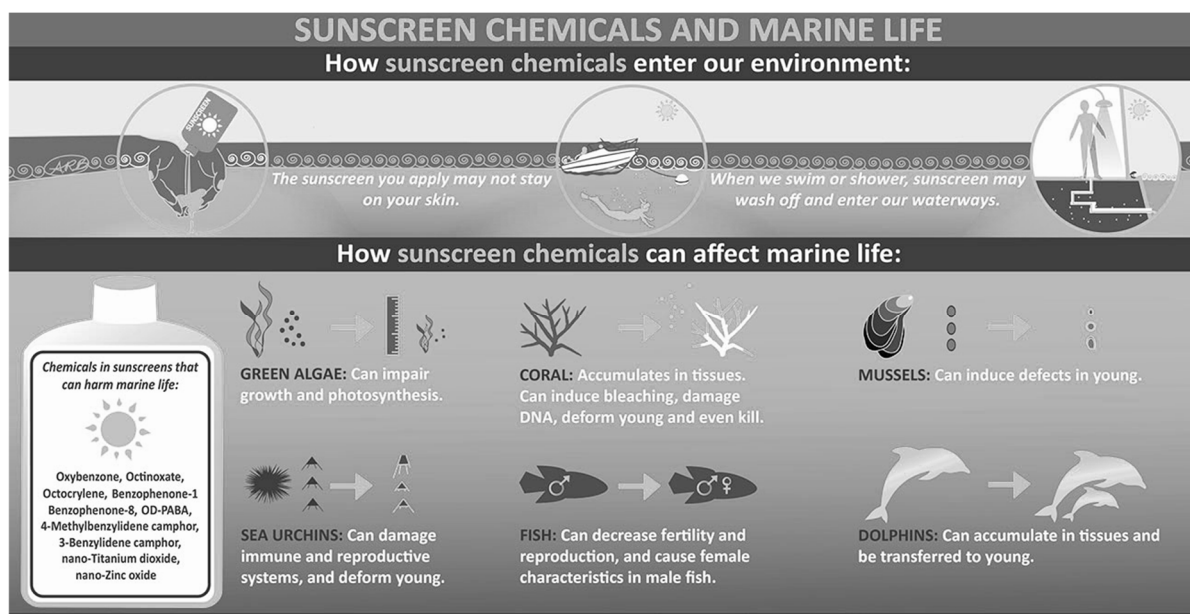


Figure 6. Infographic: Sunscreen Chemicals and Marine Life (NOAA 2020).

Given the possible negative consequences of using such ingredients, cosmetic scientists have begun to investigate natural compounds that offer safer alternatives. In addition, the ability of organisms to self-renew and reproduce ensures that supplies are potentially sustainable. This is especially true for photosynthetic organisms using simply light energy, carbon dioxide and basic nutrients (Witcover et al. 2013). Indeed, the use of plants as a source of new cosmetic ingredients is an option favoured by many companies (Kole et al. 2005).

1.3 Photoprotection in Marine Microalgae

Microalgae are unicellular prokaryotic and eukaryotic photosynthetic microorganisms which exist individually, or in chains or groups. Depending on the species, their sizes can range from a few micrometres (μm) to a few hundred micrometres. There are two groups of prokaryotes (Cyanophyta and Prochlorophyta) and different divisions of eukaryotes (Chlorophyta, Rhodophyta, Phaeophyta, Bacillariophyta, and Chrysophyta) (Mutanda 2013). They are generalists and can therefore develop in freshwater, marine and highly saline environments, living in/on both the water column and sediment (Thurman 1997).

Marine algae are one of the most extensively studied marine organisms. These marine organisms have attracted special interest because they are good sources of nutrients and functional materials. Many studies have reported biological activities, including antioxidant, anti-cancer, anti-hypertension, hepatoprotective, immunomodulatory, and neuroprotective activity. Marine algae are already used in a wide range of foods, supplements, pharmaceuticals, and cosmetics and are often claimed to have beneficial effects on human health. One particular interesting feature in marine algae is their richness in photoprotective substances. Intertidal and epipelagic marine algae are exposed to the highest levels of UVR, and even planktonic and benthic organisms may experience harmful levels to depths >20 m (Booth & Morrow 1997, Núñez-Pons et al. 2018).

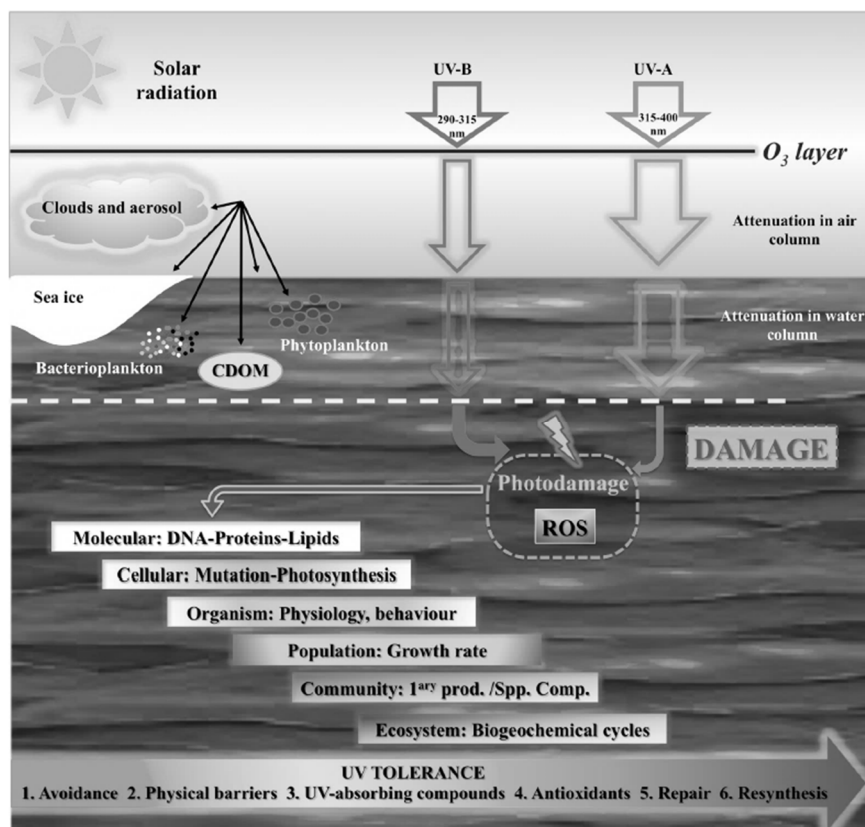


Figure 7. Negative effects of ultraviolet radiation (UVR) on the marine environment. Main factors involved in the attenuation of light through the air and water column and mechanisms of UV tolerance in biological systems by mitigating strategies and repair processes. UV-R may affect organisms through molecular and/or cellular damages, genetic mutations, or by causing disturbances at population and community levels, interfering with physiological functions (e.g., growth, reproduction and behaviour), and species interactions with effects on the ecosystem and biogeochemical cycles. ROS, reactive oxygen species; CDOM, coloured dissolved organic matter (Núñez-Pons et al. 2018).

Cellular damage from UV exposure can occur by direct photochemical reaction, e.g., thymine dimerization in DNA (Rogers 2007), or via the photodynamic production of reactive oxygen species (ROS) such as singlet oxygen ($^1\text{O}_2$) and superoxide radical ($\text{O}_2^{\cdot-}$) (Eastman 2005). Reduced O_2 intermediates, such as hydrogen peroxide (H_2O_2), superoxide radicals ($\text{O}_2^{\cdot-}$), hydroxyl radicals ($\cdot\text{OH}$) and singlet oxygen ($^1\text{O}_2$) are produced as a result of electronic excitation after UV-R absorption and reduction of molecular O_2 . Most of the production of ROS involves the activation of intermediate molecules in cells (e.g., aromatic amino acids), which absorb UVR, and enter into an excited state leading to the production of extremely reactive hydroxyl radicals in an iron-catalysed Fenton reaction. UVA-generated ROS trigger several toxic responses in organisms, including impair of DNA, enzymes, membrane proteins and lipids (especially those containing polyunsaturated fatty acids), as well as photooxidative stress of photosystem components in photoautotrophs (Tyrrell 1991, Lesser 2006). In organisms that perform oxygenic photosynthesis, an excess of UVB light can interfere with the thylakoid photochemistry, leading to a decrease in O_2 , electron transport, Rubisco activity and CO_2 fixation rates (Gómez et al. 2007). Such processes consequently lead to photoinhibition or photoinactivation, bringing repercussions to the first levels of food webs (Fig. 7) (e.g. Dring et al. 1996). Accordingly, algae exposed to high levels of solar UVR have evolved biochemical defences against such damage, protection that includes the elaboration of natural UV-absorbing sunscreens, the expression and regulation of antioxidant enzymes (superoxide dismutase, catalase, glutathione reductase and ascorbate peroxidase), the accumulation and cycling of small-molecule antioxidants (ascorbate, flavonoids, carotenoids, tocopherols, glutathione, polyphenols), and molecular repair (Fig. 7) (e.g. Núñez-Pons et al. 2018). Specifically, photoprotective substances such as mycosporine-like amino acids (MAAs), sporopollenin, scytonemin and sulfated polysaccharides, are synthesized to counteract and minimize photodamage induced by high UVR (Eastman 2000, Carreto & Carignan 2011). These substances can be used for photoprotection to provide the skin with adequate protection against UVR-induced photodamage (Rogers 2007).

1.3.1 Photoprotective Substances

1.3.1.1 Mycosporine-like Amino Acids

Mycosporine-like amino acids (MAAs) are low-molecular-weight (<400 Da), water-soluble molecules with maximum absorption bands in the UV spectrum between 310 and 360 nm (Fig. 8) and have been reported as the strongest UVA-absorbing compounds in nature (Daniel et al. 2004). Mycosporines were first identified in fungi as having a role in UV-induced sporulation (Favre-Bonvin 1976). Their relatives the MAAs have since been found in a diverse variety of freshwater and marine organisms (more than 380 marine species) including cyanobacteria, macro- and microalgae, corals as well as many marine invertebrates such as sea anemones, limpets, shrimp, sea urchins and vertebrates including fish and fish eggs (Karentz 1991, Shick & Dunlap 2002, Sinha et al. 2007). The highest amount of MAAs is produced in seaweeds, being highest in red algae, followed by brown and green algae, respectively (Carreto & Carignan 2011). The type and accumulation of MAAs in marine algae varies based on season, climate, depth, and environmental variables (i.e., salinity, temperature, and nutrient availability) (Peinado et al. 2004). Unlike photosynthetic pigments, MAAs are invoked to function as passive shielding substances by dissipating the absorbed radiation energy in the form of harmless heat without generating photochemical reactions. In the organisms, MAAs not only function as “nature’s sunscreen compounds” but also serve as antioxidant molecules scavenging toxic oxygen radicals (Oren

& Gunde-Cimerman 2007). Up to now, more than 30 different chemical structures of MAAs have been elucidated. Further roles include acting as compatible solutes to protect cells against salt stress where they are involved in protection against desiccation or thermal stress in certain organisms and as intracellular nitrogen reserves (Oren & Gunde-Cimerman 2007).

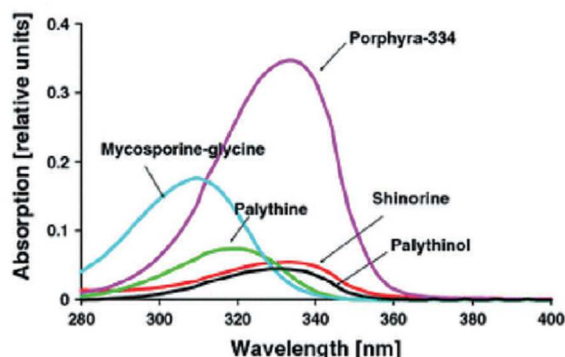


Figure 8. Absorption spectra of some MAAs (Siezen 2011).

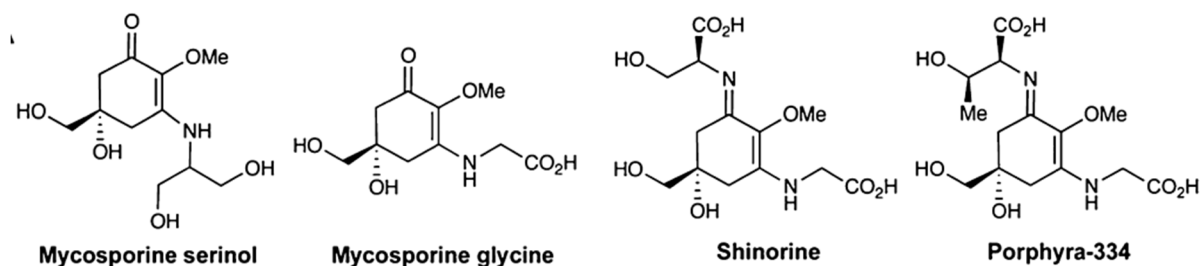


Figure 9. Chemical structures of representative mycosporines and MAAs from fungi (mycosporine serinol) and cyanobacteria (mycosporine-glycine, shinorine and porphyra-334); from Balskus & Walsh (2010).

The chemical structure of MAAs is based on either a cyclohexenone or cyclohexenimine ring structure (chromophore) with amino acid substituents (Fig. 9). The conjugated double bonds within the molecule result in broad band absorptions with wavelength maxima (λ_{max}) ranging from 310 nm in the ultraviolet-B for cyclohexenone based structures (280–315 nm) to 360 nm in the UVA (315–400 nm) for cyclohexenimine based structures (Karentz et al. 1991). Changes in the λ_{max} are caused by substituent effects with organisms generally containing a variety of MAAs protecting across a wide UV band range.



Figure 10. The shinorine biosynthesis gene cluster from *Anabaena variabilis*.

In 2010, the initial steps in the biosynthesis of mycosporines and MAAs in *Anabaena variabilis* were elucidated (Balskus & Walsh 2010). A cluster of four genes (Fig. 10) was found to be responsible for conversion of the common pentose phosphate pathway intermediate sedoheptulose 7-phosphate into shinorine (Fig. 11). In the first steps, a dehydroquinone synthase (DHQS) homologue 2-*epi*-5-*epi*-valiolone synthase and an *O*-methyltransferase convert the precursor into 4-deoxy-gadusol, after

which an ATP-grasp homologue and an (NR)peptide synthetase homologue attach glycine and serine to generate mycosporine-glycine and shinorine. Genome data mining subsequently identified this gene cluster in several cyanobacteria, fungi, dinoflagellates and even in an actino-bacterium (Balskus & Walsh 2010, Singh et al. 2010). In cyanobacteria, all gene clusters contain the first three genes to generate the main intermediate mycosporine-glycine, while additional genes vary. Most clusters encode a conserved D-Ala D-Ala ligase homologue, presumably also to couple amino acids to the mycosporine core, while others encode a (NR)peptide synthetase and/or conserved transporter, or combinations of these. Intracellularly, MAAs are found distributed in the cytoplasm of cells although it has also been suggested that they can be released extracellularly into colonial mucilage in *Phaeocytis* sp. providing enhanced UV protection to themselves and possibly to other community members (Marchant et al. 1991).

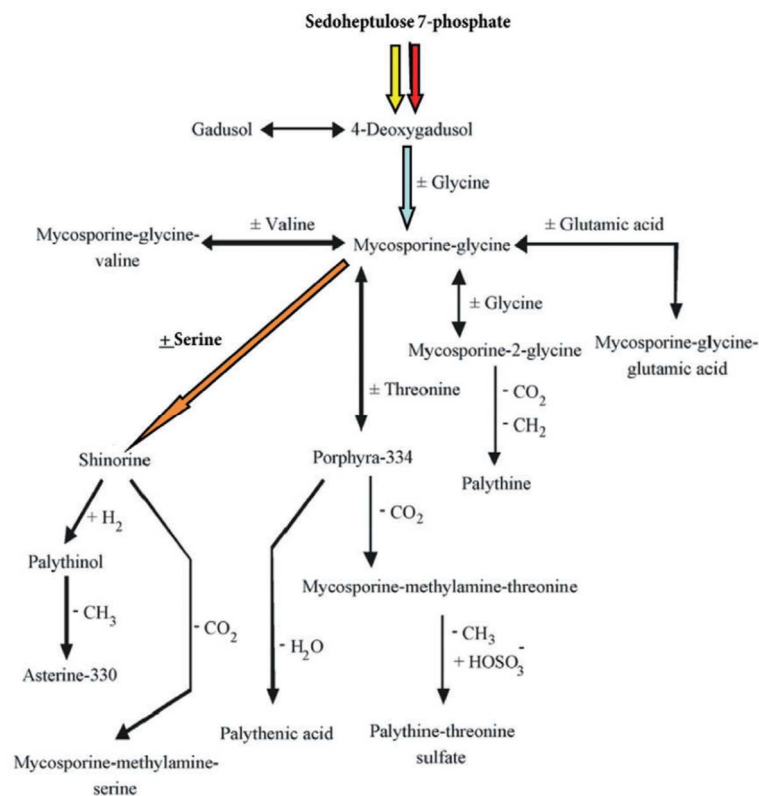


Figure 11. Biosynthetic pathways for the assembly of mycosporine and MAAs from sedoheptulose 7-phosphate.

1.3.1.2 Scytonemin

Contrary to MAAs, scytonemin is exclusively synthesized by cyanobacteria (Garcia-Pichel & Castenholz 1991). They produce this indole alkaloid as part of their response strategy for survival in environmentally stressed conditions, particularly in pulsed-irradiation conditions such as in intertidal flats. It is found as a yellow (oxidized) to red brown (reduced) lipid-soluble pigment in the extracellular sheaths or other polysaccharide structures (Fig. 12), depending upon the redox and acid-base conditions during the process of extraction (Garcia-Pichel & Castenholz 1991).

The structure of scytonemin consists of a dimeric carbon skeleton composed of fused symmetric heterocyclic units with a conjugated double-bond distribution that allows strong absorption of UVA

radiation with a maximum absorption at 384 nm. Three derivatives of scytonemin pigments such as dimethoxy scytonemin, tetra methoxy scytonemin, and scytonin have been reported from *Scytonema* sp. (Fig. 13) (Bultel-Poncé et al. 2004). Purified scytonemin has a maximum UV absorption at 384 ± 2 nm, although it also absorbs significantly at 252, 278 and 300 nm (Sinha et al. 1998, Rastogi et al. 2013). In addition to its UVA absorbing properties, scytonemin also has strong anti-proliferative and anti-inflammatory activities (Stevenson et al. 2002a, b).

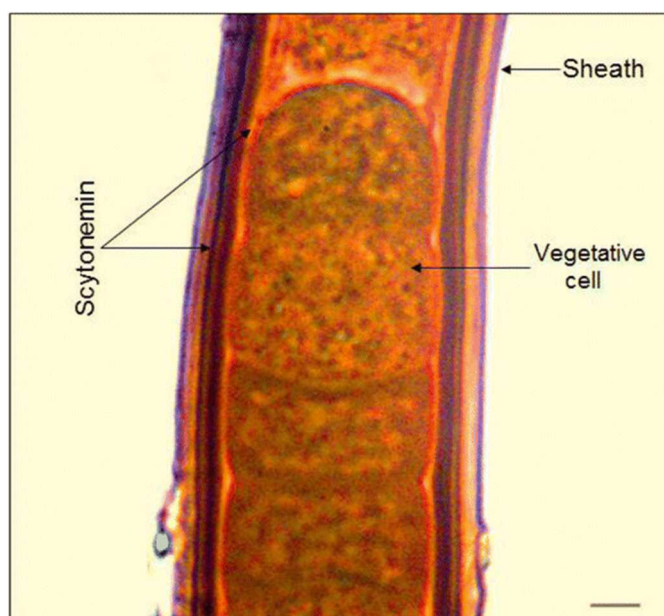


Figure 12. A filament of *Lyngbya* sp. showing the vegetative cells inside a polysaccharide sheath with yellow-brown pigment, scytonemin (scale bar, 10 μ m) [Image from R.P. Rastogi]

The biosynthesis of scytonemin probably involves tryptophan and tyrosine derivatives that absorb ambient UV radiation (Fig. 14A) (Proteau et al. 1993). Several cyanobacterial genomes have been explored to identify the genes responsible for scytonemin biosynthesis (e.g. Sorrels et al. 2009). The predicted structures of the gene products suggest that the assembly of scytonemin occurs in the periplasmic space (Soule et al. 2007). It has been suggested that the biosynthesis of scytonemin is regulated by a cluster of 18 genes (ORFs: NpR1276–NpR1259) transcribed unidirectionally (Soule et al. 2009). A total of eight genes have been found to involve in the biosynthesis of tryptophan and tyrosine, while the function of other genes does not show any significant homology with functionally characterized proteins (Fig. 14B) (Soule et al. 2009). The biosynthesis of scytonemin has been explored at genetic or molecular level in some cyanobacteria and some genetic variations was found to exist between genome clusters, but the majority of the scytonemin synthesizing genes showed high degree of amino acid sequence similarity (e.g. Balskus & Walsh 2009). Recently, the biosynthetic pathway of scytonemin has been heterologously expressed using the bacterium *Escherichia coli* (Malla & Sommer 2014). Moreover, the precise mechanism of scytonemin biosynthesis is still ambiguous. However, based on recent study, it may be concluded that the scytonemin biosynthesis in cyanobacteria is a highly conserved process (Balskus et al. 2011). Scytonemin production has not been observed in other organisms, but aquatic animals presumably accumulate scytonemins via the food chain or from symbiotic bacterial partners, as they lack the shikimate pathway for synthesizing precursors. Some derivatives of scytonemin have been discovered (Fig. 14B) suggesting that scytonemin may be the parent for a whole family of related molecules with subtle changes in radiation absorption.

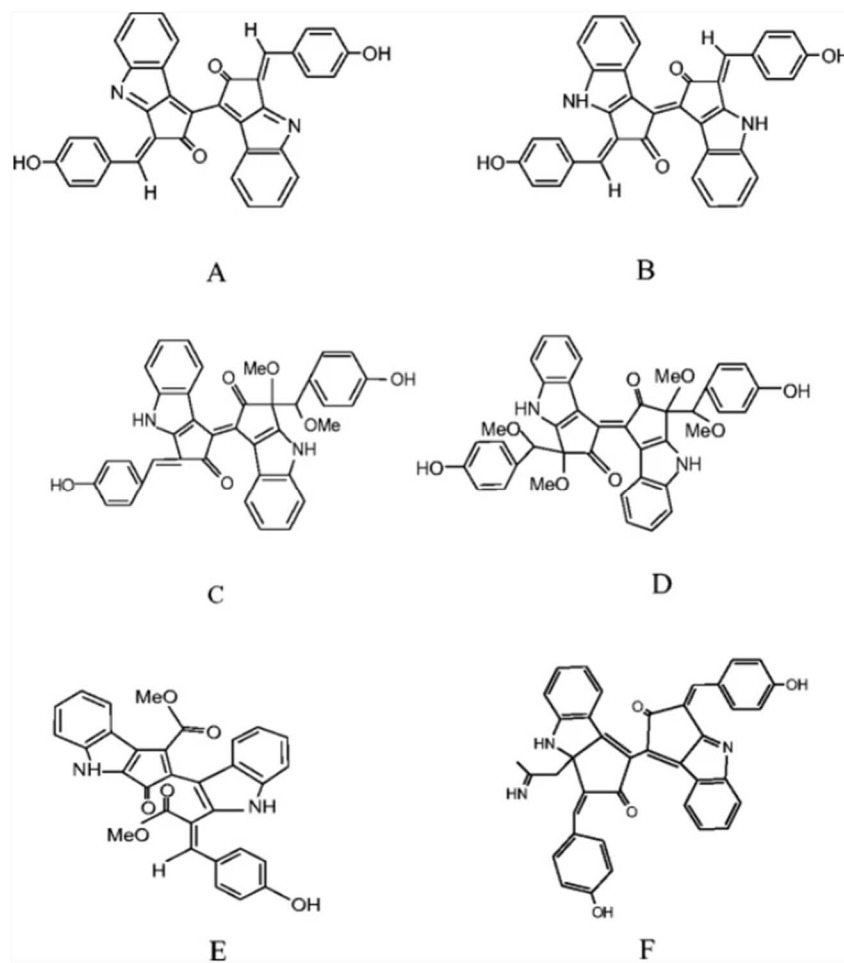


Figure 13. Chemical structure of scytonemin and its derivatives. (A) Oxidized scytonemin; (B) reduced scytonemin; (C) dimethoxyscytonemin; (D) tetramethoxyscytonemin; (E) scytonin; and (F) scytonemin-3a-imine

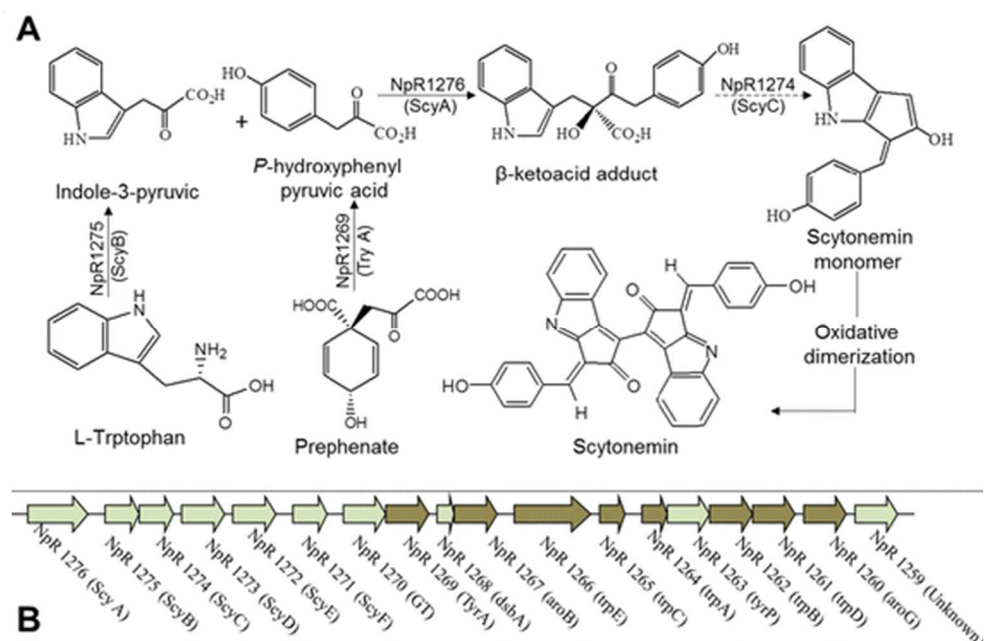


Figure 14. A proposed pathway of scytonemin biosynthesis in cyanobacteria (A) and genes associated with scytonemin biosynthesis (B) in *N. punctiforme* Rastogi et al. 2015

1.3.1.3 Sporopollenin

Sporopollenin is an acetolysis-resistant inert biopolymer possessing a complicated structure with aliphatic (mainly isoprenoid) and aromatic components variably present. It is found in the cell wall of some algae (Atkinson et al. 1972, Pickett-Heaps & Staehelin 1975) and in plant pollen and spores (Shaw & Yeadon 1964, Osthoff & Wiermann 1987, Guilford et al. 1988). Xiong et al. (1997) observed that UVB tolerant chlorophyte species of *Characium terrestre*, *Coelastrum microporum*, *Enallax coelastroides*, *Scenedesmus* sp., *Scotiella chlorelloidea*, *Scotiellopsis rubescens*, and *Spongiochloris spongiosa* contain large amounts of sporopollenin. The biopolymer was reported to be present also in *Dunaliella salina* zygotes (Komaristaya & Gorbulin 2006) and in the cell wall of *Chlorella protothecoides* (Fig. 15) (He et al. 2016).

Rozema et al. (2001) has demonstrated the UVB absorbing property of extracts containing sporopollenin. The UVB screening role of sporopollenin is evidenced by the high UVB optical density of the sporopollenins isolated from UVB tolerant chlorophytes and its increase upon UVB exposure. Xiong et al. (1997) showed that the sporopollenin content (mean \pm SE) increased from $0.73\pm 0.12\%$ to $0.85\pm 0.14\%$ (w/w) in *Scenedesmus* sp. and from $0.58\pm 0.10\%$ to $0.73\pm 0.09\%$ in *Enallax coelastroides* upon UVB exposure. Aside from its UVB screening role, the presence of sporopollenin in the cell wall of *Pediastrum duplex* has been associated with the resistance of this chlorophyte to microbial decomposition in natural waters (Gunnison & Alexander 1975). The presence of sporopollenin in the cell wall of *Chlorella fusca* also has been associated to its resistance to extreme extraction procedure (Atkinson et al. 1972). Since sporopollenin is a non-toxic, safe natural material that has the ability to absorb UV-B radiation and to bind heavy metal (Arslan et al. 2004), its use in the cosmetic treatment of skin against age-related/sun-related wrinkle formation and as a chelating agent of ion-exchangers in wastewater purification has been patented in the United States in 2007 (<http://www.patentgenius.com/patent/7182965.html>).

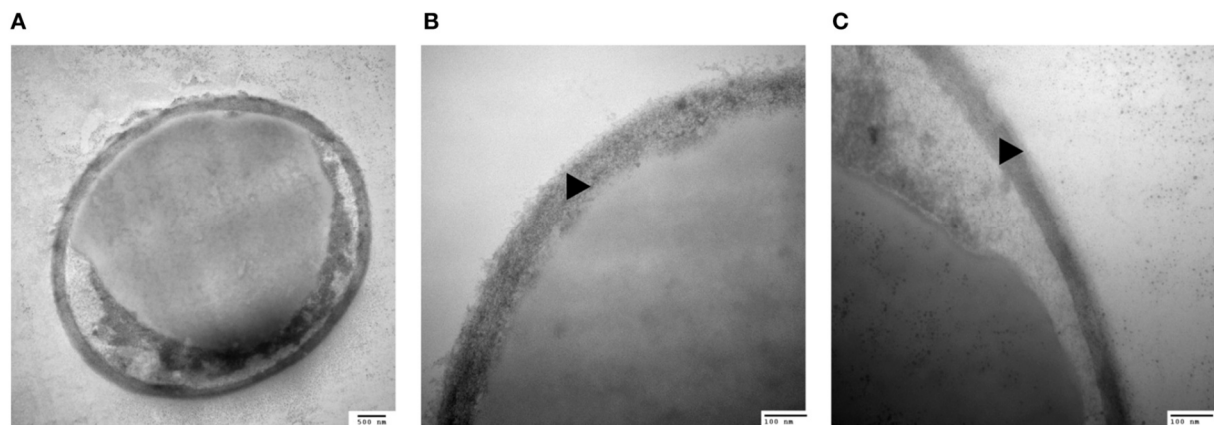


Figure 15. Identification of sporopollenin in the cell wall of *Chlorella protothecoides*. (A) Following 2-amino ethanol treatment were examined using TEM ($\times 30K$). (B) The same with (A). (C) Similar with (A, B) but at higher magnitude ($\times 120K$) (He et al. 2016).

1.3.1.4 Sulfated Polysaccharides

Marine algae are considered as the most important source of non-animal sulfated polysaccharides, and chemical structures of these polymers differ according to class and species of algae (Misurcova et al 2015). Carrageenan and fucoidan are the major sulfated polysaccharides found in red and brown

algae, respectively. Carrageenans are widely used in food, pharmacy, dairy, and cosmetic products due to the unique physical functional properties, such as thickening, gelling, emulsifying, and stabilizing properties (Pangestuti & Kim 2014). These sulfated polysaccharides have been considered as safe additives for many commercial products in many countries. In addition to their unique physical functions, carrageenan composition in cosmetic and skin care products has often been found with antioxidant, tonifying, cleaning, hydrating, and revitalizing bioactivities. Recently, photoprotective effects of carrageenan (κ , ι and λ) in UVB-induced human keratinocytes (HaCaT) cells have been reported (Thevanayagam et al. 2014). Carrageenan has shown significant protection against the detrimental effects of UVB-induced apoptosis in HaCaT cells and has decreased the release of reactive oxygen species (ROS). The accumulation of excess ROS has been related to skin diseases including skin aging and cancers. Therefore, antioxidants are usually viewed as preventive agents against UV-related skin diseases. We assumed that the photoprotective activity of carrageenan may also correlate to their immunomodulatory properties. Carrageenan has been known as an immunomodulator, which induces the expression of cyclooxygenase-2 (COX-2) and the release of prostaglandin-E₂ (PGE₂) (Nantel et al. 1999). Based on an in vivo experiment in SKH-1 hairless mice, Tripp et al. (2003) suggested that COX-2 expression is an important factor for keratinocyte survival and proliferation after acute UV irradiation. Inhibition of COX-2 expression has been demonstrated to reduce epidermal keratinocytes proliferation. Taken together, it may be hypothesized that immunomodulatory activities and ROS scavenging activities of carrageenan might play an important role in their photoprotective mechanisms. The addition of carrageenan to a broad spectrum of skin care and cosmetic products might decrease UV-induced photodamage compared with sunscreen alone.

Fucoidan is the most commonly sulfated polysaccharide isolated from brown algae. In general, these linear polysaccharides have a backbone of α -linked L-fucose residues with various substitutions. Fucoidan structures and bioactivities are different among brown algae species (Pangestuti & Kim 2013). Recent findings have reported the photoprotective activity of fucoidan isolated from brown algae including *Ecklonia cava*, *Undaria pinnatifida*, *Costaria costata*, and *Fucus evanescens* (e.g. Moon et al. 2009). The photoprotective activity of fucoidan has been determined in UVB-irradiated human dermal fibroblast and mice models. Most studies report that the photoprotective activity of fucoidan is mediated through the suppression of matrix metalloproteinase-1 (MMP-1) activity. MMP-1 is a major enzyme implicated in the collagen damage and photoaging of UV-irradiated human skin. More precisely, these sulfated polysaccharides downregulate the expressions of NF- κ B, which, in turn, diminish MMP-1 expression. Recently, it was reported that topical applications of low-molecular-weight fucoidan have stronger photoprotective activity than high-molecular-weight fucoidan (Kim et al. 2018). The rationale for this is that low-molecular-weight fucoidan is mostly absorbed before irradiation. This low-molecular-weight fucoidan seems to be involved in photoprotective effects rather than UV filtering effects. Photoprotective activity in orally administered fucoidan, in addition to topical applications, has been reported. This information on the bioavailability of fucoidan might have stimulated further research on the relationship between the oral administration of fucoidan and their bioavailability, mode of action, and potency in skin care and cosmetic products.

The soluble cell-wall polysaccharides of different red microalgae species (e.g. *Porphyridium cruentum*, *Dixoniella grisea*, *Rhodella reticulata*) have a common structural feature: galactan heteropolymers (molar mass $2\text{--}7 \times 10^6 \text{ g mol}^{-1}$) that contain sulfate residues (e.g. Dubinsky et al. 1992). The polysaccharides are anionic due to the presence of GlcA and half-ester sulfate groups. In the species studied, the main sugars of the polymers are xylose, glucose, and galactose, but in different ratios.

Additional minor sugars (methylated sugars, mannose, arabinose, and ribose) have also been detected. The polymers have different sulfate contents (1–9%, w/w), with the sulfate groups being attached to glucose and galactose in the 6 or 3 position (Lupescu et al. 1991).

In particular, the polysaccharide of *Porphyridium* sp. (Fig. 16) was found to have anti-inflammatory, anti-irritating (Matsui et al. 2003), and antioxidant (Tannin-Spitz et al. 2005) activities. Due to these bioactivities, this sPS has already been introduced into a wide range of cosmetic products of a leading global cosmetics company (Arad & Levy-Ontman 2010).

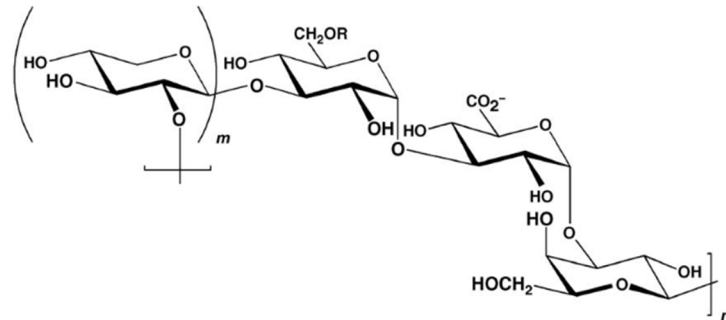


Figure 16. Proposed structure of a linear building block in the *Porphyridium* sp. polysaccharide (Geresh et al. 2009).

1.3.2 Antioxidant Defense Strategies

Algae apply two defensive strategies for cope on ROS before they can damage to cellular difference components (Fig. 17). The first system comprises antioxidant enzymes (high molecular weight) such as superoxide dismutases, glutathione reductase, catalases, ascorbate peroxidase and non-enzymatic (low molecular weight) that comprise ascorbate, flavonoids, carotenoids, glutathione, tocopherols and phenols. The second mechanism is repair enzymes that repair and remove damaged macromolecules. The enzymatic antioxidants are important in the detoxification of the destructive effects of formed ROS by electron transport ($O_2^{\cdot -}$, H_2O_2 , HO^{\cdot}), but the non-enzymatic antioxidants are more effective in the prevention of ROS production by the excitation energy transfer (1O_2) (Jahan et al. 2017, Pikula et al. 2019).

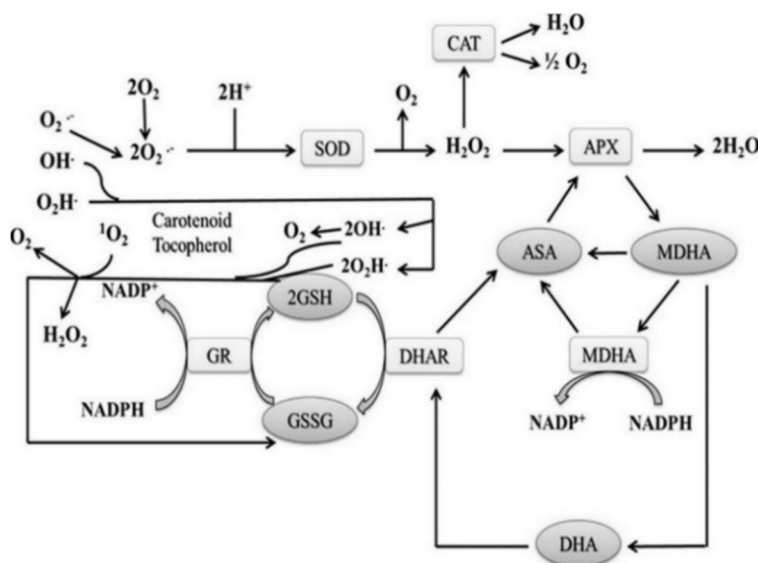


Figure 17. Enzymatic and non-enzymatic antioxidants in algae. ASA, Ascorbate; APX, Ascorbate peroxidase; CAT, Catalase; DHA, Dehydroascorbate; GSH, Glutathione; GR, Glutathione reductase; GSSG, glutathione disulfide; MDHA, Monodehydroascorbate; SOD, Superoxide dismutase; DHA, Dehydroascorbate reductase (Gill & Tuteja 2010).

ROS in low concentration have significant roles in the defence against infection, the cell signalling and the apoptosis. O_2^- , OH^\cdot and H_2O_2 have more signalling capacity because they can transfer of membranes via aquaporins (Reczek & Chandel 2015). The transduction of H_2O_2 - based signals is centred on sulphur chemistry, with the main player being the reversible oxidative modification of cellular sulphur-containing groups (e.g., cysteine residues and thioredoxin), which in turn results in disturbances of metabolism and signalling pathways in microorganisms. H_2O_2 oxidized cysteine thiol groups of phosphatases in mitogen activated protein kinase (MAPK) pathways, which act in signalling response for various environmental stimuli. Late studies showed moreover change of gene expression, ROS have an essential role for resistance under oxidative stress by post-translational changes. Some of mitogen-activated protein kinase family includes extracellular signal-regulated kinases, JNK, and p38 play a role in cellular processes including proliferation, differentiation, and apoptosis regulated by ROS (Veal et al. 2007, Lushchak 2011, Morano et al. 2012).

1.3.2.1 Non-Enzymatic Constituents

1.3.2.1.1 Ascorbate

Ascorbic acid (ascorbate, vitamin C) is a water-soluble antioxidant that acts as substrate for ascorbate peroxidase, electron donor for $^{\cdot}OH$ radical, good scavenger, reducing antioxidant and donating its electrons to ROS. Ascorbate suppresses H_2O_2 through ascorbate-glutathione cycle (Wheeler et al. 1998).

1.3.2.1.2 Flavonoids

Flavonoids are a well-known important group of secondary metabolites in land plants and were also detected in microalgae from different evolutionary lineages (Goiris et al. 2014). They are involved in various processes ranging from UV protection to signalling and pigmentation (Stafford 1991, Winkel-Shirley 2001a, b, Koes et al. 2005, Markham 2006, Agati & Tattini 2010).

Flavonoids form a large heterogeneous group of components, all of which are derived from a common chalcone precursor, which in its turn is formed from the end product of the phenylpropanoid pathway. In the phenylpropanoid pathway, the amino acid phenylalanine is converted into *t*-cinnamic acid by the enzyme phenylalanine ammonia lyase (PAL), which is further converted into *p*-coumaroyl-CoA. In the first step of flavonoid synthesis, three acetate units are added onto *p*-coumaroyl-CoA by chalcone synthase, yielding a chalcone (Fig. 18). After formation of the chalcone, an array of isomerases, reductases, hydroxylases, glycosyltransferases, and acyltransferases form a variety of flavonoid subclasses such as flavanones, flavones, isoflavonoids, flavonols, flavandiols and proanthocyanidins. Several studies have demonstrated that algae are capable of forming *p*-coumaric acid, the precursor of the flavonoid synthesis as the enzyme PAL has been detected in the microalgae *Chlorella pyrenoidosa* (Chen et al. 2003) as well as in the cyanobacteria *Anabaena variabilis* and *Nostoc punctiforme*, suggesting that this enzyme was already present in the ancestors of the chloroplasts (Moffitt et al. 2007). For instance, the flavonols quercetin ($2-4 \mu\text{g g}^{-1}$) and kaempferol ($4-7 \mu\text{g g}^{-1}$) were detected in a study on the influence of UV radiation on the chlorophyte *Scenedesmus quadricauda* (Kováčik et al. 2010) while the flavonols quercetin, rutin and myricetin were found (ng per 10^{10} cells) in the diatom *Phaeodactylum tricorutum* in a study on the antioxidant response to Cu-induced oxidative stress (Rico et al. 2013).

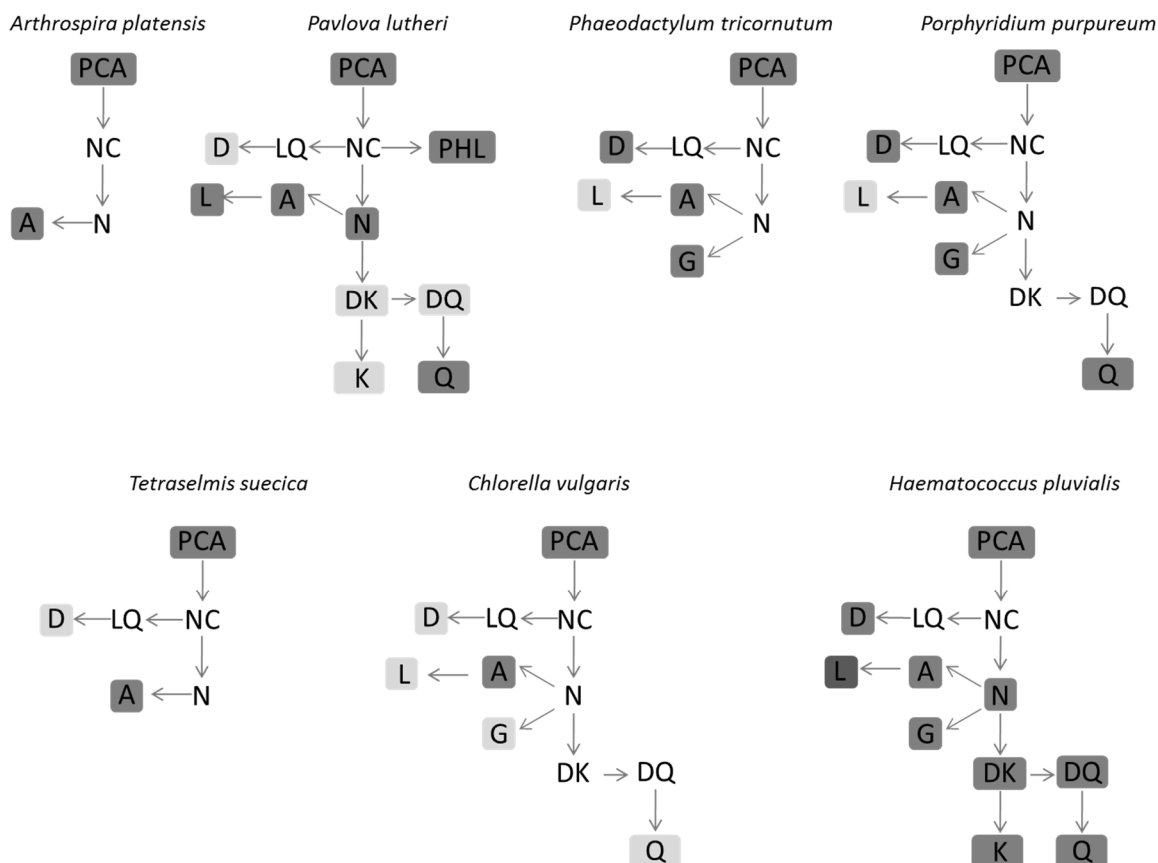


Figure 18. Metabolomics-based reconstruction of tentative flavonoid pathways present in selected microalgae (Goiris et al. 2014). Minor components are marked in light grey, whereas major components are indicated in dark grey. PCA, *p*-coumaric acid; NC, naringenin chalcone, N, naringenin, PHL, phloretin; LQ, liquiritigenin; D, daidzein; A, apigenin; G, genistein; L, luteolin; DK dihydrokaempferol; DQ, dihydroquercetin; K, kaempferol; Q, quercetin.

1.3.2.1.3 Carotenoids

Carotenoids are isoprenoid and lipophilic compounds and are coloured yellow, orange or red that 750 kinds of carotenoid are exist in plants and microorganisms (Concepcion et al. 2018). Carotenoids include carotenes such as lycopene, α -carotene and β -carotene, and xanthophylls with oxygen as hydroxyl groups (e.g. lutein), as oxy-groups (e.g. canthaxanthin) or as a combination of both (e.g. astaxanthin). Some of xanthophylls (violaxanthin, antheraxanthin, zeaxanthin, neoxanthin, lutein, loroxanthin, astaxanthin and canthaxanthin) produced by microalgae whereas others (diatoxanthin, diadinoxanthin and fucoxanthin) also synthesized by brown algae. Carotenoids have antioxidant characterizes and cause maintain of cells against free radicals, inhibition of lipid peroxidation, increase the stability of the photosynthetic apparatus and protection of integrity membranes (Sasso et al. 2012, Katsumata et al. 2014, Di Pietro et al. 2016).

Carotenoids play an important role in photosynthetic light-harvesting complexes; they absorb the solar spectrum in the blue-green region and transfer the energy to chlorophylls (Hashimoto et al. 2015). Many studies have reported a strong correlation between increased UVB irradiation and carotenoid accumulation in terrestrial and marine plants (Shen et al. 2017). As an example, Hupel et al. (2011) demonstrated that UVB irradiation increased the carotenoid contents in brown algae *Pelvetia canaliculata*.

Photoprotective effects of fucoxanthin (Fig. 19) derived from marine brown algae against UVB-induced photoaging have been reported (Heo & Jeon 2009). Photoprotective activity of fucoxanthin has been determined by various in vitro and in vivo methods such as comet assay, human dermal fibroblast, and hairless mice irradiation. ROS scavenging activity is mainly considered to be a mechanism of action underlying the photoprotective activity of fucoxanthin (e.g. Liu et al. 2016). Carotenoids, including fucoxanthin, are known as a singlet oxygen quencher. These photosynthetic pigments mitigate the harmful effects associated with UV irradiation by dissipating the excess energy as heat and returns to the initial ground state. Recently, fucoxanthin has been demonstrated to stimulate filaggrin promoter activity in UV-induced sunburn (Matsui et al. 2016). Filaggrin is a UV-sensitive gene that reflects the state of the skin damage. This stimulation of a UV-sensitive gene promoter by fucoxanthin suggested that other protective mechanisms of fucoxanthin might be exerted by the promotion of skin barrier formation through the induction of UV-sensitive gene expression.

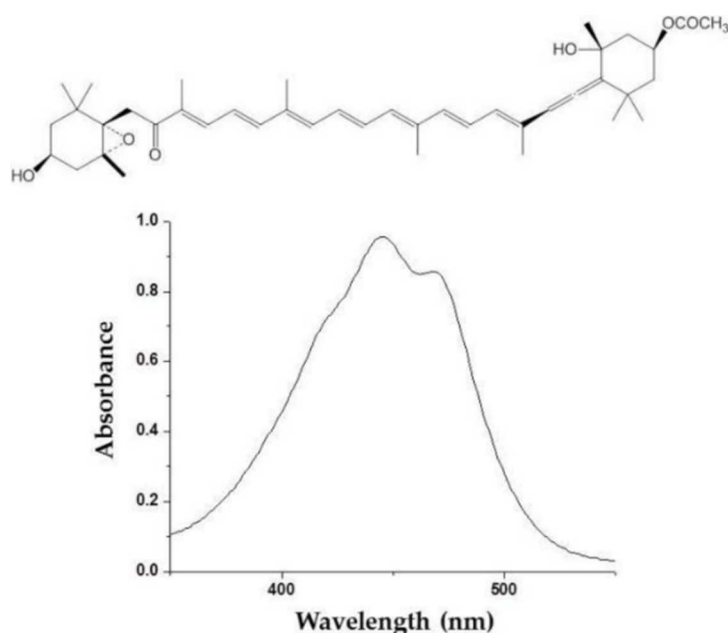


Figure 19. Molecular structure and ultraviolet (UV) absorption spectra of fucoxanthin from brown algae (e.g. diatoms).

Photoprotection mechanisms of fucoxanthin might also be achieved by oral administration. It has been shown that photodamage on the skin or eyes can be protected by biological compounds in tissues, which come from nutritional sources via the bloodstream. Stahl & Sies (2012) reported the concentration of carotenoids in human skin and demonstrated that there are considerable differences in the patterns in each skin layer. As an example, high concentrations of carotenoids are found in the skin of the forehead, the palm of the hand, and dorsal skin. Meanwhile, lower concentrations are found in the skin of the arm and the back of the hand of the human body (Stahl & Sies 2012). In the human body, fucoxanthin absorption strongly depends on a number of factors, including the amount and type of dietary lipids consumed, the stability of the matrix to which the carotenoid is bound, and additional dietary factors such as dietary fibre. The esterified fucoxanthin is likely to be incorporated into the lipid core in chylomicron and carried into a variety of tissues, including the skin (Pangestuti & Kim 2011).

Recently, it has been reported that skimmed milk is an excellent food matrix for fucoxanthin application in terms of stability and bioavailability (Mok et al. 2018). An in vivo pharmacokinetic study

with a single oral administration of fucoxanthin fortified in skimmed milk showed the highest absorption of fucoxanthinol and amarouciaxanthin A (two prime metabolites of fucoxanthin). Considering the potency of fucoxanthin as a photoprotective substance, further research studies are needed to verify photoprotective mechanisms of fucoxanthin oral consumption and the bioavailability of fucoxanthin (and its derivatives) in human skin.

1.3.5.1.4 Glutathione

The Tripeptide glutathione (Fig. 20) is the major low molecular weight thiol and formed of glutamate, cysteine, and glycine. Reduced glutathione by oxidizing itself into oxidized glutathione via ascorbate-glutathione cycle causes the regeneration of ascorbate. Glutathione involves in adjust redox potential for amino acids and proteins, scavenging oxidative damage, non-specific reductant, substrate/cofactor for enzyme-catalysed reactions, reconstruction of protein disulphide bonds and suppression of H₂O₂ and organic peroxides (ROOH) (Foyer & Halliwell 1997).

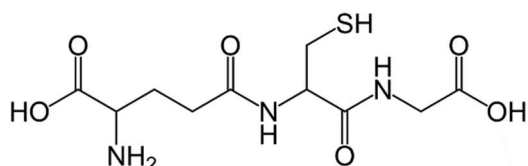
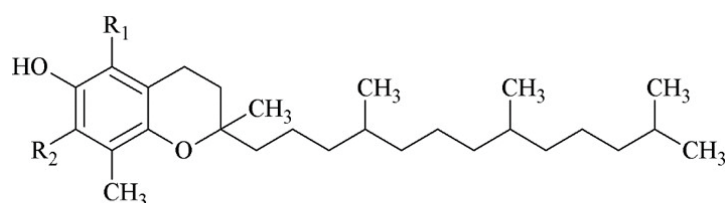


Figure 20. Chemical structure of Glutathione.

1.3.2.1.5 Tocopherols

Tocopherols (vitamin E) have an aromatic ring and a long hydrocarbon chain. Tocopherols play in oxidation-reduction-reactions by the aromatic ring. Tocopherols destroy reactive types of oxygen and protect unsaturated fatty acids from oxidation. Among the four tocopherols (α -, β -, γ and δ -tocopherols), α -tocopherol is a key antioxidant because it can suppress ¹O₂, reduce O₂⁻ and finish lipid peroxidation reaction (Fig. 21) (Takenaka et al. 1991).



Tocopherol	R ₁	R ₂
α -	CH ₃	CH ₃
β -	CH ₃	H
γ -	H	CH ₃
δ -	H	H

Figure 21. Tocopherol structures. The table indicates the number and position of methyl groups on the aromatic ring.

1.3.5.1.6 Phenolic Compounds

In organic chemistry, phenols, sometimes called phenolics, are a class of chemical compounds consisting of a hydroxyl group (—OH) bonded directly to an aromatic hydrocarbon group.

In selected microalgae and cyanobacteria strains, 6 phenolic compounds (gallic acid, catechin, epicatechin, protocatechuic acid, and chlorogenic acid) have been identified and quantified in extracts by reverse phase high performance liquid chromatography (RP-HPLC) (Jerez-Martel et al. 2017).

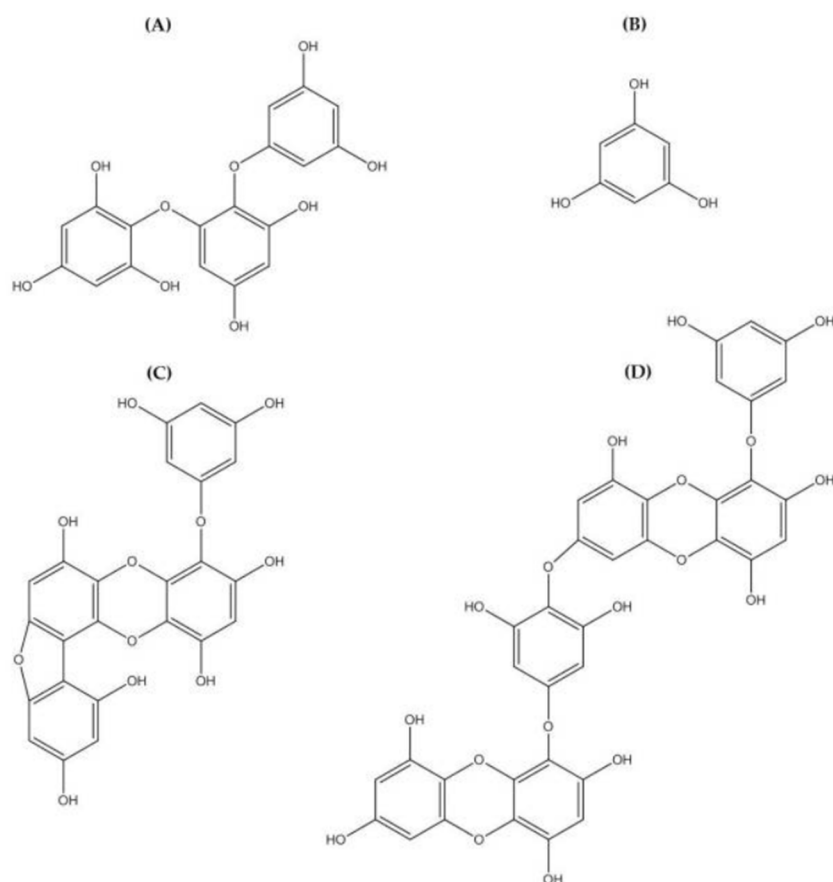


Figure 22. Chemical structure photoprotective polyphenol isolated from marine brown algae. Triphlorethol-A (A), phloroglucinol (B), fucofuroeckol-A (C), and dieckol (D) (Pangestuti et al. 2018).

Polyphenols are bioactive substances characterized by the presence of more than one phenolic group (a hydroxyl group bound to an aromatic ring). The hydroxyl (–OH) group bound to the aromatic ring acts as an electron donor, giving it to a free radical or other reactive species. This underlies the inhibition of ROS and ROS-mediated damage on macromolecules, which in turn inhibit the activation of the signal transduction pathways such as the MAPK signalling pathway.

Polyphenolic compounds are a class of secondary metabolites with diverse biological functions. These bioactive substances are divided into several classes according to the number of phenol rings and structural elements that bind these rings to one another (Ignat et al. 2011). The three main groups of polyphenols are phenolic acids, flavonoids, and tannins. Marine algae-derived polyphenols have been investigated for their photoprotective activities. Dieckol (phlorotannin), phloroglucinol, fucofuroeckol-A, and triphlorethol-A (Fig. 22) isolated from marine brown algae exhibited prominent protective effect against photodamage induced by UVB radiation, as demonstrated in many studies (e.g. Vo et al. 2018). To understand the cellular and molecular photoprotective mechanisms of phloroglucinol, Piao and his colleagues developed it in UVB-irradiated mice and a HaCaT cell model. Phloroglucinol (10 μ M) scavenged free radical and protects macromolecules damage in UVB-irradiated HaCaT cells (Kim et al. 2012). In addition, phloroglucinol treatment significantly inhibited the UVB-induced upregulation of MMP-1 and phosphorylation of mitogen-activated protein kinases (MAPK) and activator protein-1 (AP-1) binding to the MMP-1 promoter (Piao et al. 2012). Phloroglucinol has

been demonstrated to be safe and effective when applied in the mouse skin irradiated with UVB (Piao et al. 2014). The findings confirm the effectiveness of phloroglucinol as potential cosmeceutical leads for the formulations of sun-protective lotions and creams (Pangestuti et al. 2018).

As mentioned in the many scientific reports, polyphenolic compounds represent an interesting class of active substance in the protection of UV-light-induced skin damage. Up to a certain concentration, marine algal polyphenol did not exert any toxic effect, anticipating its potential use as a safe photoprotector that can be utilized in skin care products (Pangestuti et al. 2018).

1.3.2.2 Antioxidant Enzymes

1.3.2.2.1 Superoxide Dismutase

Superoxide dismutase (SOD) is a metalloprotein and first line of defence against oxidative stress that catalyzes the dismutation of superoxide radicals into oxygen and hydrogen peroxide. SOD include three isoforms that determined by their metal centre cofactors: Cu/ZnSOD found in the thylakoid membranes and cytosol of higher plants, certain dinoflagellates and charophycean green algae, MnSOD located in mitochondria, and FeSOD found in the chloroplast stroma. The SOD activity enhanced by abiotic stresses and acts a defence tool (Davies 2000, Mallick & Mohn 2000).

1.3.2.2.2 Catalase

Catalase (CAT) is tetrameric enzyme contain heme that has a main role to convert H_2O_2 into H_2O and O_2 . CAT has three groups. Manganese catalases exist in prokaryotes. Catalase peroxidases act as both catalases and peroxidases and have been found in prokaryotes and some eukaryotes. Classical catalases (cat) include heme groups and covert H_2O_2 to H_2O and O_2 in a two-step process. First, one molecule of H_2O_2 is reduced to water and the Fe^{3+} of the catalase is altered to $cat(Fe[V]O)$. Second, the $cat(Fe[V]O)$ is converted back to Fe^{3+} while another molecule of H_2O_2 is reduced to H_2O and O_2 (Mate et al. 1999).

1.3.5.2.3 Ascorbate Peroxidase

Ascorbate peroxidase (APX) is a heme enzyme and converts the H_2O_2 into H_2O through ascorbate as electron donor. APX is existed in plants and algae. Two cytosolic APX (cAPX) isoenzymes have been showed in the red algae *Galdieria partita* and *G. sulphuraria* (Sano et al. 2001, Oesterhelt et al. 2008).

1.3.5.2.4 Glutathione Reductase and Glutathione Peroxidase

Glutathione reductase (GR) is a flavoprotein oxidoreductase that exists in eukaryotes and prokaryotes. GR is a great enzyme of the ascorbate-glutathione cycle and have a necessary function in defence system against ROS by maintain the reduced status of GSH. Like Ascorbate peroxidase, Glutathione peroxidase decomposes H_2O_2 to H_2O by GSH (Edwards et al. 1990, Romero-Puertas et al. 2006).

2. Objectives and Aims of the Study

UVR affects organisms through molecular and/or cellular damages, genetic mutations, interfering with physiological functions such as growth and reproduction. It clearly indicates the need of a potent, stable, and broad-spectrum group of agents which are devoid of their hazardous effects to the skin and environment. Here, mycosporine like amino acids (MAAs) stand as a good example due to their excellent antioxidant and sun protection activities, particularly against UVA radiation, without causing any known harmful effects (Bhatia et al. 2011). MAAs are becoming important as compounds of interest to supplement and/or even replace commercially available sunscreens, particularly as the requirement for natural products and replacement of petrochemical based products is growing. Until now only one product called Helioguard® 365 that contains MAAs from the red macroalga *Porphyra umbilicalis* has been commercialized (Llewellyn & Airs 2010). An MAA containing product originating from marine microalgae is not yet on the market.

As pointed out in the introduction besides MAAs there are several naturally occurring photoprotective compounds as well as antioxidative defences in marine microalgae and cyanobacteria which might be utilizable as additives in sun protective agents. Therefore, the presence, amounts and in some cases the composition of antioxidant enzymes (superoxide dismutase, catalase, glutathione reductase and ascorbate peroxidase), small-molecule antioxidants (ascorbate, flavonoids, carotenoids, tocopherols, glutathione, polyphenols), as well as photoprotective substances such as sporopollenin, scytonemin and sulfated polysaccharides were also analysed in the present study.

Under the assumption that sub-Arctic marine microalgae may be rich sources for UV-absorbing/screening compounds due to high UV radiation in the environment, selected microalgae from the BioPol ehf culture collection of northern Icelandic algal strains were screened for their potential to adapt under controlled laboratory conditions in small scale experiments as well as further up-scales to 100 L combined with UV-exposure and processing optimizations.

Specifically tested were:

- the presence of photoprotective compounds and antioxidative defence systems,
- the potential of induction of the synthesis of photoprotective compounds and antioxidative defence systems by variation of the length and composition of UV/PAR exposure,
- the stability of these compounds during handling processes such as harvest, drying and storage,
- the potential to scale up systems and increase the final product yield.

3. Material and Methods

If not otherwise mentioned, all chemicals used in this study were of the highest purity from Sigma/Aldrich.

3.1 Algal Strains and Culture Conditions

3.1.1 Algal Species

Initially 50 microalgae species were selected for the experiments due to their reliable growth patterns.

Table 1. List of microalgae and cyanobacteria which were used in the experiments, including specifications of growth conditions (media, temperature, light conditions, and nitrogen (N) source). Furthermore, the laboratory code contains besides the name and taxonomic order initials information regarding year of isolation, habitat, and location.

No	Species	Laboratory Code (e.g., year and location of isolation, group designation)	Medium	Optimum growth by		
				T [°C]	PAR [$\mu\text{mol m}^{-2} \text{s}^{-1}$]	N-source
Cyanobacteria						
1	<i>Nodularia sp.</i>	15CY-P-No-ISA	BG-11	16	30	NaNO ₃
2	<i>Nodularia harveyana</i>	14CY-P-NH-HRU	BG-11	16	30	NaNO ₃
3	<i>Synechocystis I</i>	15CY-P-SYI-SKA	BG-11	16	30	NaNO ₃
4	<i>Synechocystis II</i>	14CY-P-SYII-SKA	BG-11	16	30	NaNO ₃
5	<i>Merismopedia sp</i>	15CY-P-ME-SKA	BG-11	16	30	NaNO ₃
6	<i>Phormidium autumnale</i>	13CY-EPS-PA-SKA	BG-11	16	30	NaNO ₃
7	<i>Chroococcus turgidus</i>	13CY-P-CT-ISA	BG-11	16	30	NaNO ₃
8	<i>Spirulina subsalsa</i>	14CY-P-SS-SKA	BG-11	16	30	NaNO ₃
9	<i>Synechococcus I</i>	14CY-P-SYN-SKA	BG-11 b	16	15	NaNO ₃
10	<i>Synechococcus II</i>	15CY-P-SYN-SKA	BG-11	16	30	NaNO ₃
Chlorophyceae						
11	<i>Dunaliella tertiolecta</i>	15CH-P-DT-WF	f/2	18	80	urea
12	<i>Chlorella salina</i>	16CH-P-CS-SKA	f/2	18	80	urea
Rhodophyceae						
13	<i>Porphyridium marinum</i>	14RHO-P-PM-SKA	PES	14	50	NaNO ₃
14	<i>Porphyridium purpureum</i>	13RHO-P-PP-SKA	f/2b	18	50	NaNO ₃
Prymnesiophyceae						
15	<i>Isochrysis galbana</i>	13PR-P-IG-SKA	f/2	18	50	NaNO ₃
16	<i>Emiliana huxley</i>	15PR-P-EH-SKA	L1	18	50	NaNO ₃
Dinophyceae						
17	<i>Amphidinium carterae</i>	14DINO-P-AC-SKA	L1	18	50	NaNO ₃
18	<i>Alexandrium tamarense</i>	14DINO-P-AT-SKA	L1	18	50	NaNO ₃
Bacillariophyceae (diatoms)						
19	<i>Coscinodiscus sp.</i>	13DIA-P-CSP-SKA	f/2 Si	14	40	urea

20	<i>Coscinodiscus wailesii</i>	14DIA-P-CW-SKA	SWES Si	14	40	urea
21	<i>Navicula gregaria</i>	14DIA-B-NG-HRU	f/2 Si	14	40	urea
22	<i>N. cancellata</i>	15DIA-B-NCA-SKA	f/2 Si b	14	40	urea
23	<i>N. clementis</i>	14DIA-B-NCL-HRU	f/2 Si	14	40	urea
24	<i>N. directa</i>	15DIA-B-ND-SKA	f/2 Si	14	40	urea
25	<i>N. perminuta</i>	15DIA-EPS-NP-SKA	f/2 Si	14	40	urea
26	<i>N. hamiltonii</i>	15DIA-B-NH-ISA	f/2 Si b	14	40	urea
27	<i>N. spicula</i>	14DIA-B-NS-ISA	f/2 Si	14	40	urea
28	<i>Cylindrotheca closterium</i>	15DIA-P-CC-SKA	SWES Si	14	40	NaNO ₃
29	<i>Achnanthes borealis</i>	15DIA-B-AB-ISA	f/2 Si	14	40	urea
30	<i>A. cf. brevipes var. parvula</i>	15DIA-EPS-AB-SKA	f/2 Si	14	40	urea
31	<i>A. pseudogroenlandica</i>	14DIA-B-AP-ISA	f/2 Si	14	40	urea
32	<i>Amphora abludens.</i>	14DIA-P-AA-SKA	f/2 Si	14	40	urea
33	<i>A. acutiuscula.</i>	14DIA-B-AA-HRU	f/2 Si b	14	40	urea
34	<i>A. coffeaeformis</i>	14DIA-B-AC-HRU	f/2 Si b	14	40	urea
35	<i>A. laevis var. laevis</i>	15DIA-B-AL-ISA	SWES Si	14	40	urea
36	<i>Gyrosigma fasciola</i>	15DIA-P-GF-SKA	SWES Si b	14	40	urea
37	<i>G. tenuissimum</i>	14DIA-P-GT-SKA	SWES Si	14	40	urea
38	<i>Cymbella minuta</i>	14DIA-P-CM-SKA	f/2b Si	14	40	NaNO ₃
39	<i>Pinnularia ambigua</i>	15DIA-P-PA-SKA	f/2 Si	14	40	NaNO ₃
40	<i>Amphipleura rutilans</i>	15DIA-P-AR-SKA	f/2 Si b	14	40	urea
41	<i>Trachyneis aspera</i>	14DIA-P-TA-SKA	SWES Si	14	40	urea
42	<i>Entomoneis gigantea</i>	14DIA-P-EG-SKA	f/2 Si	14	40	urea
43	<i>Cocconeis costata</i>	15DIA-P-CC-SKA	f/2 Si	14	40	urea
44	<i>C. fasciolata</i>	14DIA-B-CF-SKA	f/2 Si	14	40	urea
45	<i>C. placentula</i>	14DIA-B-CP-SKA	f/2 Si	14	40	urea
46	<i>Diatoma mesodon</i>	15DIA-P-DM-SKA	f/2 Si	14	40	urea
47	<i>Diploneis didyma</i>	15DIA-B-DD-SKA	f/2 Si	14	40	urea
48	<i>D. bombus</i>	15DIA-B-DB-SKA	f/2 Si	14	40	urea
49	<i>D. ovalis</i>	14DIA-B-DO-SKA	f/2 Si	14	40	urea
50	<i>Pleurosigma elongatum</i>	15DIA-P-PE-SKA	SWES Si	14	40	urea

Abbreviations: PAR, photosynthetic active radiation measured in PFR, Photon fluence rates; P, phytoplankton species; B, benthic species; EPS, epispammic; SKA, Skagatrönd (Húnaflói); HRU, Hrótafjörður; ISA, Ísafjörður
Growth media: f/2b, f/2 Brackish Medium (f/2 Medium diluted 1:1 with sterilised freshwater, (Guillard 1975); f/2 + Si, f/2 Medium enriched with silicate; f/2b +Si, f/2 Brackish Medium enriched with silicate; f/2, f/2 Medium (Guillard 1975); BG-11 (Stanier et al. 1971); SWES Si, Medium enriched with silicate (Werner 1982); L1, (Guillard & Hargraves 1993); PES, (Andersen et al. 1991)

3.1.2 Cultivation

Prior to cultivation in liquid culture, the microalgae were purified from bacterial contaminants by spreading cells on 1.5% medium agar plates with 5 µg mL⁻¹ tetracycline and 5 µg mL⁻¹ kanamycin (Guillard 1975). The absence of bacteria was verified by epifluorescence microscopy (BX51, Olympus Corporation, Tokyo, Japan/Axiophot, Carl Zeiss AG, Oberkochen, Germany) using the dye 4',6-diamidino-2-phenylindol (DAPI). Subsequently each isolate was maintained in culture in 500 mL flasks (250 mL culture volume) under sterile conditions at 16±2°C, 12:12 h light: dark (L:D) regime and at an irradiance of 30-80 µmol photons m⁻² s⁻¹ using Master TL-D 18W/840 light (Phillips, Germany), corresponding to species specific optima (cf. Table 1, Fig. 23). Cultures were adapted to the standard culturing conditions described above at a saturating nitrogen concentration of 800 µM, ca. 90% of original medium, for two weeks. The nitrogen to phosphorous ratio of the medium during all experiments was 17:1. Furthermore, sodium nitrate (NaNO₃) was used as main nitrogen source

besides urea for Chlorophyceae and most diatoms. Artificial seawater salt (Tropic Marin Classic®, GmbH Aquarientechnik, Wartenberg) dissolved in de-ionised water was used with a salinity of 30 and pH of 8.3, corresponding to environmental factors recorded at the sampling sites from which the species originated in northern Iceland. Salinity, pH and conductivity were measured using handheld probes (YK-31SA, YK-2001PH SI Model 33, Engineered Systems and Designs-Model 600, Philips W9424).

Photon fluence rates (PFR, 400–700 nm) were measured with an underwater spherical quantum sensor LI-193SA connected to a Licor Data Logger LI-250A (LI-COR Lincoln, NE, USA).



Figure 23. Cultivation of microalgae and cyanobacteria in different locations. A) 2016: in the climate chamber at BioPol ehf which included a temperature gradient (ca. 3 °C difference, measured between the highest and the lowest shelf). The overall temperature change per hour was besides others also seasonal related and was $\pm 3.8^{\circ}\text{C}$ (measured on the highest shelf); B) 2018: at the BioPol laboratory in which no temperature gradient was possible. The maximum temperature change per hour was $\pm 5.5^{\circ}\text{C}$ (depending on season); C), D) since 2019 in an external facility which provides the optimal temperature gradient from the highest to lowest shelf (difference 3°C). The overall temperature change per hour is $\pm 0.2^{\circ}\text{C}$ (measured on the highest shelf) and is seasonal independent.

3.2 Experimental Designs

3.2.1 First Screening for Photoprotective Compounds and Scavenging Activities

The small-scale experiments were conducted in batches of 10 species per run in 2016 (cf. Fig. 24), resulting overall in five runs. The trials started by filling ten 1 L UV transparent quartz glass flasks (Technical Glass Products, Inc. Painesville, Ohio, U.S.A.) and ten standard 1 L Isolab borosilicate Erlenmeyer flasks (control) each with 250 mL fresh culture medium, add 250 mL dense algal culture ($8.8 \times 10^6 - 8.3 \times 10^9$ cells per millilitre) and incubating them at the species-specific optimal temperature ($16 \pm 2^\circ\text{C}$) for 336 hours under a 12:12 hours light to dark regime in two incubators (New Brunswick Innova 42 Incubator, Eppendorf, Hamburg, Germany). In the case of the UV screening assays two UV lamps (Exo Terra® PT2225 Mini Compact Top Canopy, 30 cm, equipped with each one Reptile UVB200 PT2341, 25 W, Rolf C. Hagen Inc., Montreal, Canada) were inserted into the trial incubator (Fig. 24A), whereas the control assays were illuminated in a second incubator using PAR only as described in 3.1.2. The UV light was measured using a handheld probe (OAI Model 308 UV Light Meter, OAI Instruments, Milpitas, U.S.A.).



Figure 24. Screening experiments A) view inside the trial incubator with the two inserted Exo Terra® canopy UV-lamps, B) and C) examples of batches of two times 10 flasks (UV assay and control assay).

The UV light equipment applied during the experiments is commonly used for terrarium illumination and was employed in this study due to a) safety issues, b) easy handling and purchase as well as c) already pre-assembled defined UV spectra which are similar to the natural light spectrum (cf. Fig. 25).

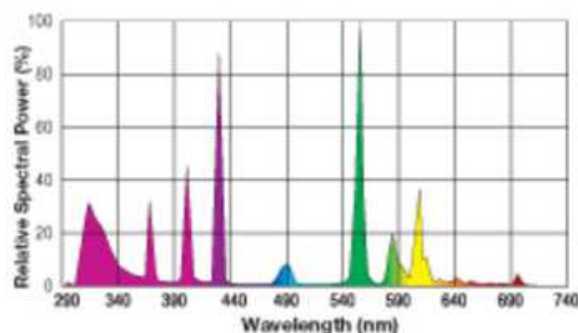


Figure 25. Spectrum of the combined UV and PAR bulbs from Exo Terra® (UVB200 PT2341) used during the first screening experiments.

The first samples were taken at the beginning of the experiments to obtain the cell numbers at $t=0$ h (cf. paragraph 3.3). Every two days, 5 mL of the medium were replaced by fresh medium in all test and control assays to prevent nutrient depletion. The position of replicate flasks was randomly changed

every second day to eliminate any location effect due to minor changes in external conditions. After 336 hours incubation all test and control assays were harvested and processed as described in 3.4 and a sub sample was used to determine the growth (3.3). The biochemical analysis is described in 3.5. Due to the unannounced use of solvent soaked fish samples in the lyophilisator prior to the freeze drying of the samples from the UV assay, resulting in negative MAA results, the experiment had to be repeated in 2017 using this time only 20 different species in two batches.

3.2.2 Induction of Photoprotective Compounds and Antioxidative Defenses

The compound initiation trials were conducted by variation of the duration of UV exposure and the use of different UV/PAR sources. Overall, two different UV/PAR sets with three spectra in each set were utilized (cf. Fig. 26) in these trials in order to cover the assimilation of an array of potential photoprotective compounds and components of the antioxidative defense system by four selected species which showed during the first screening trials promising activities (*Synechocystis* I and II, [3, 4]; *Synechococcus* I and II, [9, 10] in Table 1).

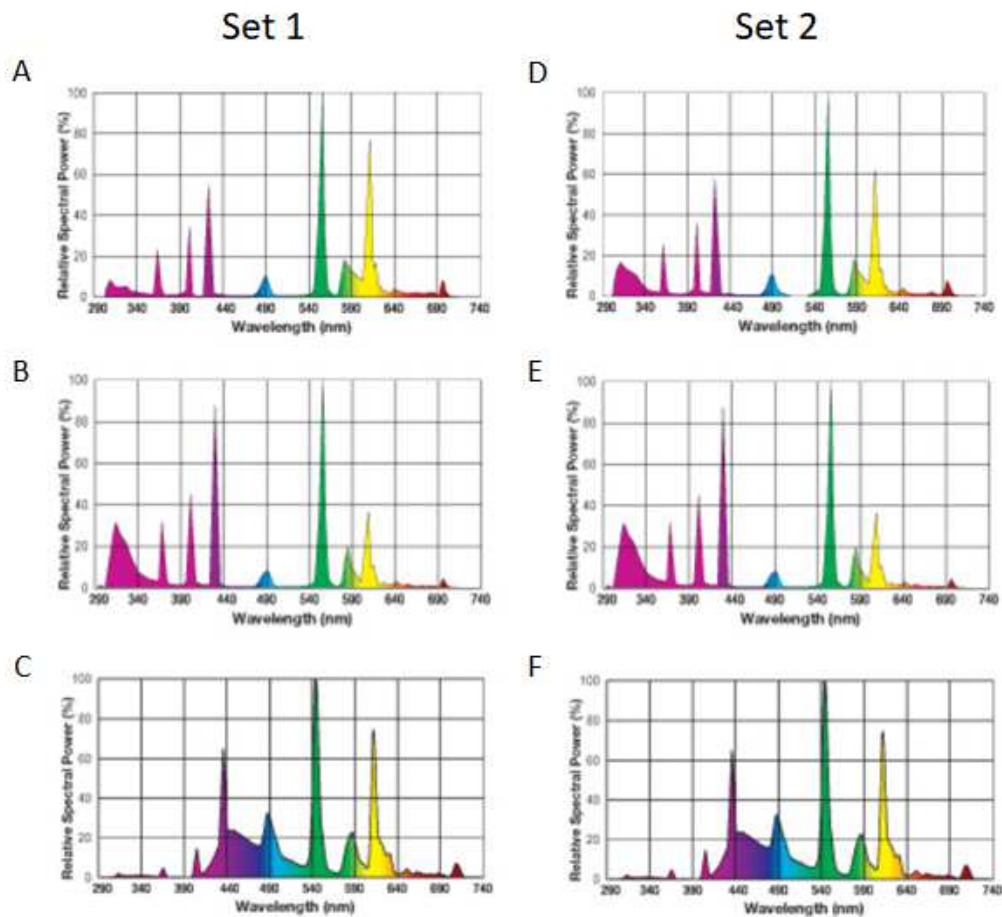


Figure 26. Spectra of the combined 25 W UV and PAR bulbs from Exo Terra© used during the induction experiments. Set 1 consisting of A) UVB100 PT2187, B) UVB200 PT2341, C) Natural Light PT2191 and Set 2 consisting of D) UVB150 PT2189, E) UVB200 PT2341, C) Natural Light PT2191. The utilization of different bulbs became necessary because there is no combined UVB and UVA bulb in the necessary size commercially available.

The experiments were conducted in 2018 in four 1 L UV transparent quartz glass flasks (Technical Glass Products, Inc. Painesville, Ohio, U.S.A.) per experiment with additional air bubbling for mixing as well as CO₂ and oxygen supply of the assays (Fig. 27). The position of the flasks was changed every day to eliminate any location effects due to changes in external conditions. Furthermore, ventilators were placed on one side of the experimental set up to prevent overheating of the test assays. As control, assays were handled as described in 3.1.2. The UV exposure time was varied as follows: 12: 12, 16: 8, 20: 4 and 8: 16 hours light to dark photoperiods. In addition, 24- and 72-hours continuous illumination were also tested. As control PAR illuminated assays were utilized. Samples were taken at the beginning of the experiments to obtain the cell numbers at t=0 h. After 336 hours incubation, all test and control assays were harvested and processed as described in 3.4 and sub samples from each assay were used to determine the growth (3.3). The following biochemical analysis focussed on MAAs (c.f. 3.5.1.1.1), scytonemin (covered by the alkaloid screening c.f. 3.5.4), sulfated polysaccharides (3.5.1.4), selected components of the antioxidative defence system (flavonoids 3.5.2.1.2, phenolic compounds 3.5.2.1.6), and scavenging activity (DPPH, 3.5.3.1). In addition, the 24 h and 72 h assays were analysed regarding their enzyme activities (SOD, CAT, APX, GR, 3.5.2.2).



Figure 27. One of the two experimental set ups for the induction of photoprotective compounds and antioxidative defense systems by variation of exposure times to slightly different UV light sources, using two selected cyanobacteria species which showed promising compound activities in the first screening.

3.2.3 Photoprotective Compound Stability

3.2.3.1 Alternative Harvest Methods

Three flocculation methods: ferric chloride, chitosan, and alkaline flocculation, were tested for each species. These three methods were selected because they are commonly used in studies on microalgae flocculation and they also differ with respect to the flocculation mechanism: the metal salt ferric chloride (Iron (III) chloride) induces flocculation predominantly through charge neutralization

(Wyatt et al. 2012), the cationic polymer chitosan (from crab shells) induces flocculation through a bridging mechanism, and alkaline flocculation causes flocculation predominantly through a sweeping mechanism (Brady et al. 2014, Vandamme et al. 2015). Alkaline flocculation was induced by addition of sodium hydroxide. The use of different harvest treatments was therefore further tested regarding their effect on photoprotective compounds as well as components of the antioxidative defense systems (Fig. 28). The experiments to obtain biomass were conducted in four 1 L UV transparent quartz glass flasks - two flasks for each species. As control, assays were handled under standard conditions as described in 3.1.2. For UV-light equipment in these trials an Exo Terra® Dual Top Canopy PT2233, 90 cm, equipped with PT2172 Repti Glo 10.0/T8 (75 cm, 25 W, Rolf C. Hagen Inc., Montreal, Canada) was used (Fig. 29). The trials started by filling the four 1 L UV transparent quartz glass flasks and two standard 1 L Isolab borosilicate Erlenmeyer flasks (controls) each with 250 mL fresh culture medium, add 250 mL dense cyanobacteria cultures ($8.0 \times 10^9 - 8.3 \times 10^9$ cells per millilitre) of *Synechococcus* I and II, [9, 10] incubating them at a temperature of $16 \pm 0.5^\circ\text{C}$ under a 12:12 hours light to dark regime.



Figure 28. Test of gravitational sedimentation, pH treatment with calcium hydroxide (pH 9) as well as chitosan as flocculant (last bottle) as alternative harvest methods for high biomass amounts.

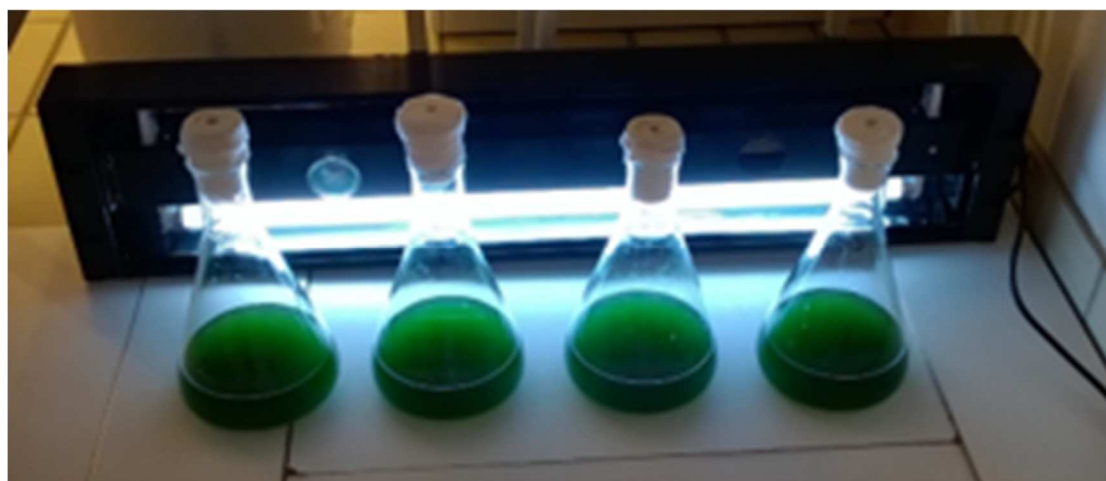


Figure 29. Set up to gain biomass for the tests of alternative harvest methods and drying temperatures and their effects on photoprotective compounds as well as components of the antioxidative defence systems.

For harvesting purposes, the culture broth was distributed to two times five 50 mL centrifuge tubes (45 mL test volume in duplicates) per species after 336 h. The control assays were centrifuged, the supernatants discarded, and the biomasses directly used for biochemical analysis, whereas the other five assays were used for the different flocculants. Sodium hydroxide (NaOH_2), Iron (III) chloride (FeCl_3), and chitosan (poly-(D)glucosamine) (PG) were utilized in form of stock solutions. Stock solutions of 0.5 M NaOH and $10 \text{ g} \cdot \text{L}^{-1} \text{ FeCl}_3$ were prepared in deionized water. For chitosan, $5 \text{ g} \cdot \text{L}^{-1}$ of stock solution was prepared in 0.01 M HCl . NaOH was applied at pH 8, 9 and 10 after pretesting

(data not shown). A series of test experiments were carried out to determine the minimum dosage of flocculant required for induction of flocculation in both tested species (cf. Figure 37). Jar test experiments were carried out in a volume of 100 mL. During addition of the flocculant, the cyanobacteria suspensions were intensively mixed (350 rpm) for 10 min, followed by gentle mixing (250 rpm) for 20 min (Vandamme et al. 2012). The suspensions were subsequently allowed to settle for 30 min. The supernatant was sampled in the middle of the clarified zone and absorbance was measured at 750 nm. The separation efficiency η_a was calculated as:

$$\eta_a = \frac{OD_i - OD_f}{OD_i} \times 100$$

in which OD_i is the absorbance before flocculation and OD_f is the absorbance after flocculation and settling.

After the optimization experiments, assays were incubated for 6 h at 4°C in darkness. The supernatants were decanted and the remaining cell numbers in the supernatant determined under the microscope. The biomasses were weighted and used in the biochemical analysis as described in 3.5, focussing on MAAs (c.f. 3.5.1.1.1) scytonemin (covered by the alkaloid screening c.f. 3.5.4), sulfated polysaccharides (3.5.1.4), flavonoids (3.5.2.1.2), phenolic compounds (3.5.2.1.6), and scavenging activity (DPPH, 3.5.3.1).

3.2.3.2 Effects of Drying Temperatures and Storage Lengths

The identical set up, species and parameter were used during the experiments as described in 3.2.3.1, focussing explicit on MAA, scytonemin and sulfated polysaccharide concentrations. After 336 h the culture broths were distributed as described in paragraph 3.2.3.1, cells were harvested by centrifugation, the supernatant discarded and the biomasses dried at five different temperatures (35, 45, 60 and 70°C) in aluminium trays for 24-64 h. As control crude biomass samples were used. After drying the biomasses were weighted and used for biochemical analysis as described in 3.2.4.1. The effects of different storage length on MAA concentrations prior to the extraction were also tested. Two times 45 mL samples from the experiment were kept frozen for 7, 21, 56 and 168 days, utilizing a freezer ($63 \pm 12^\circ\text{C}$) and subsequently used for biochemical analysis.

3.2.4 Experiments in 100 L Photobioreactors (PBRs)

To gain more biomass for further biochemical analysis and to test if an up-scale of the UV equipment might be successful in terms of high yields of UV protective compounds, further experiments in photobioreactors (PBRs) became necessary. In the following bubble column PBRs, made from UV transparent ACRYL (KUS-Kunststofftechnik, Recklinghausen, Germany) were chosen.

3.2.4.1 Conventional Bubble Column PBRs

The handling and optimization experiments were conducted in two 100 L bubble column PBRs (\emptyset 400/390 mm, length 1000 mm, Fig. 28), using *Synechococcus* I [9] and II [10, Table 1] in parallel. The up scales were identical for both species and included the following capacity steps: 4 x 2 L (Fig. 30E), 4 x 5 L (Fig. 30B, D), 40 and 80 L. The latter two steps took already place in the PBRs (Fig. 30A), using a temperature of $17 \pm 2^\circ\text{C}$ and a light to dark cycle of 12:12 hours during all steps of the upscales and the

following experiments. The trials started by filling 20 L fresh BG11 culture medium into each PBR and replace the standard illumination by UV-light equipment, utilizing for each reactor an Exo Terra® Dual Top Canopy PT2233, 90 cm (Rolf C. Hagen Inc., Montreal, Canada) (cf. Fig. 31 for the light spectrum). During five runs two different linear fluorescent bulbs (PT2162 Repti Glo 5.0/T8 and PT2172 Repti Glo 10.0/T8, both 75 cm, 25 W) were employed. In addition, two distinct semi-continuous culture conditions (exchange of 30 L medium and addition of nutrients for 30 L medium both in weekly intervals) versus batch culture as well as urea as NaNO_3 replacement were tested. Apart from the first trial which lasted 672 h, the standard length for each experiment was 504 h. Samples were taken at $t=0$, $t=168$ h, $t=336$ h and $t=504$ h (if applicable at $t=672$ h, but not considered in the results part) and immediately processed as described in 3.4 (lyophilisation time varied between 23.5 and 48 h). In addition, sub samples from each assay were used to determine the growth (3.3).



Figure 30. Up scales, comprising different volumes of 2 L and 5 L flasks and 5 L bubble columns (B, D, E) as well as experiments in the two 100 L PBRs (A, C).

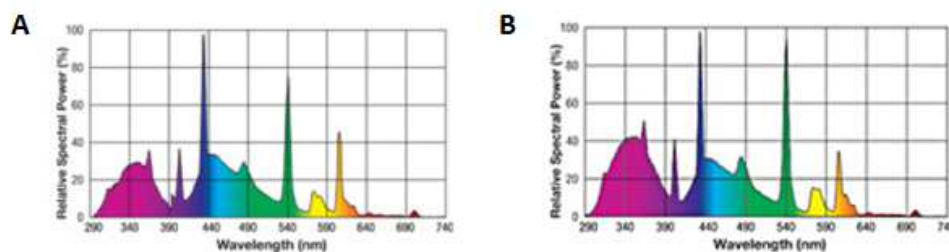


Figure 31. Spectra of the two linear fluorescent bulbs from Exo Terra® used in the experiments in 100 L PBRs A) PT2162 Repti Glo 5.0/T8 and B) PT2172 Repti Glo 10.0/T8, 25 W.

During the first experiment it became clear that particularly the MAA analysis needed basic improvements to monitor the compound accumulation in the cells over time and was therefore adapted to a fast testing method for MAA presence (cf. 3.5.1.1.2). All further biochemical analysis followed the protocols given in 3.5, focussing on MAAs (c.f. 3.5.1.1.1 and 3.5.1.1.2), scytonemin (c.f.

3.5.4), sulfated polysaccharides (3.5.1.4), selected components of the antioxidative defence system (flavonoids 3.5.2.1.2, phenolic compounds 3.5.2.1.6), and scavenging activity (DPPH, 3.5.3.1).

3.2.4.2 Internally Illuminated Bubble Column PBR

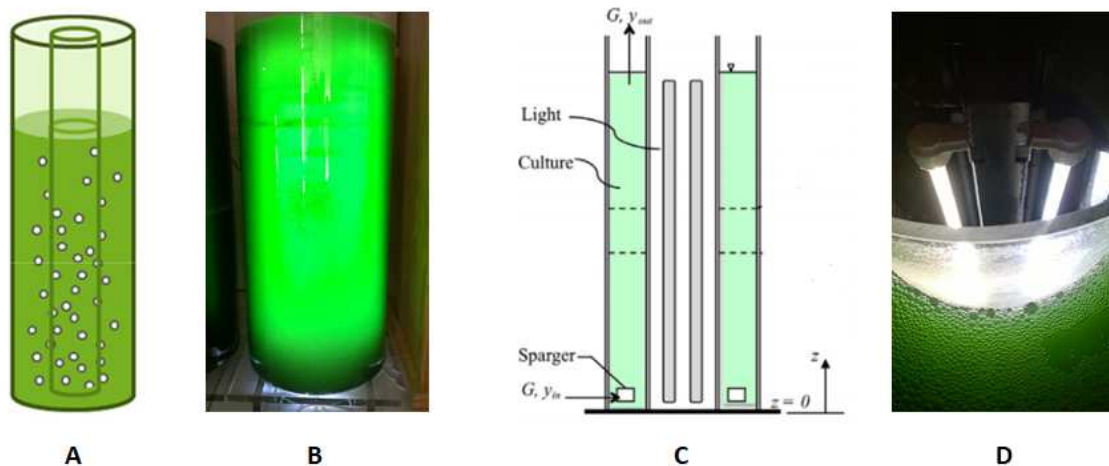


Figure 32. Bubble column PBR with annular design in overview (A, B), schematic illustration of the functional elements (C) and view on the internal illumination (D). Measurements outer cylinder: \varnothing 400/390 mm, L = 1000 mm, inner cylinder: \varnothing 200 mm, L = 1000mm.

To optimize the penetration and evenness of the UV-light reaching the cells, including necessary air ventilation for cooling, a bubble column PBR with annular design was chosen (Fig. 32). The cyanobacteria culture was placed in the space between the inner cylinder and the outer cylinder as illustrated in Figure 30B. The bottom plate in the space containing the culture was provided with four sparger for CO₂ and oxygen supply which were connected to a pump (HAILEA ACO-9720, 20W, 30 L/min). An additional sparger was inserted in the bottom plate of the inner cylinder for cooling the UV bulbs with air to prevent overheating. As UV light supply a light controller (Exo Terra® PT2235) equipped with two linear fluorescent bulbs (PT2162 ReptiGlo 5.0/T8, 60 cm, 20W; for spectrum see Fig. 31A) was utilized. The upscale of the model organism *Synechococcus* II [10] was conducted as described in 3.2.3.1. The experiment ran for 504 h. Measurements were conducted daily (e.g. chlorophyll a), and samples were taken, processed and compound concentrations analysed in order to monitor closely the accumulation of UV protective substances such as MAAs (c.f. 3.5.1.1.1 and 3.5.1.1.2), scytonemin (3.5.1.2), sulfated polysaccharides (3.5.1.4), selected components of the antioxidative defence system (flavonoids 3.5.2.1.2, phenolic compounds 3.5.2.1.6, enzymes 3.5.2.2), and scavenging activity (DPPH 3.5.3.1).

3.3 Determination of Growth

Growth was monitored by conducting cell counts and by measuring dry matter. Counting of cells during the experiments were performed under a light microscope (BX51, Olympus Corporation, Tokyo, Japan / Axiophot, Carl Zeiss AG, Oberkochen, Germany), using a Neubauer improved counting

chamber with 0.1 mm depth (LO Laboroptik GmbH, Germany). During the long-term experiments, cell counts were conducted every second day. Only cells were counted, which exhibited red fluorescence under ultraviolet light. At least 500 cells were counted in each sample at a 400× magnification. The specific growth rate (μ) was calculated with the following equation:

$$\mu = \frac{\ln_{c_1} - \ln_{c_0}}{t_1 - t_0}$$

where c_1 and c_0 are the number of cells at time t_1 and t_0 .

Dry cell weight (DCW) or dry weight was measured in triplicates by using 0.45 μm cellulose acetate filters (WHA10404006 Whatman®). Filters were pre-dried for 10 min at 105°C to remove any moisture. Subsequently 40 mL of the algal culture was filtered and dried for 24 h at 70°C and then weighed to measure the dry weight, then expressed as grams per litre.

3.4 Harvest and Processing

For the extraction of crude biomass, 10 mL of algal culture was centrifuged at 8000× g for 10 min at 4°C (Heraeus Biofuge Primo R, Thermo Fisher Scientific GmbH, Dreieich Germany), and the pellet was purified by washing twice with double-distilled water. This sample was used for extracting different antioxidants, and the amounts of enzymatic and non-enzymatic antioxidants as well as other biochemical parameters were determined, including protein, chlorophyll a, carbohydrates, and lipids. In addition, this method was used as standard method in all experimental controls prior to analysis.

For MAA analysis, harvested cells were washed twice with distilled water and processed by lyophilization (23-72 h; Modulyo desk top lyophilisator 3981, Edwards High Vacuum Int, Sussex, England). This step was replaced by drying of the biomass in a dehydrator (Zociko Dehydrator, model no. FDTHQQZ).

3.5 Biochemical Analysis

3.5.1 Sunscreen Compounds

3.5.1.1 Mycosporine-like amino acids (MAAs)

3.5.1.1.1 LC-Analysis

MAAs were identified and analysed according to the method of Karsten et al. (2009). Briefly, three replicate samples were extracted for 1.5–2 h in screw-capped centrifuge vials filled with 1 mL 25% aqueous methanol (v/v) and incubated in a water bath at 45°C. After centrifugation at 5,000 g for 5 min, 700 L of the supernatants were evaporated to dryness under vacuum. Dried extracts were re-dissolved in either 700 L 100% methanol, distilled water or the HPLC eluent [2.5% aqueous methanol (v/v) plus 0.1% acetic acid (v/v) in water]. After centrifugation at 5,000 g for 5 min the extracts were passed through a 0.2 μm membrane, and afterwards analysed with an Agilent HPLC system. MAAs in

all extracts were one after another separated on three different stainless-steel HPLC columns. The mobile phase was always 2.5% aqueous methanol (v/v) plus 0.1% acetic acid (v/v) in water. MAAs were detected online with a photodiode array detector at 330 nm, and absorption spectra (290–400 nm) were recorded each second directly on the HPLC-separated peaks. Identification was done by comparison of spectra and retention times with databases and literature. Quantification was made using the molar extinction coefficients given in Karsten et al. (1998).

3.5.1.1.2 Spectrophotometric Analysis

For screening purposes during the experiments, the MAAs were extracted from the crude biomass in 100% HPLC-grade methanol by overnight incubation at 4°C. After extraction, aliquots were centrifuged (8000x g, 5 min), and supernatants were transferred to new Eppendorf tubes and subjected to evaporation at 38 °C (dehydrator). The residues were redissolved in 600 µL sterile double-distilled water followed by the addition of 100 µL chloroform with gentle vortexing. After centrifugation (8000 g, 5 min), the photosynthetic pigment-free uppermost water phase was transferred carefully into new Eppendorf tubes and filtered through sterilized microcentrifuge syringe-driven filter (13 mm, PVDF, 0.22 µm, Jet Biofil) to obtain the partially purified MAAs. Spectroscopic analysis between 200 and 400 nm was performed using a UV/Vis spectrophotometer (ATI Unicam 5625 UV/VIS Spectrometer, Richmond Scientific Ltd., Chorley, United Kingdom). The peaks were analysed with the software provided by the manufacturer.

3.5.1.2 Scytonemin

For extraction of scytonemin, samples of harvested cyanobacterial biomass were dried and grounded with a mortar and pestle. Cells were suspended in 100% acetone and kept overnight at 4°C. After centrifugation, samples were filtered through Whatman no. 1 filter paper, and absorbance-specific filtered contents were measured on a UV-VIS spectrophotometer (ATI Unicam 5625 UV/VIS Spectrometer, Richmond Scientific Ltd., Chorley, United Kingdom). The absorbance of the filtrate was measured at 384 nm (scytonemin maximum), 490 nm (pooled carotenoid) and 663 nm (chlorophyll a). The value of the absorbance at 750 nm was subtracted from all measured absorbances. The cellular scytonemin content was calculated using the trichromatic equation:

$$A_{384}^*(\text{Scyt}) = 1.04A_{384} - 0.79A_{663} - 0.27A_{490}$$

where A_{λ} is the measured absorbance at λ . In the absence of an absorption coefficient for scytonemin, the unit represents the absorbance of 1 mg dry weight of material extracted in 1 mL acetone in a cuvette with 1 cm path length. Specific content is expressed as ' A_{λ} mg⁻¹'. During the experiments, this method was replaced by the protocol given by Scholz & Liebezeit (2006) (c.f. 3.5.4).

3.5.1.3 Sporopollenin

Sporopollenin is the only natural biopolymer resistant to the action of acetolysis, therefore, the preservation of cell walls in the preparation after performance of acetolysis shows the presence of sporopollenin (Dickinson & Bell 1973). The cells were washed in succession with chloroform: methanol mixture (1:2, by volume), 1 N. NaOH, 0.1 M sodium acetate, and icy acetic acid. The mixture for acetolysis (acetic anhydride: concentrated sulfuric acid, 9:1 by volume) was then added to the cells in

Eppendorf tubes, placed in a boiling water bath (90-95°C) for 10 min and then cooled. During the treatment, the conditions of preparations was controlled under a microscope, the results of treatment were registered by photomicrography using the digital photo camera Infinity 1.

3.5.1.4 Sulfated Polysaccharides (sPS)

Dissolved polysaccharides were collected from the medium by centrifugation. Subsequently, the supernatant was dialyzed to remove salts, frozen, and lyophilized. The resulting powder was used for the following analyses.

The crude SPs extracts were estimated for their chemical composition. Total sugars (TSs) content was determined by the phenol-sulfuric acid analysis using galactose as standard (Dubois et al. 1956) using a spectrophotometer (ATI Unicam 5625 UV/VIS Spectrometer, Richmond Scientific Ltd., Chorley, United Kingdom) at 490 nm. After acid hydrolysis of the soluble polysaccharides (1 mL of HCl for 5 h at 100°C), free sulfate (FS) was measured by the BaCl₂/gelatine method (Dodgson & Price 1962). Contaminant proteins (CPs) content was measured by Bradford's method (1976), using bovine serum albumin as the standard. Sulfate content was determined after hydrolysis of the polysaccharide sample with 2 M HCl for 2 h at 100°C, according to the method of Terho & Hartiala (1971).

3.5.2 Antioxidant Defense System

3.5.2.1 Non-Enzymatic Constituents

3.5.2.1.1 Ascorbate

For estimation of ascorbic acid, 1 g of the microalgae sample was ground and homogenized in 5 mL of 4% trichloroacetic acid (TCA); the volume was made up to 10 mL with double-distilled water and centrifuged at 2000× g for 10 min. The supernatant was treated with activated charcoal or bromine. Dehydroascorbic acid reacts with 2, 4-dinitro phenyl hydrazine to form osazones, which dissolve in sulphuric acid to give an orange coloured solution whose absorbance was measured spectrophotometrically at 540 nm (Roe & Kuether 1943).

3.5.2.1.2 Flavonoids

Total flavonoid content was determined by a calorimetric method (Zishen et al. 1999). Approximately 0.5 mL of each extract with the concentration of 100 µg/mL was added with 1 mL 100 % methanol to make up to 3 mL. The mixture was left for 5 min after the addition of 0.4 mL distilled water and 0.3 mL of 5% sodium nitrite (NaNO₂). Approximately 2 mL of 1 M sodium hydroxide (NaOH) and distilled water was added to make up to 10 mL after 0.3 mL of 10% aluminium chloride (AlCl₃) was added and left at room temperature for 1 min. The mixture was left for 15 min after being shaken. The absorbance was measured at 510 nm and the concentrations of total flavonoids were determined as quercetin equivalents per mg of extracts, QE/mg.

3.5.2.1.3 Carotenoids

First, 4 mL of crude liquid algae samples were extracted with 5 mL of acetone 80% (acetone/water: 80/20, v/v), and were sonicated for 15 min. The extraction was carried out in the dark at 4°C. The

Lichtenthaler (1987) equation was used to calculate the concentration of carotenoid and chlorophyll contents.

$$\begin{aligned}\text{Chlorophyll (a)} &= (12.25 A_{663.2}) - (2.79 A_{646.8}) \\ \text{Chlorophyll (b)} &= (21.5 A_{646.8}) - (5.10 A_{663.2}) \\ \text{Total Carotenoids} &= (1000 A_{470}) - (1.82 \text{ Chlorophyll (a)}) - (85.02 \text{ Chlorophyll (b)}) / 198\end{aligned}$$

The absorbance was acquired at λ_{470} for carotenoids, and $\lambda_{663.2}$ nm and $\lambda_{646.8}$ nm for chlorophyll. The total carotenoids are expressed by mg/g and mg/mL for freeze-dried algae and for crude liquid algae (fresh algae), respectively.

3.5.2.1.4 Glutathione

For the estimation of reduced glutathione, 1 g of sample was homogenized to a 20% homogenate using 5% TCA. The precipitated protein was centrifuged at 1000×g (4°C) for 10 min. The homogenate was cooled on ice and 0.1 ml of supernatant was used for the estimation of reduced glutathione. Reduced glutathione was measured by reacting it with 5, 5'-dithio-bis 2-nitro benzoic acid (DTNB) and the compound formed was read spectrophotometrically at 412 nm (Moron et al. 1979).

3.5.2.1.5 Tocopherols

Tocopherol was estimated using Emmerine–Engel reaction, which is based on the reduction of ferric to ferrous ions by tocopherol, which then forms a red colour with 2,2 dipyridyl. Tocopherols were first extracted with xylene and was read at 460 nm (Rosenberg 1992).

3.5.2.1.6 Phenolic Compounds

Polyphenols were extracted from the microalgal culture using 80% ethanol. Total phenol estimation was carried out using the Folin–Ciocalteu reagent. Phenols react with phosphomolybdic acid in Folin–Ciocalteu reagent in alkaline medium and produce a blue coloured complex (Molybdenum blue) and the colour intensity was measured at 650 nm (Malik 1980).

3.5.2.2 Antioxidant Enzyme Activities

3.5.2.2.1 Superoxide dismutase (SOD, EC1.15.1.1)

Microalgal cells were homogenized in 0.5 M phosphate buffer (pH 7.5) and centrifuged at 10,000 x g for 10 min at 4°C. To the supernatant, added 1.5 mL Na₂CO₃ (1 M), 200 mL methionine (200 mM), 100 mL nitroblue tetrazolium (NBT) (2.25 mM), 100 mL EDTA (3 mM), 100 mL riboflavin (60 μM) and 1.5 mL phosphate buffer (pH 7.8, 0.1 M) to determine the inhibition of NBT. The absorbance was recorded at 560 nm and one unit of SOD per milligram of protein was defined as the amount causing 50% inhibition of photochemical reduction of NBT (Dhindsa et al. 1981).

3.5.2.2.2 Catalase (CAT, EC 1.11.1.6)

For catalase assay, 50 mg biomass was homogenized in 2 mL phosphate buffer (0.5 M, pH 7.5), centrifuged at 12,000 rpm at 4°C for 30 min and the supernatant was collected. A reaction mixture containing 1.6 mL phosphate buffer (pH 7.3), 100 μL EDTA (3 mM), 200 μL H₂O₂ (0.3%) and 100 μL supernatant was taken in a cuvette and CAT activity in supernatant was determined by monitoring the disappearance of H₂O₂, by measuring a decrease in absorbance at 240 nm against a blank of same reaction mixture without H₂O₂ (Nakano & Asada 1981).

3.5.2.2.3 Ascorbate peroxidase (APX, EC 1.11.1.1)

For analysis of ascorbate peroxidase activity, 100 μL of microalgal supernatant was added with 1 mL phosphate buffer (pH 7.3), 100 μL EDTA (3 mM), 1 mL ascorbate (5 mM) and 200 μL H_2O_2 (0.3%). The reaction was followed for 3 min at a wavelength of 290 nm against a blank of same reaction mixture without H_2O_2 (Nakano & Asada 1981).

3.5.2.2.4 Glutathione reductase (GR, EC 1.6.4.2)

The method of Smith et al. (1988) was used to assay GR activity spectrophotometrically by following the reduction of Ellman's reagent (5,5'-dithiobis-(2-nitrobenzoic acid), DTNB). The reaction mixture contained 1.0 mL 200 mM potassium phosphate (pH 7.5) with 1 mM EDTA, 0.5 mL 3 mM DTNB in 10 mM phosphate buffer, 0.25 mL H_2O , 0.1 mL 2 mM NADPH, 0.05 mL GR standard or algal sample (kept at 47°C), and 0.1 mL 2 mM glutathione disulphide (GSSG). The components were added in the order listed to a 4.5-mL cuvette and the reaction was initiated by the addition of GSSG. Temperature was maintained at 25°C. The increase in absorbance at 412 nm was monitored using a Shimadzu UV-120-02 spectrophotometer. The reaction rate was calculated from the linear portion of a standard curve and expressed as U/mg protein.

3.5.3 Scavenging Activity Assays

The extraction procedure included three steps, each with different solvents (hexane, dichloromethane, and methanol). In the first step, two grams of freeze-dried samples was soaked in 200 mL of solvent and shaken for 24 hours, prior to filtration. The filtrate was suspended in 200 mL of the next solvent, which was treated as described above. The process was repeated for the last solvent. After extraction, all solvents were pooled, and kept at -18°C until further analysis.

3.5.3.1 2,2-Diphenyl-1-picrylhydrazyl-free-radical-scavenging activity (DPPH)

Stable DPPH radicals were subject to scavenging by the components of extracts, using a modified method proposed by Brand-Williams et al. 1995. A 2 mL fraction of extract was mixed thoroughly with 2 mL freshly prepared 3×10^{-5} M DPPH solution in dimethyl-sulfoxide (DMSO). The reaction mixture was incubated for 1 h, and the absorbance of the supernatant was measured at 517 nm using an UV-VIS spectrophotometer.

3.5.3.2 Superoxide-anion-scavenging assay (SAS)

The superoxide-anion-scavenging effect was tested following Nagai et al. (2003). A reaction mixture consisting of 0.48 mL of sodium carbonate buffer (pH 10.5) 0.05 M, 0.02 mL xanthine 3 mM, 0.02 mL EDTA 3 mM, 0.02 mL BSA 0.15%, 0.02 mL NBT (nitro blue tetrazolium salt) 0.75 mM, and 0.02 mL extract was incubated at 25 °C for 10 min. Then, the reaction was started by adding 6 mU xanthine oxidase maintaining 25°C temperature conditions. The reaction was stopped by adding 0.02 mL CuCl_2 6 mM after 20 min. The absorbance was measured at 560 nm.

3.5.3.3 Hydrogen-peroxide-scavenging activity (HPS)

Hydrogen-peroxide-scavenging activity was determined according to Rice-Evans et al. (1995). A sample comprised of 80 μL extract, 100 μL PBS (0.1 M, pH 5.0), and 20 μL H_2O_2 (10 mM) prepared in a

Eppendorf cap and incubated at 37°C for 5 min. Thereafter, 30 µL ABTS (2,2-azinobis (3-ethyl-benthiazoline)-6-sulfonic acid) (1.25 mM) and 30 µL peroxidase (1-unit x mL⁻¹) were added. The absorbance at 405 nm was recorded after incubating the mixture at 37°C for 10 min.

3.5.3.4 Ferric-reducing antioxidant power assay (FRAP)

The FRAP assay was carried out as suggested by Omidreza et al. (2005), with a modified concentration. FRAP reagents were freshly prepared for each measurement by mixing 2,4,6-tripyridyl triazine (TPTZ) 10 mM with HCl 40 mM, acetate buffer (0.3 M, pH 3.6) and ferric chloride 20 mM in double-distilled water in a ratio 1:10:1. A 180 µL volume of pre-warmed FRAP reagent (37°C) was added along with 20 µL of the sample solution and incubated at 37°C for 30 minutes, prior absorbance measuring at 593 nm.

3.5.4 Screening for Compound Classes

Table 2. Methods used during the phytochemical screenings.

Compound group	Extraction Solvent	Calibration standard	Method	Ref.
Alkaloids	EtOH (99%)	Piperine C ₁₇ H ₁₉ NO ₃	Mayer's and Wagner's reagent*	Scholz & Liebezeit (2006)
Saponins	EtOH (99%)	Saponin S4521	Frothing test	Scholz & Liebezeit (2006)
Tannins	EtOH (99%)	Tannic acid C ₇₆ H ₅₂ O ₄₆	Gelatine-Saltblock test	Scholz & Liebezeit (2006)

For the phytochemical screening, the harvested biomass of each species was weighted, equalized to a final weight of 2 g fresh weight and sonicated 3 times for 2 min under cooling conditions (Branson 2800, Emerson Electric Co, Ferguson, Missouri, United States). The homogenized biomass was then extracted in an all-glass filtration chamber (1 h), using 50 mL ethanol (99.5%) following the methods referenced in Table 2.

3.5.5 Gross Compositions

3.5.5.1 Chlorophyll *a*

Initially, chlorophyll was extracted with 90% acetone over 24 h in darkness at -80°C. Chlorophyll *a* was determined spectrophotometrically (Shimadzu UV-vis spectrophotometer UV-1603, Kyoto, Japan) and corrected for phaeopigments, according to Lorenzen (1967).

From 2018 onwards, a probe was used for chlorophyll *a* quantification (TriLux fluorometer with a CTG Hawk which powers and displays data, Chelsea Technologies Ltd, West Molesey, United Kingdom).

3.5.5.2 Proteins

Protein was measured using the Lowry method as described by Herbert et al. (1971) with bovine serum albumin as a standard. In brief, 5 mL 1.0 N NaOH was added to the biomass aliquot and incubated for 5 min in a boiling water bath (95°C, Typ 1083, GFL mbH, Burgwedel, Germany). After cooling, 2.5

mL of the reactive mixture (5% Na₂CO₃ + 0.5% CuSO₄ x 5 H₂O in 1.0% Na-K-Tartarate; ratio 25:1 v/v) were added and incubated for 10 min at room temperature. This was followed by the addition of 0.5 mL Folin-phenol reagent (1.0 N) and incubation for another 15 min. After centrifugation (Omnifuge 2.0 RS, Heraeus Sepatch, Osterode, Germany), the intensity of the resulting blue colour was determined at 650 nm.

3.6 Statistical Analysis

Measures were carried out in triplicate ($n = 3$), and the results are given as mean values and standard deviations. The results were statistically analysed using a one-way ANOVA with a statistical difference of 5% and the Tukey TSD test of the IBM SPSS software version for multiple comparisons.

4. Results

4.1 First Screening for Photoprotective Compounds and Scavenging Activities

Table 3. Results from the first screening of 50 microalgae and cyanobacteria species listed in Table 1 (pages 26-27). Data depicted in red were obtained from the second experiment.

No	Growth μ {day ⁻¹ }	Sunscreen compounds				Antioxidant Defence System						Scavenging Activities				Further compounds					
		MAAs	Scytonemin	Sporopollenin	SPs	Non enzymatic Constituents			Enzymes												
					Ascorbate	Flavonoids	Carotenoids	Glutathione	Tocopherols	Phenolics	SOD	CAT	APX	GR	DPPH	SAS	HPS	FRAP	Alkaloids	Saponins	Tannins
Cyanobacteria																					
1	1.393	+			+	++		+	+	++	+	+	+	+	+	+	+	+			++
2	1.36	+			+	++		+	+	++					+						++
3	1.73	+			+	+++	+	+	++	+++	+	+	+	+	++	+	+	+			+
4	1.39	+			+	++	+	+	+	+++	+				+	+	+				
5	1.46	+				++	+	+	+	+++	+	+			+						
6	1.33	+	+		+	++		+	+	+++	+	+			+	+					+
7	1.31	+				++	+	+	+	+++	+	+			+						
8	1.42	+				++	+	+	+	+++	+	+	+	+	+						+
9	1.69	+	+		+	+++	++	+	++	+	+	+	+	+	+	+	+	+	+		+
10	1.58	+	+		+	++		+	+	+	+		+	+	+						+
Chlorophyceae																					
11	0.49	+	+		+	++	++	++	+	+	+	+			+						+
12	0.53	+			+	+	++	++	++	+	+	+			+						
Rhodophyceae																					
13	0.22				+	+	++	++	+	+	+	+	+	+	+	+	+	+			+
14	0.23				+	+	++	++	+	+	+	+			+	+					
Prymnesiophyceae																					
15	0.18				+	+	+	+	+	+	+					+					
16	-0.05					+	+	+	+	(+)	+	+			+						

Dinophyceae

17	0.19 0.13	+	+	+	++	++	+	++		+		+					+
18		+	+	+	+	+	+	++	+	+	+	+	+	+	+	+	++

Bacillariophyceae (diatoms)

19	0.07 0.11 0.05 0.14 0.13 0.09 0.06 0.06 0.03 0.04 0.05 0.15 0.15 0.12 0.14 0.09 0.08 0.07 0.08 0.08 0.03 0.08 0.1 0.13 0.1 0.08 0.09 0.05 0.06 0.1		+	+	+	+	+	++		+		+	+				+	
20		+	+			+	+	+	+	+	+	+	+	+	++		+	
21		+	++		+	+	+	++	+	+		+	+	+	+		+	
22		+	++		+	+	+	++	+	+	+	+	+	+	+		+	
23		+	+	+	+	+	+	+	+	+		+					+	+
24		+	+			+	+	+	+	+	+		+	+	+	++		
25		+	+	+	+	+	+	+	+	+		++	+	+	+			
26		+	+			+	+	+	+	+		+	+	+	+			
27		+	++			+	+	+	+	+	+		+	+				
28		+	+++	+	+	+	+	+	+	+		+	+	+		++		
29		+	+	+	+	+	+	+	+	+		+	++	+				+
30			+	+	+	+	+	+	+	+		+		+	+			
31			+	+	+	+	+	+	+	+		+						
32		+	++	+	+	+	+	+	+	+	+		+					
33			+		+	+	+	+	+	+		+	++	+	+			+
34		+	++		+	+	+	+	+	+		+	+	+	+			+
35		+	++		+	+	+	+	+	+	+		++		+			
36		+	+	+		+	+	+++		+	+	+	+	+				+
37		+	+			+	+	+	+	+		+	+	+	+			
38			++			+	+	+	+	+		+		+		++		
39		+	+	+		+	+	+	+	+		+	+	++	+	+		+
40			+	+		+	+	+	+	+		+	+		+			
41			+++	+		+	+	+	+	+		+						+
42			+		+	+	+	(+)	+	+		+	+	+	+			
43		+	+		+	+	+	+	+	+		+		++	+			
44			++		+	+	+	+	+	+		+	+	++	+			
45		+	+		+	+	+	++		+	+	+				++		
46		+	+		+	+	+	+	+			+	+		+			
47		+	+		+	+	+	+	+			++	+		+			+
48		+	+		+	+	+	+	+	+		+	+	+	+			
49		+	+		+	+	+	+		+		+			+			
50		+	+	+	+	+	+	+		+		+						

The results of the first screening for photoprotective compounds and scavenging activities in 50 selected species were, apart from the presence of ascorbate, carotenoids, glutathione, and tocopherols, highly variable and showed group as well as species specific adaptations in response to UV exposure (Table 3, in the following numbers behind species names in square brackets refer to the numbers in Tables 1 and 3). Ascorbate, carotenoids, glutathione, and tocopherols were detected in all tested species although distinct differences regarding the compound concentrations became visible (+ = present in low concentration; (+) = test not conclusive; ++ = medium concentration; +++ = strong concentration). Also, phenolic compounds were present in all species, except the prymnesiophyte *Emiliana huxley* [16], which deceased during the UV experiments in both runs (negative growth rate μ in comparison to the control, c.f. Table 3). Above average concentrations of phenolic compounds were recorded in assays from cyanobacteria, being the highest in *Synechocystis I* [3], *Synechocystis II* [4], *Merismopedia sp* [5], *Phormidium autumnale* [6], *Chroococcus turgidus* [7], and *Spirulina subsalsa* [8].

From the four sun protective compounds, sulfated polysaccharides (sPS) were the most common found in the present study, being detected in 76% of the tested species, as of which *Synechocystis I* [3], *Synechococcus I* [9], *Cylindrotheca closterium* [28], and *Trachyneis aspera* [41] showed the highest sPS concentrations. Furthermore, the cyanobacteria specific indole alkaloid scytonemin was only detectable in three of the tested species, namely *Phormidium autumnale* [6], *Synechococcus I* [9], and *Synechococcus II* [10], whereas the biopolymer sporopollenin was merely observed in one chlorophyte: *Dunaliella tertiolecta* [11]. Analysing all 50 species for the presence of MAAs after the first exposure experiments was completely unsuccessful. In contrast, in the repetition run, utilizing only 20 species and the exact same experimental design as before (c.f. 3.2.1), 12 species showed at least traces of the compound and qualified them therefore for further inducement experiments. From these 20 species, all cyanobacteria [1-10] were tested positive for the presence of MAAs as well as both chlorophytes, namely *Dunaliella tertiolecta* [11] and *Chlorella salina* [11].

Regarding the enzymatic components of the antioxidative defense system, such as superoxide dismutase (SOD), catalase (CAT), ascorbate peroxidase (APX), and glutathione reductase (GR), a highly heterogeneous distribution of the activities among species and species groups was recorded. Only 18% of the 50 tested species showed activities of all four enzymes tested during this first screening: *Nodularia sp.* [1], *Synechocystis I* [3], *Spirulina subsalsa* [8], *Synechococcus I* [9], *Porphyridium marinum* [13], *Alexandrium tamarense* [18], *Coscinodiscus wailesii* [20], *Navicula cancellate* [22], and *Amphora laevis var. laevis* [35]. From the four tested enzymes, SOD was the most abundant among the tested species (86%), followed by catalase (84%), glutathione reductase (36%) and ascorbate peroxidase (32%). Values varied between 0.02-159 U/mg protein for SOD, 0.05-176 U/mg protein for CAT, 0.01-114 U/mg protein for APX and 0.8-259 U/mg protein for GR, being the highest for individual representatives of the cyanobacteria such as *Spirulina subsalsa* [8], *Phormidium autumnale* [6], and *Synechococcus I* and *II* [9, 10].

The screening for scavenging activities of the tested species, using 2,2-diphenyl-1-picrylhydrazyl-free-radical-scavenging activity (DPPH), superoxide-anion-scavenging assay (SAS), hydrogen-peroxide-scavenging activity (HPS) and ferric-reducing antioxidant power assay (FRAP), showed for 92% of the species DPPH activities, being the highest for *Synechocystis I* [3], *Navicula perminuta* [25] and *Diploneis didyma* [47]. In contrast, all other scavenging activity assays were found to be far lower abundant among species than compared to the DPPH assay, ranging from 44% (HPS) over 66% (SAS) to 72%

(FRAP). In this context, the above average activities of *Nodularia sp.* [1], *Nodularia harveyana* [2], *Navicula directa* [24], *Cylindrotheca closterium* [28], *Cymbella minuta* [38] and *Cocconeis. placentula* [45] in the FRAP assay as well as of *Coscinodiscus wailesii* [20], *Cocconeis costata* [43] and *C. fasciolata* [44] in the HPS assay are noteworthy.

Finally, the screening for the presence of further compound classes showed some group specific characteristics. While tannin tests were negative for all tested species, sporadic saponin and alkaloid activities were observable. Alkaloids were detected in three cyanobacteria (*Phormidium autumnale* [6], *Synechococcus I* [9], and *Synechococcus II* [10]) and both dinoflagellates *Amphidinium carterae* [17] and *Alexandrium tamarense* [18], whereas saponins were only traceable in six diatoms (*Navicula clementis* [23], *Achnanthes borealis* [29], *Amphora acutiuscula* [33], *A. coffeaeformis* [34], *Gyrosigma fasciola* [36], *Pinnularia ambigua* [39] and *Diploneis didyma* [47]).

4.2 Induction of Photoprotective Compounds and Antioxidative Defense

Due to the promising results obtained from the first screening, fast growth and favourable handling characteristics, overall four cyanobacteria were chosen for the next step of the investigation: *Synechocystis I* and II, [3, 4]; *Synechococcus I* and II, [9, 10] in Table 1, focussing on the presence of MAAs, scytonemin, sulfated polysaccharides as photoprotective compounds, selected components of the antioxidative defense system (flavonoids, phenolic compounds, enzymes), and DPPH scavenging activity. The experimental designs for this part are described in 3.2.2, utilizing two different UV/PAR sets with three spectra in each set. The UV exposure time was varied as follows: 12: 12, 16: 8, 20: 4 and 8: 16 hours light to dark photoperiods. In addition, 24- and 72-hours continuous illumination were also tested. The results are presented in Figures 33-36.

Basically, all photoprotective compounds and components of the antioxidative defense system as well as the antioxidant activity increased in all tested UV treatments compared to the PAR control, independent of the exposure time. Comparing the presence and concentrations of sun protective compounds between the four cyanobacteria and the different treatments a highly diverse picture arises (Figs. 33A-36A). While sulfated polysaccharides (sPS) were the main photoprotective compound in *Synechocystis I* apart from the occurrence of a high sole scytonemin concentration in the 8 h UV I treatment ($0.181 \pm 0.009 \text{ mg} \cdot \text{g DW}^{-1}$), MAAs and scytonemin were mainly present in *Synechococcus I* and II besides sPS. Concentrations of sPS ranged in *Synechocystis I* from 0.016 ± 0.003 to $0.117 \pm 0.002 \text{ mg} \cdot \text{g DW}^{-1}$, being the highest in the 8 h UV II exposure (Fig. 33A). In *Synechocystis II*, sPS concentrations were in average significantly lower ($p \leq 0.05$) than compared to *Synechocystis I*. At least one MAA sample was tested positive in the 72 h UV I assay in *Synechocystis II* (Fig. 34A). It was not possible to identify the MAA (c.f. Table 4). Furthermore, scytonemin was present in the 16 h (UV I and II) and 20 h (UV I) assay. In all cases the concentrations of scytonemin were significantly lower than compared to the ones detected in *Synechocystis I*, ranging between 0.03 and $0.09 \pm 0.01 \text{ mg} \cdot \text{g}^{-1} \text{ DW}$. In contrast to all other tested cyanobacteria in this experimental series, the main response of *Synechococcus I* to the different UV/time treatments was scytonemin besides sPS, reaching highest concentrations in the 16 h (UV I), 20 h (UV I and II) and 8 h (UV I) assay (Fig. 35A). The in general significantly weaker responses of *Synechococcus I* to UV set II as well as the 24 and 72 h exposure to UV set I are noteworthy. SPS concentrations, which were in some cases the only sunscreen compound detectable in this species (e.g. 24 h UV I), ranged between 0.016 - $0.101 \pm 0.005 \text{ mg} \cdot \text{g DW}^{-1}$, being the highest in the 8 h exposure to UV II assay. MAAs were detected in 62.5% of the tested samples with

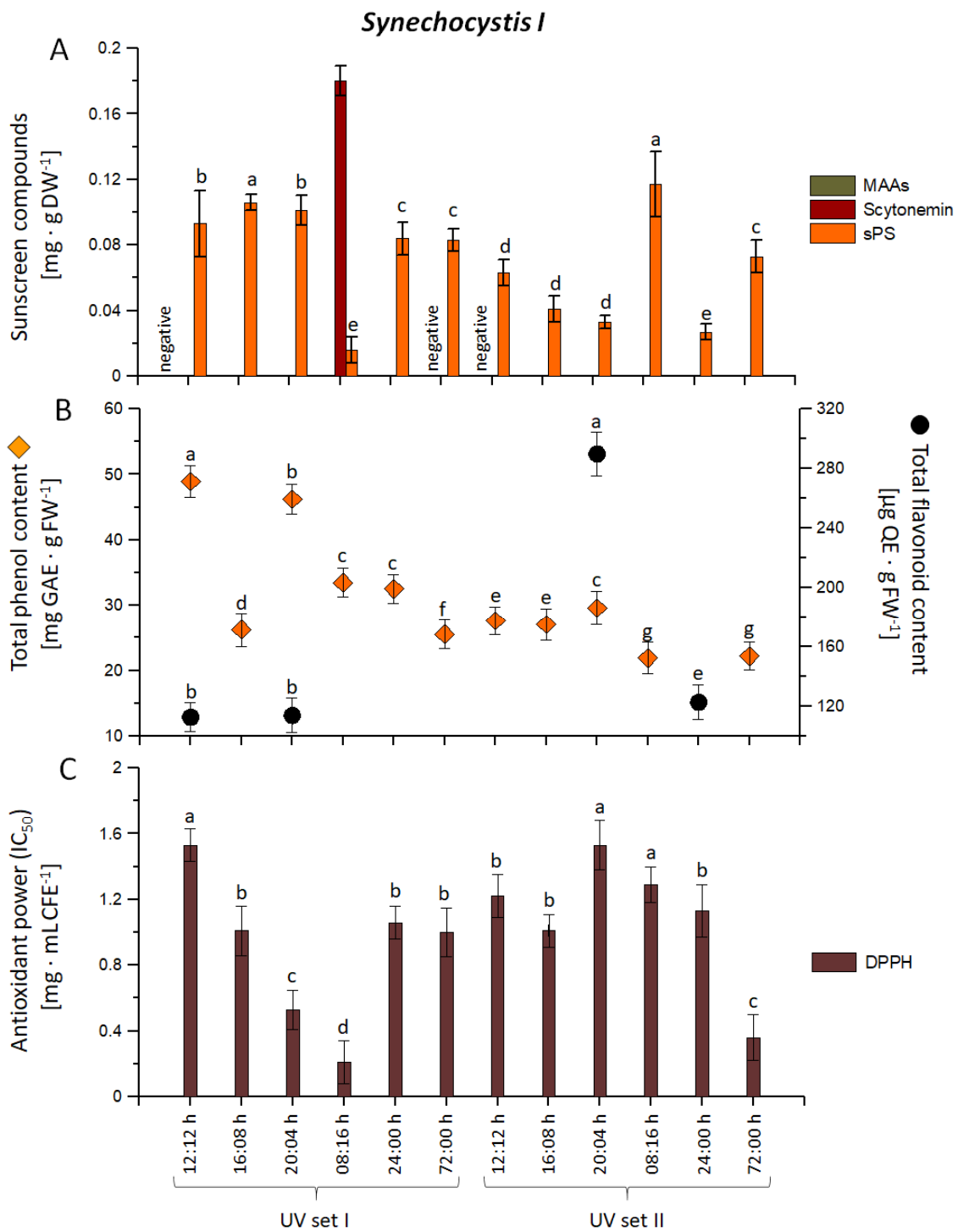


Figure 33. Results of the induction experiments using the coccoid cyanobacteria *Synechocystis I* (no [3] in Table 1)) and two different UV/PAR sets in combination with different exposure lengths. Depicted are the concentrations of mycosporine-like amino acids (MAAs), scytonemin, and sulfated polysaccharides (sPS) as sunscreen compounds (A), total phenol and flavonoid contents as part of the antioxidative defense system (B), as well as the IC₅₀ values of the antioxidant power of cell free extracts measured as 2,2-Diphenyl-1-picrylhydrazyl (DPPH) scavenging activity (C). Only positive values for the MAA concentration are depicted in Figure A. If tested and no concentration was detected the value is designated as “negative”. All other samples were not analysed for the presence of MAAs. Data are presented as means ± SD (n=3) and different letters indicate significant difference among treatments. The results of the control assay (PAR only) were: MAAs, Scytonemin: negative; sPS: 0.03 mg · g DW⁻¹; phenolic compounds: 3.6 µg QE · g FW⁻¹; flavonoids: negative; DPPH: negative.

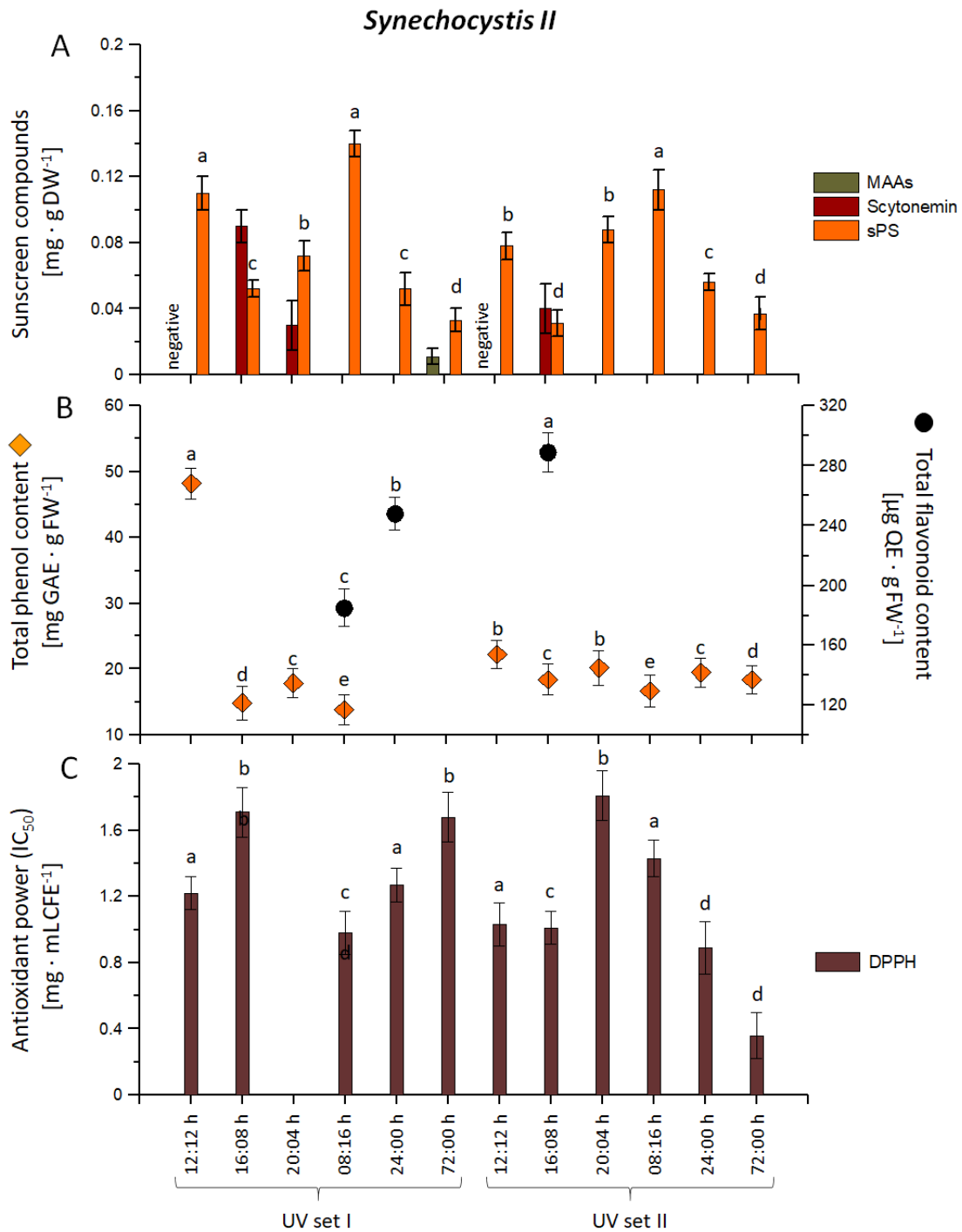


Figure 34. Results of the induction experiments using the coccoid cyanobacteria *Synechocystis II* (no [4] in Table 1) and two different UV/PAR sets in combination with different exposure lengths. Depicted are the concentrations of mycosporine-like amino acids (MAAs), scytonemin, and sulfated polysaccharides (sPS) as sunscreen compounds (A), total phenol and flavonoid contents as part of the antioxidative defense system (B), as well as the IC₅₀ values of the antioxidant power of cell free extracts measured as 2,2-Diphenyl-1-picrylhydrazyl (DPPH) scavenging activity (C). Only positive values for the MAA concentration are depicted in Figure A. If tested and no concentration was detected the value is designated as “negative”. All other samples were not analysed for the presence of MAAs. Data are presented as means ± SD (n=3) and different letters indicate significant difference among treatments. The results of the control assay (PAR only) were: MAAs: negative; scytonemin: 0.042 mg · g DW⁻¹; sPS: 0.036 mg · g DW⁻¹; phenolic compounds: 3.3 µg QE · g FW⁻¹; flavonoids: negative; DPPH: negative.

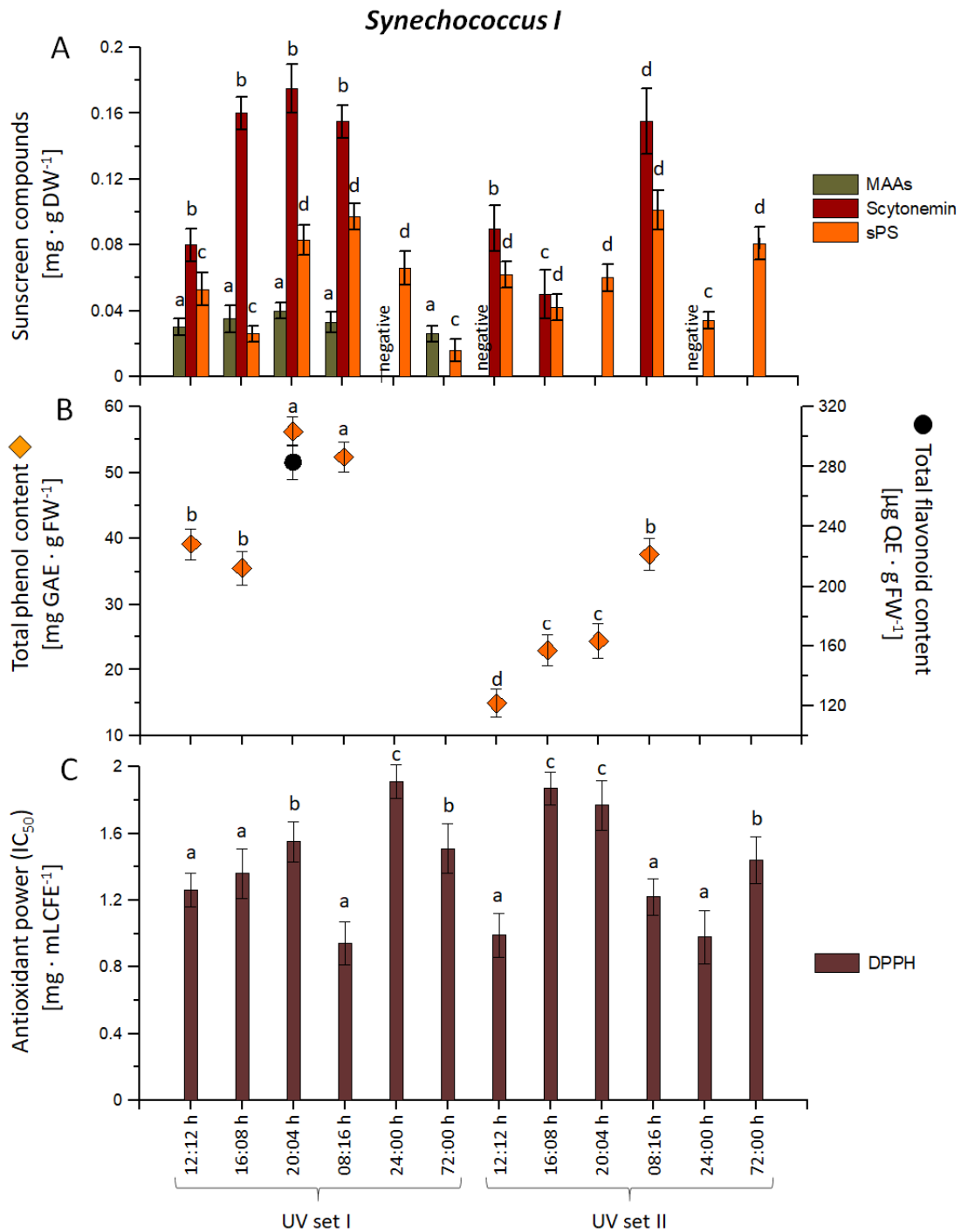


Figure 35. Results of the induction experiments using the coccoid cyanobacteria *Synechococcus I* (no [9] in Table 1) and two different UV/PAR sets in combination with different exposure lengths. Depicted are the concentrations of mycosporine-like amino acids (MAAs), scytonemin, and sulfated polysaccharides (SPS) as sunscreen compounds (A), total phenol and flavonoid contents as part of the antioxidative defense system (B), as well as the IC₅₀ values of the antioxidant power of cell free extracts measured as 2,2-Diphenyl-1-picrylhydrazyl (DPPH) scavenging activity (C). Only positive values for the MAA concentration are depicted in Figure A. If tested and no concentration was detected the value is designated as “negative”. All other samples were not analysed for the presence of MAAs. Data are presented as means ± SD (n=3) and different letters indicate significant difference among treatments. The results of the control assay (PAR only) were: MAAs: negative; scytonemin: 0.038 mg · g DW⁻¹; SPS: 0.031 mg · g DW⁻¹; phenolic compounds: 3.9 µg QE · g FW⁻¹; flavonoids: negative; DPPH: negative.

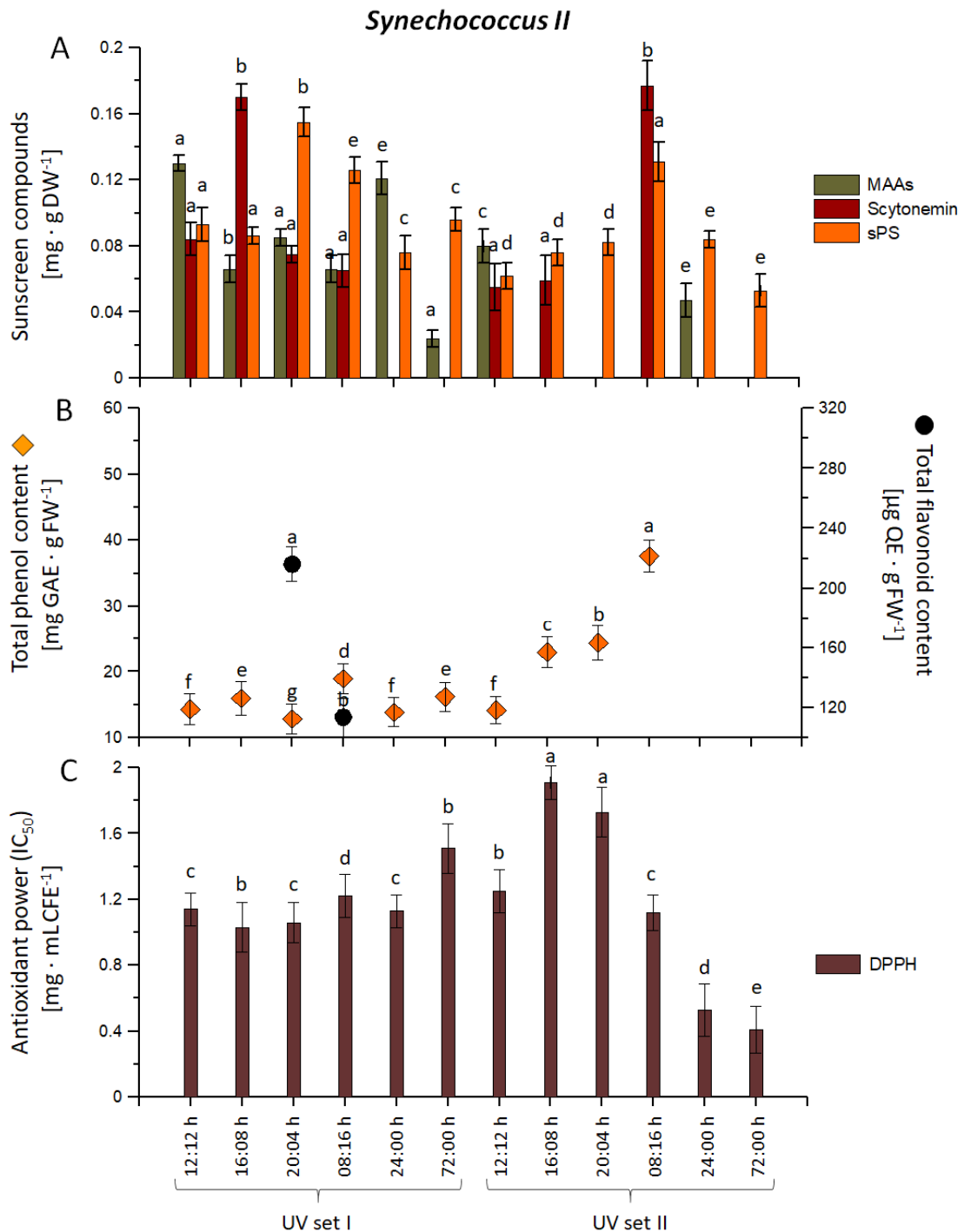


Figure 36. Results of the induction experiments using the coccoid cyanobacteria *Synechococcus II* (no [10] in Table 1) and two different UV/PAR sets in combination with different exposure lengths. Depicted are the concentrations of mycosporine-like amino acids (MAAs), scytonemin, and sulfated polysaccharides (sPS) as sunscreen compounds (A), total phenol and flavonoid contents as part of the antioxidative defense system (B), as well as the IC₅₀ values of the antioxidant power of cell free extracts measured as 2,2-Diphenyl-1-picrylhydrazyl (DPPH) scavenging activity (C). Only positive values for the MAA concentration are depicted in Figure A. If tested and no concentration was detected the value is designated as “negative”. All other samples were not analysed for the presence of MAAs. Data are presented as means ± SD (n=3) and different letters indicate significant difference among treatments. The results of the control assay (PAR only) were: MAAs: negative; scytonemin: 0.026 mg · g DW⁻¹; sPS: 0.041 mg · g DW⁻¹; phenolic compounds: 3.0 µg QE · g FW⁻¹; flavonoids: negative; DPPH: negative.

Table 4. Survey of MAAs and derivatives found during the LC analysis (cf. Appendix for chromatogram examples).

Species	MAA	Wavelength [nm]	Retention time [h]	Concentration [mg · g DW ⁻¹]	Experiment Light: dark cycle; UV set
<i>Synechococcus I</i>					
	Palythine-serine sulfate (ester)	321	3.672	0.04	20:04 h; UV I
	Mycosporine-methylamine-serine	327	4.815	0.03, 0.08	12:12 h; UV I, II
	Mycosporine-ornithine	331	13.099	0.026	72 h; UV I
	Shinorine	333	13.058	0.035 0.033	16:08 h; UV I 08:16 h; UV I
<i>Synechococcus II</i>					
	Palythine-threonine glycoside	326	7.991	0.047	24 h; UV II
	Mycosporine-methylamine-serine	327	7.441	0.13, 0.08	12:12 h; UV I, II
	unknown* (denoted as M-328)	328	8.146	0.121	24 h; UV I
	unknown* (denoted as M-329)	329	11.541	0.066	16:08 h; UV I 08:16 h; UV I
	Asterina-330	330	11.554	0.085	20:04 h; UV I
	Palythinol	332	11.485	0.024	72 h; UV I
<i>Synechocystis II</i>					
	unknown (denoted as M-341)	341	11.487	0.011	72 h; UV I

Table 5. Monosaccharide composition of sPS detected in the four selected cyanobacteria.

Species	Monosaccharides [molar ratios*]										Substituent [% DW]
	Ara	Fuc	Gal	Glc	Man	Rha	Xyl	GalA	GlcA	UrA	
<i>Synechocystis I</i>*	5.3	2.2	5.9	31.4	3.1	2.8	2.6	-	-	16.3	1.3
<i>Synechocystis II</i>**	-	6.3	1.2	7.3	3.4	3.9	3.7	-	-	16.2	1.0
<i>Synechococcus I</i>	5.6	4.9	9.7	19.2	10.1	9.4	9.9	0.9	1.3	-	0.9
<i>Synechococcus II</i>	5.5	4.2	9.9	20.5	10.8	8.8	9.5	0.9	1.1	-	0.8

* Molar ratio calculated by comparing the absorption of the standard peaks and the sample peak as well as the composition of the extracts; Abbreviations: Ara = arabinose; Fuc = fucose; Gal = galactose; Glc = glucose; Man = mannose; Rha = rhamnose; Xyl = xylose; GalA = galacturonic acid; GlcA = glucuronic acid; UrA = uronic acid; *others: glucosamine, galactosamine; ** others:: methylhexose, glucosamine, galactosamine.

Table 6. Effects of different UVR exposure times (24 and 72 h continuous illumination, set I) on enzyme activities of the antioxidative defense system in the four selected cyanobacteria species. Data are means ± SD (n=3).

Species	SOD activity [U/mg protein]		CAT activity [U/mg protein]		APX activity [U/mg protein]		GR activity [U/mg protein]	
	24	72	24	72	24	72	24	72
<i>Synechocystis I</i>	188±1.3	136±1.0	107±1.5	103±0.3	89±8.1	101±1.1	109±1.2	88±2.3
<i>Synechocystis II</i>	109±1.0	106±3.4	103±2.3	102±4.4	64±2.3	89±0.9	114±3.3	73±2.2
<i>Synechococcus I</i>	195±5.5	133±6.3	109±3.3	106±2.0	71±2.5	86±2.1	101±5.9	89±1.8
<i>Synechococcus II</i>	222±1.3	198±1.6	108±2.1	93±3.1	87±2.5	92±3.8	103±2.1	96±1.0

concentrations varying from $0.026\text{-}0.04 \pm 0.03 \text{ mg} \cdot \text{g DW}^{-1}$. Noteworthy is in this context that almost for each exposure length a different single MAA was found, such as in the 12 h UV exposure assay the MAA mycosporine-methylamine-serine and in the 16 h assay shinorine (Table 4). In addition, all MAAs observed were solely found in the UV illumination set I. Similar to *Synechococcus* I, also in *Synechococcus* II an overall significantly weaker response in the concentration of sunscreen compounds to the second UV/PAR set was detectable ($p \leq 0.05$, Fig. 36A). In this setting, the highest scytonemin concentration ($0.177 \pm 0.015 \text{ mg} \cdot \text{g DW}^{-1}$) was recorded in the 8 h assay correlated with the highest sPS concentration ($0.131 \pm 0.012 \text{ mg} \cdot \text{g DW}^{-1}$). In the first set, sPS were the main response to UV exposure in *Synechococcus* II, ranging from $0.093\text{-}0.155 \pm 0.007 \text{ mg} \cdot \text{g DW}^{-1}$ in the 12 h and 20 h UV I assay, respectively. MAAs were detected in all samples tested in varying concentrations (UV sets I and II), being the highest in the 24 h UV I exposure assay ($0.121 \pm 0.01 \text{ mg} \cdot \text{g}^{-1} \text{ DW}$). As noted in *Synechococcus* I, each MAA was solely observed in one assay. While palythine-threonine glycoside was found in the 24 h UV II assay, palythine was detected in the UV I assay (Table 4). Asterina-330 was only recorded in the 20 h UV I exposure assay and mycosporine-methylamine-serine in the 72 h one. In addition, two not identifiable MAAs were also discovered: one in the 24 h and one in the 16 h assay of the UV I illumination set.

Regarding the composition of the cyanobacterial sPS, overall, 10 different monosaccharides have been found in the tested samples in the present study: the hexoses glucose, galactose, rhamnose and mannose, the pentoses xylose and arabinose, the deoxyhexose fucose and some acidic hexoses such as glucuronic and galacturonic acid, whereas the pentose ribose was absent in all tested cyanobacteria (Table 5). The sPS of the four cyanobacteria differed mainly in their molar ratios of glucose and mannose, being the highest in *Synechocystis* I for the former one (differences of up to 76.8%) and *Synechococcus* I and II for the latter one (up to 71.3%). In addition, characteristic difference between the species were observed when comparing the acidic hexoses. While uronic acid was only observed both in *Synechocystis*, galacturonic and glucuronic acid were characteristic in both *Synechococcus*. The analysis of the substituent groups showed neither the presence of acetate nor pyruvate. Only sulfate as substituent was detected, being the highest in *Synechocystis* I (1.3%).

Phenolic compounds as part of the non-enzymatic antioxidative defense system were detectable in the majority of assays (81%) as response to the different UV/time treatments and varied between 11.8 and $56.9 \pm 0.08 \text{ mg GAE} \cdot \text{g FW}^{-1}$, being the highest in the 20 h (UV I) assay in *Synechococcus* I (Figs. 33B-36B). In contrast, flavonoids were only found in 20.8% of the assays, being the highest in *Synechococcus* I in the 20 h (UV II) assay ($293.5 \pm 0.1 \mu\text{g QE} \cdot \text{g FW}^{-1}$) (Fig. 33B). The enzymatic part of the antioxidative defense system was only analysed for the 24 and 72 h continuous UV I exposure experiments (Table 6). As a general trend, the activity of SOD, CAT and GR decreased with increasing UV exposure time, whereas APX activities increased (up to 11.8%). The highest SOD activity was measured in *Synechococcus* II with $222.3 \text{ U/mg protein}$, while the highest CAT activity was found in *Synechococcus* I.

The radical scavenging activities in all UV treated cultures were increased compared to the non-treated cultures (controls) (Figs. 33C-36C), in which the DPPH screening was negative. Antioxidant activities varied between species and treatments, being the highest in 16 h UV I treated *Synechococcus* II ($1.91 \pm 0.02 \text{ mg} \cdot \text{mL CFE}^{-1}$) (CFE=cell free extract). Noteworthy is in this context that in most of the cases the highest concentrations of sun protective compounds and components of the non-antioxidative defense system did not correlate with the highest antioxidant activities.

4.3 Photoprotective Compound Stability

4.3.1 Alternative Harvest Methods

Three flocculation methods were performed in a systematic manner to two selected species of cyanobacteria. Compared were the flocculants sodium hydroxide (NaOH), Iron (III) chloride (FeCl_3), and chitosan (poly-(D)glucosamine). In principle, flocculation was successful for all species–flocculation method combinations, except for the species flocculated with chitosan (Fig. 37). In the further investigation, the two cyanobacteria *Synechococcus* I and II, [9, 10], were analysed regarding effects of the compound stability of MAAs, scytonemin and sulfated polysaccharides as photoprotective compounds, selected components of the antioxidative defence system (flavonoids, phenolic compounds), and DPPH scavenging activities due to the harvest of biomasses by flocculation. Compared were the results to the harvest by centrifugation as standard method (control; Fig. 38).

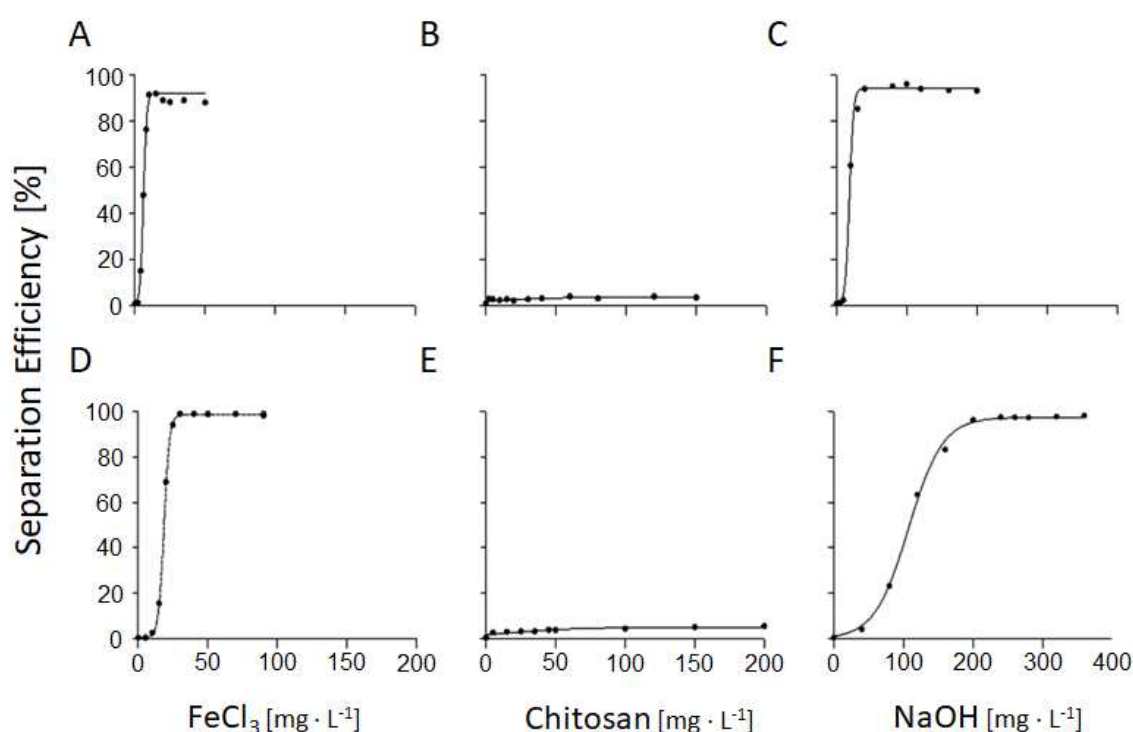


Figure 37. Results of the experiments for determination of the minimum dosage of flocculant required for induction of flocculation in *Synechococcus* I (A, B, C) and II (D, E, F), using the flocculants Iron (III) chloride (FeCl_3), chitosan, and sodium hydroxide (NaOH).

As pointed out above, chitosan did not flocculate both marine species well which was also reflected in the highest cell numbers in the supernatant after harvest (Figs. 38A and E). In contrast the lowest cell numbers in the supernatant after harvest were observed besides in the control assay, also in the NaOH III (pH 10) assay. The comparison of the compound concentrations between the different flocculation assays and the control, revealed the lowest loss of compound concentrations and activities in the NaOH III assay. In this flocculation assay yield losses only varied between 3.1-7.8% DPPH (Figs. 38D, H), 4.96-11% MAAs, 13.3-11.2% scytonemin, 15.1-4.1% sPS (Figs. 38B and F), 7.1-1.3% phenolic compounds, and 21-0.1% flavonoids (Figs. 38C and G) in *Synechococcus* I and

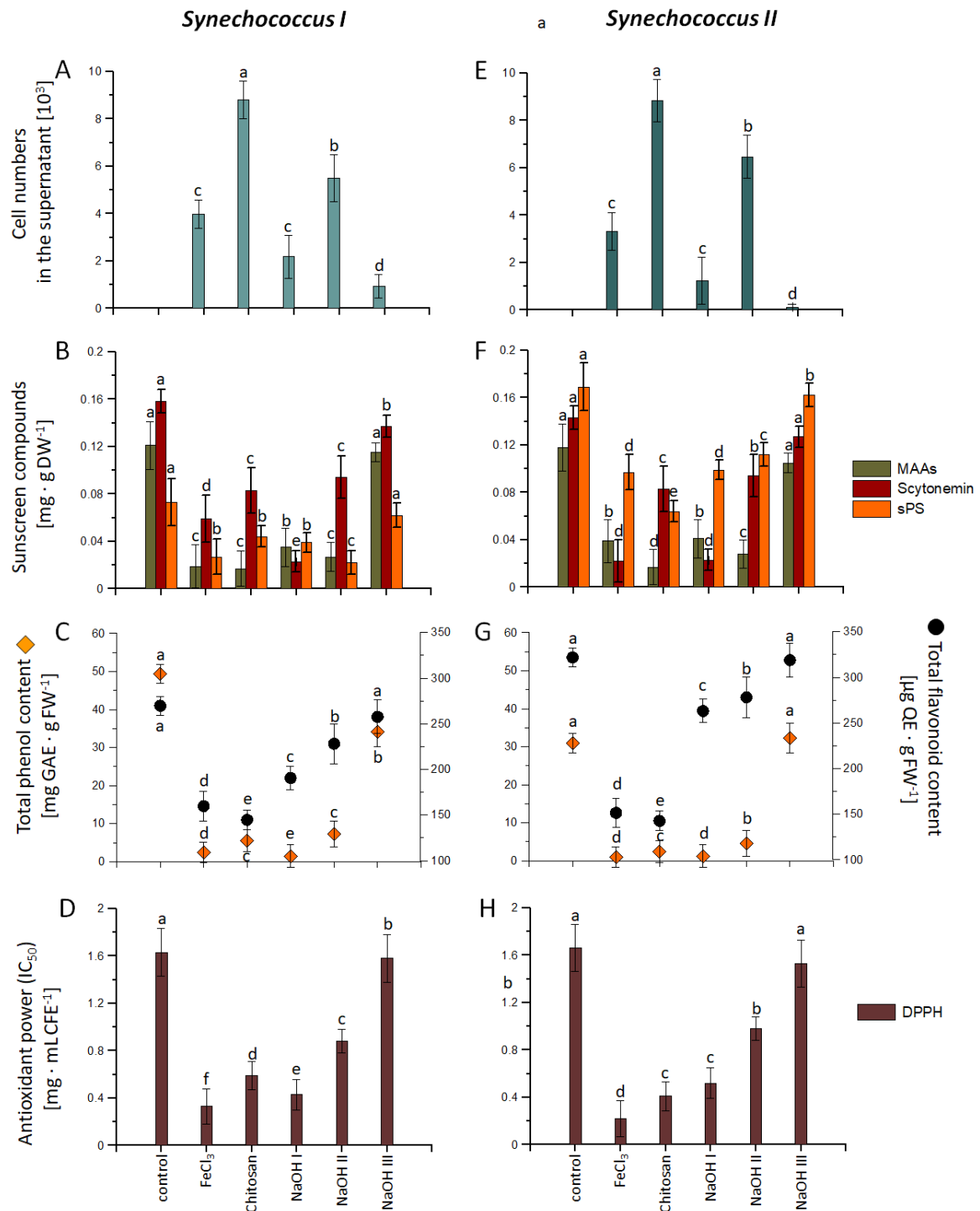


Figure 38. Results of the utilization of different harvest methods and their effects on the concentrations of mycosporine-like amino acids (MAAs), scytonemin, and sulfated polysaccharides (sPS) as sunscreen compounds (B, F), total phenol and flavonoid contents as part of the antioxidative defense system (C, G), as well as the IC_{50} values of the antioxidant power of cell free extracts measured as 2,2-Diphenyl-1-picrylhydrazyl (DPPH) scavenging activity (D, H). As model organisms the coccoid cyanobacteria *Synechococcus* I and II (no [9] and [10] in Table 1) were used. In addition, the cell numbers in the supernatant after harvest are depicted (A, E). Compared were the flocculants sodium hydroxide (NaOH), iron (III) chloride (FeCl_3), and chitosan (poly-(D)glucosamine) (PG). Sodium hydroxide was tested in three different pH values (NaOH I: pH 8; NaOH II: pH 9; NaOH III: pH 10). Data are presented as means \pm SD (n=3). Different letters indicate significant difference among treatments.

Synechococcus II, respectively. Regarding the recovery rate of the photoprotective compounds in the different flocculation assays (FeCl₃, chitosan, NaOH I, NaOH II) some significant differences were found between species, compounds, and assays. For instance, while for sPS recovery rates were in average the highest in *Synechococcus* II regardless the flocculation method used (~40% recovery in comparison to the control), the recovery rates for scytonemin were in average the highest in *Synechococcus* I (~55.3%). In contrast, the recovery rates for MAAs were in both species significantly lower than compared to the control and the NaOH III flocculation assays (in average 26% recovery rate).

4.3.2 Effects of Drying Temperatures and Storage Lengths

The experiments in this part of the study focused explicit on MAA, scytonemin and sulfated polysaccharide concentrations. As control crude biomass samples were used. After drying the biomasses were weighted and used for biochemical analysis as described in 3.2.4.1. In addition, the effects of different storage length on MAA concentrations prior to the extraction were also tested. For this test, two times 45 mL samples from the experiment were kept frozen for 7, 21, 56 and 168 days.

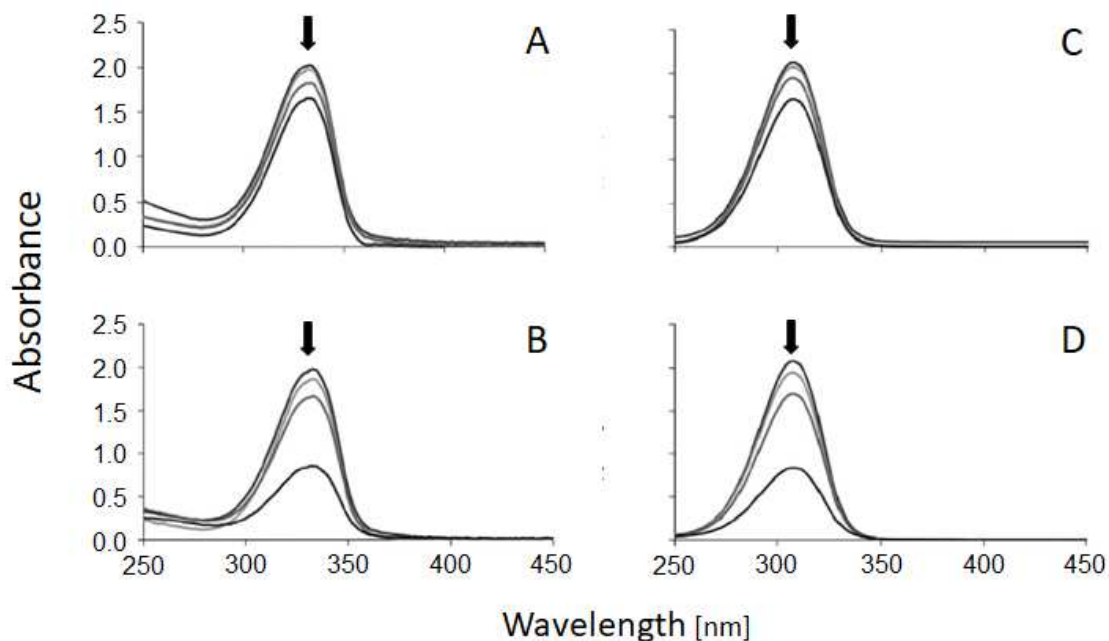


Figure 39. Stability of shinorine from *Synechococcus* I (A, B) and an unknown MAA M-328 (C, D) from *Synechococcus* II under heat stress (A, C) and different storage lengths (B, D). The down arrows denote the absorption spectra of heat treated (35 °C, 45 °C, 60 °C and 70 °C), and freeze stored (control, 3 days, 7 days, 21 days) samples from top to bottom, respectively.

The results presented in Figures 39 and 40 show a relatively high stability range of the photoprotective compound groups within a temperature range from 35 to 60°C, declining only insignificantly in samples from *Synechococcus* II (0.08% MAAs, 0.7% scytonemin, 0.8% sPS; Fig. 40C). In contrast, besides slight yield decreases of scytonemin (0.7%) and sPS (1.7%), MAA concentrations declined significantly in samples from *Synechococcus* I (5.5%, Fig. 40A). Furthermore, temperatures of 70°C led to a substantial yield loss of up to 60% in MAAs and scytonemin in *Synechococcus* I, whereas in *Synechococcus* II the concentrations were around 31 and 38% reduced. Furthermore, the sPS yield

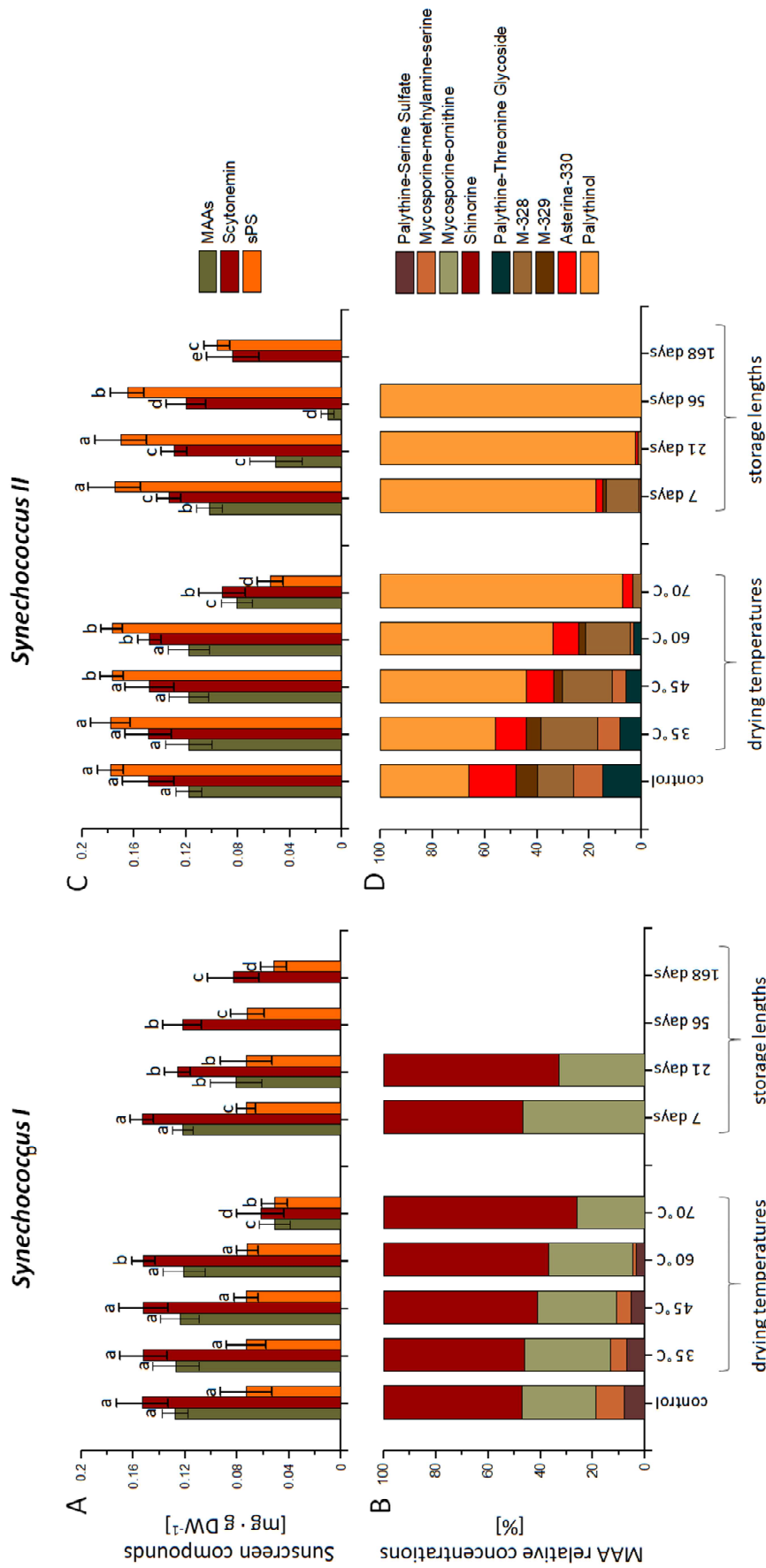


Figure 40. Results of the utilization of different drying temperatures and storage length and their effects on the concentrations of mycosporine-like amino acids (MAAs), scytonemin, and sulfated polysaccharides (sPS) as sunscreen compounds, and MAA compositions (B). As control crude biomass samples were used. Data are presented as means \pm SD ($n=3$). Different letters indicate significant differences among treatments.

was also ~30% reduced in both tested species. Regarding the MAA composition in the control assay, shinorine was most abundant in *Synechococcus* I (53%), followed by mycosporine-ornithine (28%), mycosporine-methylamine-serine (11%) and the sulfate ester of palythine-serine (8%; Fig. 40B). Conversely, palythanol was the most abundant MAA in *Synechococcus* II (34%) in the control, followed by asterina-330 (18%), palythine-threonine glycoside (15%), M-328 (14%), mycosporine-methylamine-serine (11%), and M-329 (8%; Fig. 40D). During the drying temperature experiment the relative MAA composition changed substantially. Specifically, the MAAs shinorine and M-328 were found highly stable at room temperatures up to 45°C; however, the absorbance of both MAAs decreased slowly with an increase in temperature up to 60°C, decreasing more rapidly at 70°C (Figs. 40A and C). Other MAAs besides shinorine and M-328, such as palythanol and mycosporine-ornithine were also found exceptionally temperature stable in the present study (Figs. 40B and D). On the opposite, mycosporine-methylamine-serine and palythine-serine-sulfate in *Synechococcus* I as well as palythine-threonine glycoside and M-329 in *Synechococcus* II were only stable in a temperature range up to 60°C, sharply declining over the tested temperature range and not detectable in the 70°C assay (Figs. 40B and D).

Regarding the effects of different storage lengths on MAAs, the absorbance of shinorine and M-328 decreased under different durations of storage (Figs. 40C and D). Both shinorine and M-328 were comparatively stable at 3 and 7 days of freezer storage. After 31 days storage, a drastic decrease in absorbance of the MAAs shinorine (Fig. 40C) and M-328 (Fig. 40D) was observed. Similar developments were recorded for mycosporine-ornithine and palythanol, in which the latter one was even detected after 56 days storage (Figs. 40B and D). This long-term storage instability of MAAs contrasts with the other photoprotective compounds in which scytonemin and SPs were still detectable after 168 days of freezer storage although with significant declines in concentrations (Figs. 40A and C). Specifically, the yield for scytonemin was reduced 45.8 and 43.6% in *Synechococcus* I and II, respectively, when compared to the control assay, whereas the sPS concentration declined 28.8 and 46.1% in *Synechococcus* I and II after the same storage period.

4.4 Experiments in 100 L Photobioreactors (PBRs)

4.4.1 Conventional Bubble Column PBR

Comparing effects of up-scale cultivations under different nutrient scenarios on growth, the presence and concentrations of photoprotective compounds, components of the non-enzymatic antioxidative defense system and antioxidant power of *Synechococcus* I and II, two distinct semi-continuous culture conditions (exchange of 30 L medium, designated as semi I, and addition of nutrients for 30 L medium (semi II) both in weekly intervals) versus batch culture as well as urea as NaNO₃ replacement were tested under two UV illumination sets. The results are presented in Figure 41 and show that basically in all experimental assays all sun protective compounds, polyphenols and antioxidative activities were enhanced in comparison to the control assay. In addition, the results of the purification of two MAAs and scytonemin are depicted in Figs. 42 and 43.

Growth rates varied from 1.1-1.62 ± 0.03 and 1.29-1.63 ± 0.08 μ day⁻¹ in *Synechococcus* I and II, respectively, being the lowest in the batch cultivation approaches of both tested species using UV set

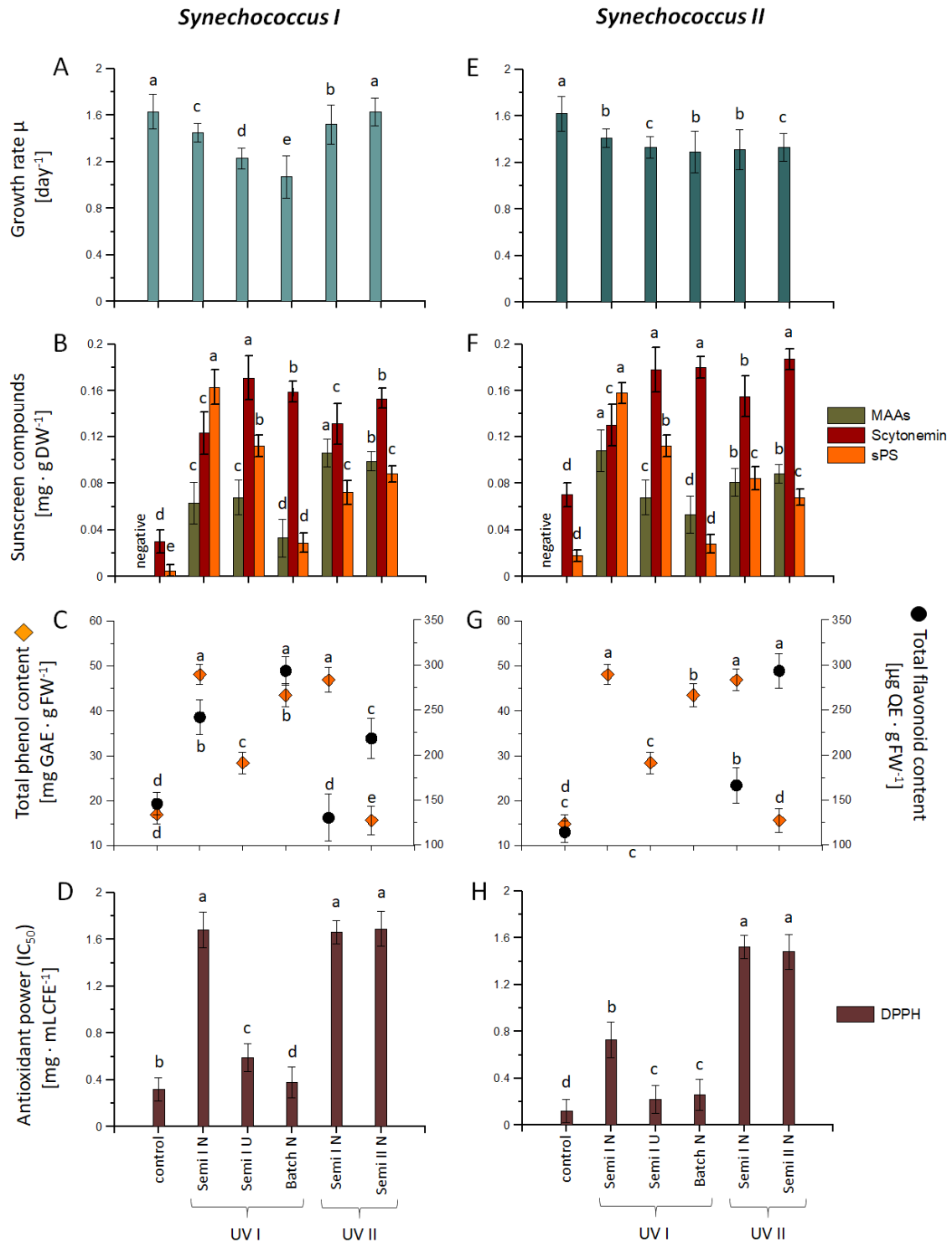


Figure 41 Results of the up-scale experiments in conventional bubble column PBRs using the coccoid cyanobacteria *Synechococcus* I (A-D) and II (E-H) (no [9] and [10] in Table 1) as model organisms. Tested were two sets of UV light equipment (UV I and UV II) as well as two distinct semi-continuous culture conditions (exchange of 30 L medium (semi I) and addition of nutrients for 30 L medium both in weekly intervals (semi II) versus batch culture as well as urea (U) as NaNO₃ (N) replacement. Depicted are the growth rates (A, E) as well as the effects on the concentrations of mycosporine-like amino acids (MAAs), scytonemin, and sulfated polysaccharides (sPS) as sunscreen compounds (B, F), total phenol and flavonoid contents as part of the antioxidative defense system (C, G), as well as the IC₅₀ values of the antioxidant power of cell free extracts measured as 2,2-Diphenyl-1-picrylhydrazyl (DPPH) scavenging activity (D, H). Data are presented as means ± SD (n=3) and different letters indicate significant difference among treatments.

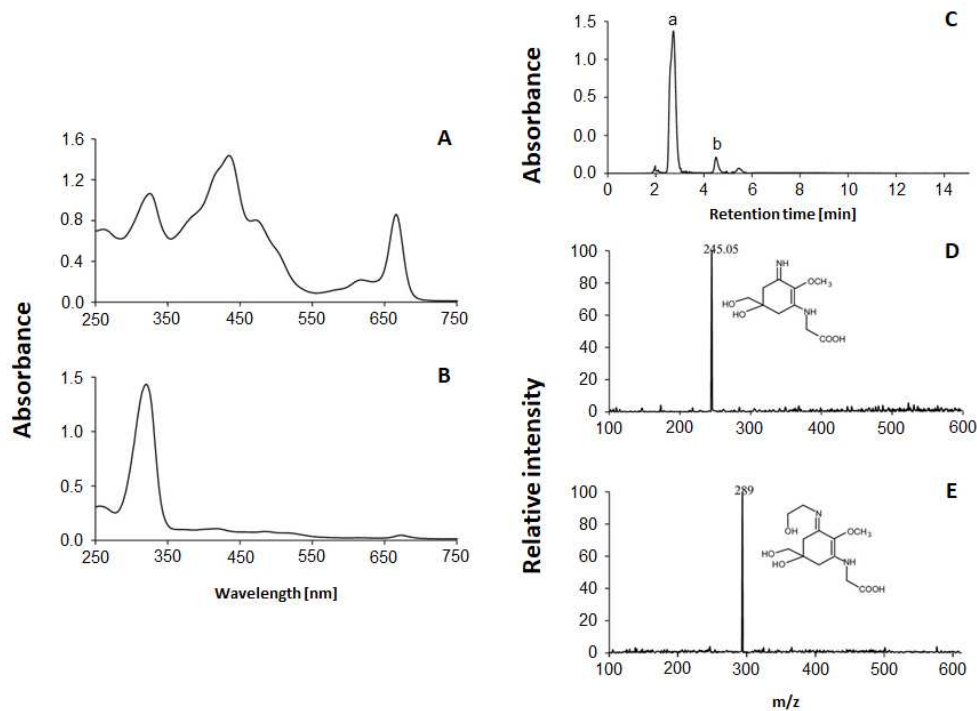


Figure 42. A-B) UV/Vis absorption spectrum of *Synechococcus* II: **A)** 100% methanolic extract showing the peaks for mycosporine-like amino acid (327 ± 2 nm), chlorophyll *a* (435 and 665 nm), and carotenoids (471 nm); **B)** Absorption spectrum of partially purified MAA prepared for HPLC analysis. HPLC chromatogram **(C)** of partially purified MAAs from *Synechococcus* II, showing the typical peaks at retention times of 2.7 min (a) and 4.3 min (b). Mass spectra of HPLC-purified MAAs, palythanol **(D)** and asterina **(E)**, showing a prominent peak at m/z 245.05 and 289, respectively.

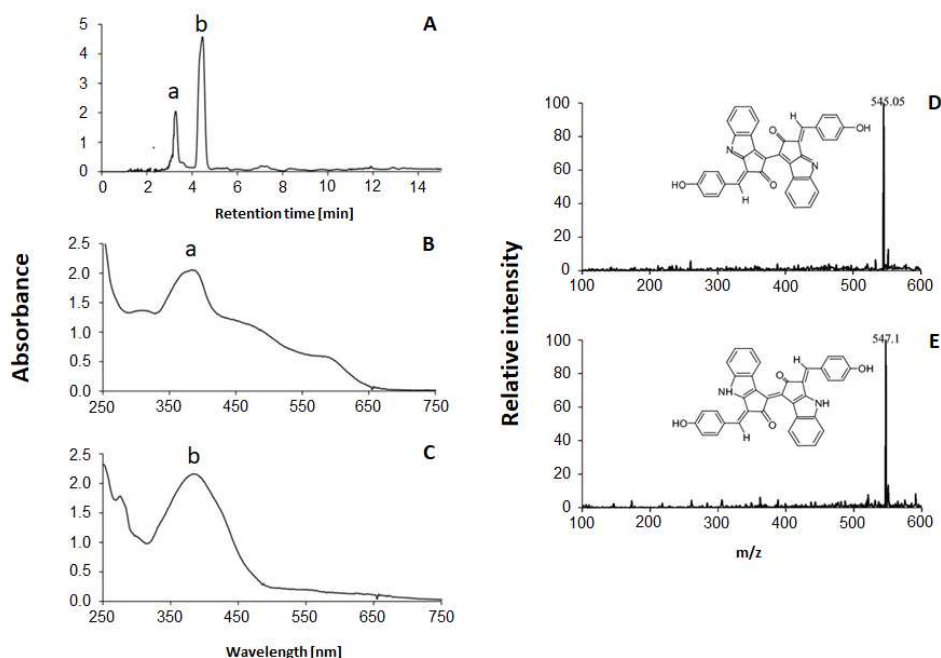


Figure 43. HPLC chromatogram **(A)** of partially purified scytonemin from *Synechococcus* II showing the typical peaks for reduced scytonemin (a) and scytonemin (b) at retention times of 3.25 min and 4.48 min, respectively. **(B)** UV/Vis spectra showing maximum absorbance at 384 nm for both reduced scytonemin and scytonemin **(C)**. Mass spectrum of HPLC-purified scytonemin **(D)** and reduced scytonemin **(E)** showing a prominent peak at m/z 545.05 and 547.1, respectively.

I (Figs. 41A and E). Only the weekly nutrient addition approach (semi II) led to an equal growth rate in *Synechococcus* I when compared to the control assay, closely followed by the weekly medium exchange approach (semi I). In both experimental approaches the UV set II in combination with sodium nitrate as N source were used (Fig. 41A). Regarding the sun protective compound concentrations obtained in the different cultivation assays, a high variability was detected in all assays, being distinctive for MAAs and sPS (Figs. 41B and F). While the highest MAA concentrations were observed in the semi I and II assays under UV II exposure in *Synechococcus* I (0.106 ± 0.012 and 0.1 ± 0.008 mg · g DW⁻¹ respectively; Fig. 41B), the highest MAA concentration for *Synechococcus* II was recorded in the semi I assay with sodium nitrate as N source under UV I illumination (0.109 ± 0.018 mg · g DW⁻¹; Fig. 41F). Furthermore, sPS concentrations were the highest in the semi I assay with sodium nitrate as N source under UV I exposure in both species (0.163 ± 0.015 and 0.158 ± 0.005 mg · g DW⁻¹), followed by the second highest sPS concentrations in the semi I assay with urea as N source (0.112 ± 0.009 mg · g DW⁻¹; Figs. 41B and F). In contrast scytonemin was found in highest concentrations in almost all experimental approaches, being the highest in *Synechococcus* II in the weekly nutrient addition assay using sodium nitrogen as N source under UV II exposure (semi II; 0.187 ± 0.009 mg · g DW⁻¹; Fig. 41F). A similar distribution pattern as found for the sPS concentrations was also recorded for the antioxidative activities, with the highest activities found in the semi I and II assays using sodium nitrate as N source, ranging between $1.66-1.69 \pm 0.15$ and $0.73-1.52 \pm 0.1$ mg · mL CFE⁻¹ in *Synechococcus* I and II, respectively (Figs. 41D and H). Total phenol contents were in both species similar and ranged from 44.6 to 48.3 ± 0.2 mg GAE · g FW⁻¹, being the highest in the semi I assay under UV I exposure with sodium nitrogen as N source (Figs. 41C and G). For flavonoids, the highest contents were detected in the batch cultivation of *Synechococcus* I (Fig. 41C) as well as the semi II assay under UV II exposure and NaNO₃ as N source in *Synechococcus* II (Fig. 41G) with 292.5 ± 0.05 and 296.8 ± 0.03 µg QE · g FW⁻¹, respectively. Finally, regarding urea as cheaper replacement for sodium nitrate, the results for the growth rates, antioxidative power and absence of flavonoids in both species points the necessity of further experiments utilizing different concentrations to get a clearer picture.

4.4.2 Internally Illuminated Bubble Column PBR

The annular PBR design was chosen in order to optimize the UV-light penetration in comparison to the conventional PBR system. As model organism *Synechococcus* II was used. Combining the results of the former experiments, sodium nitrate was used as N source and the UV illumination set I in a 12:12 h light to dark cycle was applied for an overall duration of 504 h. In addition, nutrients were supplemented in weekly intervals (every 168 hours). The results of this final experiment are presented in Figure 44, comprising cell numbers, protein contents and chlorophyll *a* (chl *a*) concentrations as growth parameters (Fig. 44A), concentrations of sun protective compounds (Fig. 43B) and components of the non-enzymatic antioxidative defense system (Fig. 44C), as well as radical scavenging activities (Fig. 44D). Relative MAA and monosaccharide composition are presented in Figure 45.

Cell numbers of *Synechococcus* II increased steadily until $t = 312$ h and reached after $t = 360$ h a plateau after which only insignificant variations were detectable ($75.4 - 78.1 \cdot 10^9$ cells ml⁻¹; Fig. 44A). Furthermore, chl *a* concentrations increased 27.1% during the experiment, being the highest at $t = 504$ h. In contrast, protein contents varied only slightly between 8.4 ± 0.11 and 12.5 ± 0.03 µg · g DW⁻¹ at $t = 0$ and $t = 216$ h, respectively.

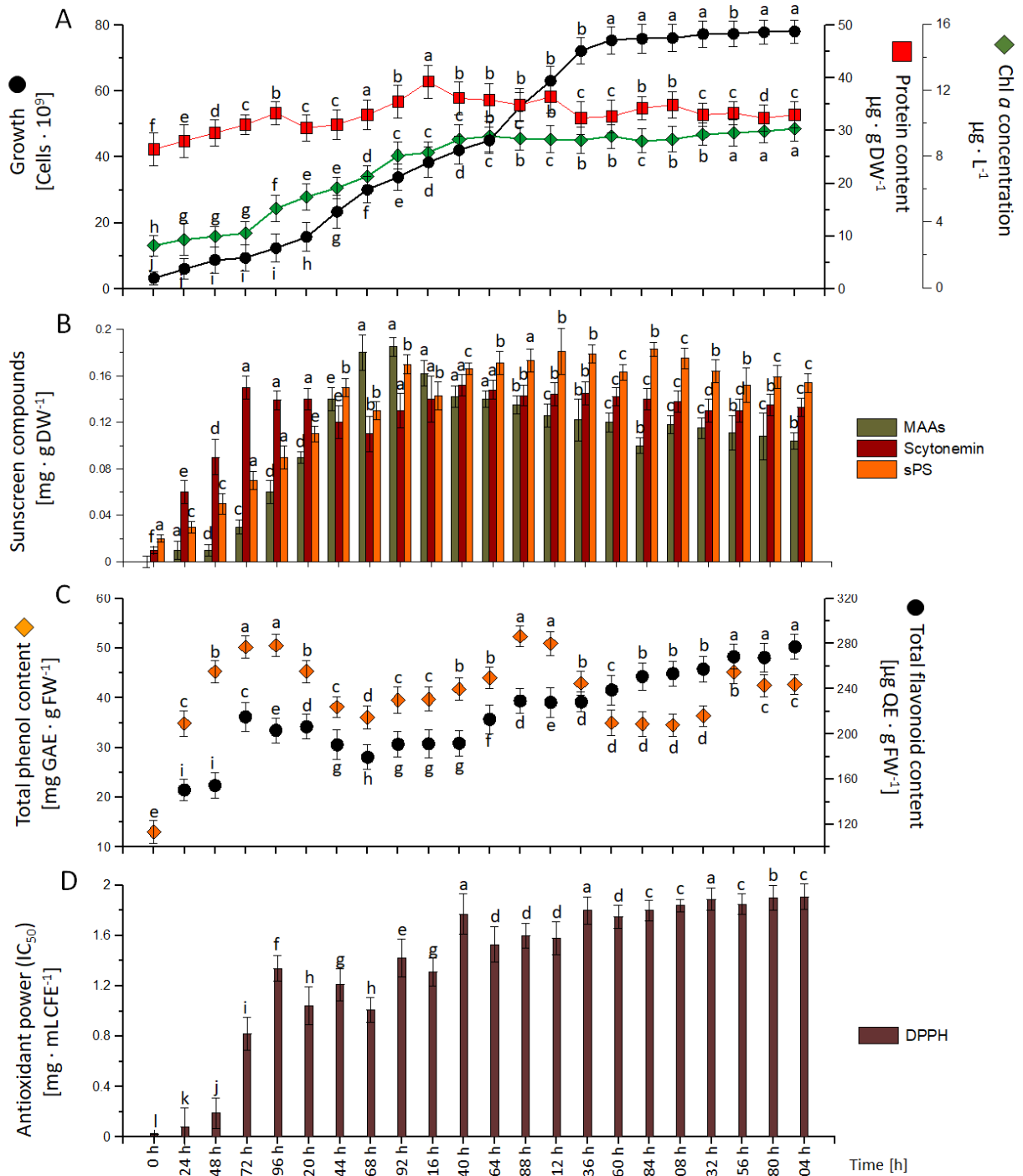


Figure 44. Results of the final experiment in an internally illuminated bubble column PBR using the coccoid cyanobacteria *Synechococcus* II (no [10] in Table 1) as model organism. Depicted are the changes over time of the cell numbers, protein content and chlorophyll *a* concentrations (A); the concentrations of mycosporine-like amino acids (MAAs), scytonemin, and sulfated polysaccharides (sPS) as sunscreen compounds (B), total phenol and flavonoid contents as part of the non-enzymatic antioxidative defense system (C), as well as the IC₅₀ values of the antioxidant power of cell free extracts measured as 2,2-Diphenyl-1-picrylhydrazyl (DPPH) scavenging activity (D). Data are means ± SD (n=3) and different letters indicate significant difference among treatments.

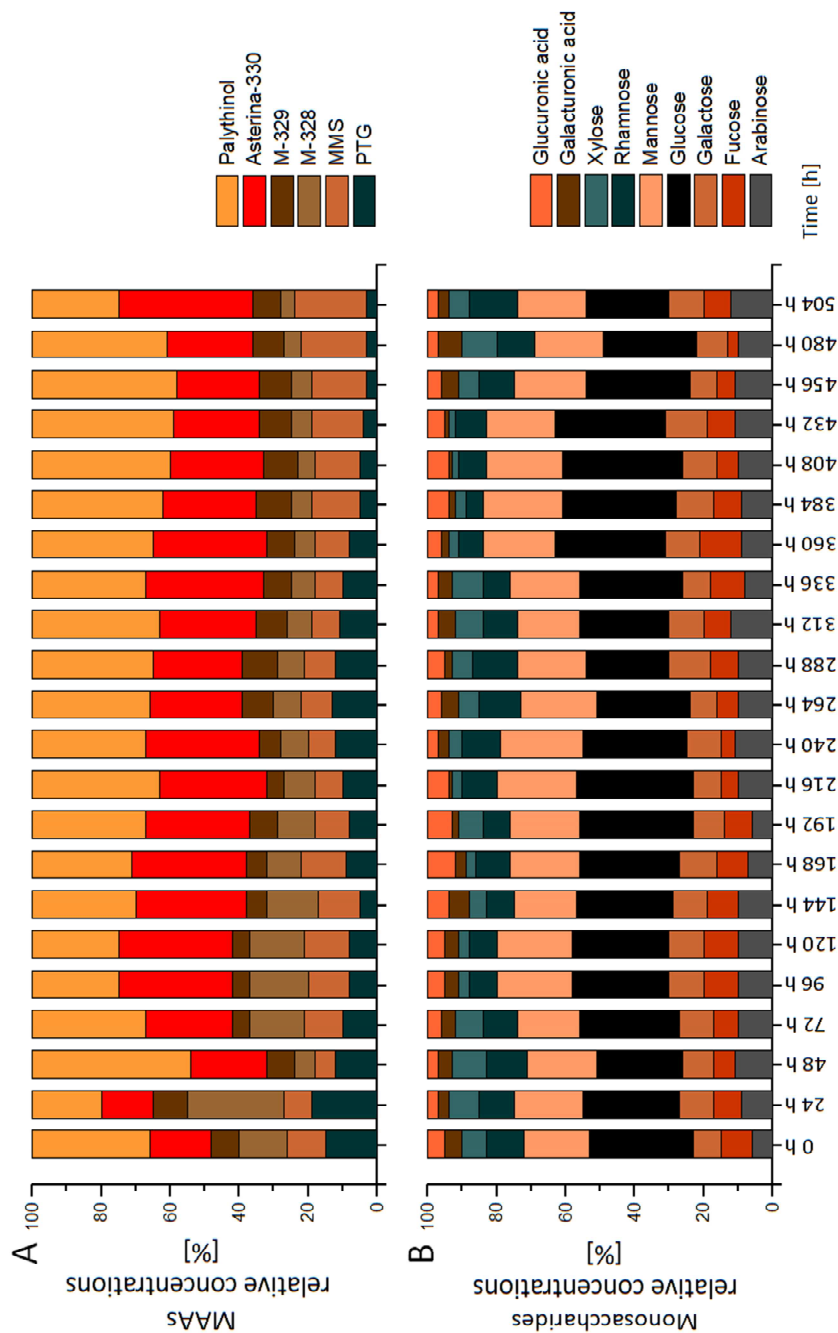


Figure 45. Development of the relative MAA (A) and monosaccharide (B) compositions during the final experiment. Abbreviations: PTG, Palythine-threonine glycoside; MMS, Mycosporine-methylamine-serine.

Photoprotective compounds increased in this experiment from the first 24 hours onwards, with scytonemin as first response sun screening compound, reaching maximum values at $t = 72$ and $t = 240$ h with 0.151 ± 0.05 and 0.152 ± 0.08 $\text{mg} \cdot \text{g DW}^{-1}$, respectively (Fig. 44B). The MAA concentration increased exponential until $t = 168$ h (0.118 ± 0.07 $\text{mg} \cdot \text{g DW}^{-1}$) and reached a maximum at $t = 192$ h with 0.185 ± 0.04 $\text{mg} \cdot \text{g DW}^{-1}$. In contrast, sPS showed several above average values during the experiment, being the highest at $t = 384$ h with 0.183 ± 0.03 $\text{mg} \cdot \text{g DW}^{-1}$. Except for $t = 24$ h, in which M-328 made up 28% of the total MAAs, palythindol and asterina-330 were the dominant MAAs throughout the experiment (Fig. 45A). While the highest abundance of palythindol was recorded at $t = 48$ h (46%), asterina-330 was predominant at $t=504$ h (39% of the total MAAs). Palythine-threonine glycoside (PTG) and mycosporine-methylamine-serine (MMS) were present during the final experiment with relative values varying between 3-19% and 6-21%, being the highest at $t = 24$ h (PTG)

and $t = 504$ h (MMS). The monosaccharide composition of the sPS from *Synechococcus* II was relatively stable during the experiment and was dominated by glucose (GLU) and mannose (MAN), varying only between 24-35% (GLU) and 18-24% (MAN) of the total monosaccharides (Fig. 45B).

Total phenolic compounds increased rapidly until $t = 72$ h (144% of the initial value) and showed a wave pattern in which two distinct maxima were observed at $t = 96$ h and $t = 288$ h with 51.4 ± 0.3 and 54.3 ± 0.2 mg GAE \cdot g FW⁻¹, respectively (Fig. 44C). Conversely, total flavonoid contents were not detected at the beginning of the experiment but increased in two steps at $t = 0-24$ h and $t = 48-72$ h about 62%. After decreasing, from $t = 240$ h onwards total flavonoid contents increased again to a maximum value of 279.1 ± 0.2 μ g QE \cdot g FW⁻¹ at $t = 504$ h.

The radical scavenging activities in the final UV experiment increased from 0.02 ± 0.005 mg \cdot ml CFE⁻¹ at $t = 0$ h rapidly to 1.35 ± 0.08 mg \cdot ml CFE⁻¹ at $t = 96$ h (Fig. 44D). Antioxidant activities varied in a similar pattern as observed for the photoprotective compounds and components of the non-enzymatic antioxidative defense system, reaching a first maximum with 1.77 ± 0.09 mg \cdot ml CFE⁻¹ at $t = 240$ h and increased from $t = 264$ h onwards until a final maximum value of 1.91 ± 0.05 mg \cdot ml CFE⁻¹ at $t = 504$ h. Overall, the antioxidative activities in this experiment were highly correlated with the contents of total phenolic compounds and flavonoids as well as scytonemin, whereas correlations with sPS were weak and MAAs in some cases even negative.

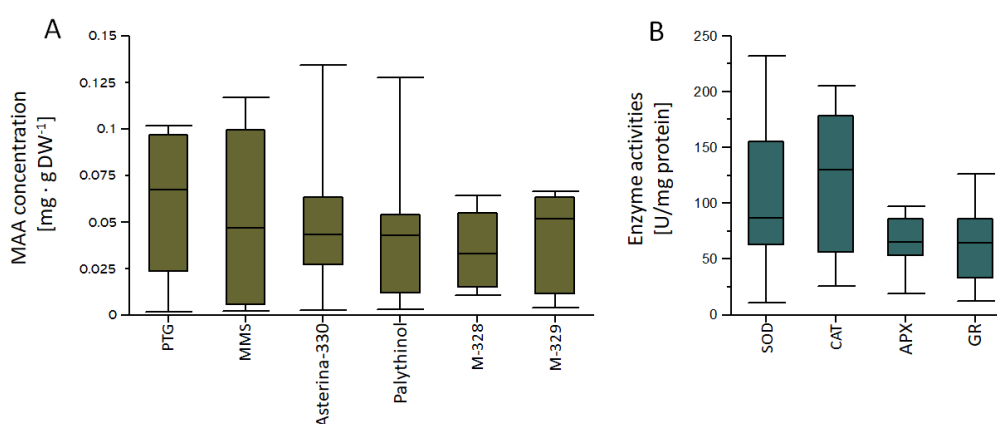


Figure 46. Box Whisker plots of the MAA yields (A) and enzyme activities (B) during the final experiment in an internally illuminated PBR using *Synechococcus* II as model organism. Abbreviations: PTG, Palythine-threonine glycoside; MMS, Mycosporine-methylamine-serine; SOD, Superoxide dismutase; CAT, Catalase; APX, Ascorbate peroxidase; GR, Glutathione reductase.

Regarding the maximum yields of MAAs during the final experiment, the highest value was recorded for Asterina-330 with 0.138 mg \cdot g DW⁻¹, followed by palythanol (0.131 mg \cdot g DW⁻¹), mycosporine-methylamine-serine (0.118 mg \cdot g DW⁻¹) and the glycoside of palythine-threonine with 0.103 mg \cdot g DW⁻¹ (Fig. 46A). Both earlier as unknown designated MAAs (M-328 and M-329) were detected during the experiment with final concentrations ranging from 0.056 and 0.069 mg \cdot g DW⁻¹ for M-328 and M-329, respectively. Furthermore, the enzymatic components of the antioxidative defense system, comprising SOD, CAT, APX and GR were recorded with maximum yields reached by SOD (232.1 U/mg protein), followed by CAT (205.3 U/mg protein), GR (126.5 U/mg protein) and APX (97 U/mg protein) (Fig. 46B).

5. Discussion

5.1. Sun Protective Compounds from Selected Cyanobacteria and their Induction

Overall, three compound groups were in focus of the present study: MAAs, scytonemin and sPS. Several abiotic factors such as different wavelength bands of UV radiation, desiccation, and nutrients and salt concentration have been found to affect the production of MAAs and scytonemin in cyanobacteria (Fleming & Castenholz 2007, 2008, Singh et al. 2008, Rastogi et al. 2010, Mushir & Fatma 2012, Rath et al. 2012). Specifically, the present survey focused on compounds with sun screening characteristics.

Though in some cases only in traces (e.g. MAAs), all three compound groups were detected in the coccoid cyanobacteria *Synechocystis* I and II as well as *Synechococcus* I and II during the first screening in which overall 50 species (40 microalgae and 10 cyanobacteria originating from northern Icelandic coastal areas) were exposed to a combined UV (UVA + UVB)/PAR source (cf. 4.1). The following experiment focused on a first enhancement of the compound concentrations in the four selected cyanobacteria by variation of the duration of exposure to two slightly different UV/PAR sets (cf. 4.2). In principle this first enhancement of photoprotective compounds in response to UV stress was successful, although for example the MAA concentrations obtained were low and only in the range of natural occurring ones found in phytoplankton communities according to literature (e.g. Laurion et al. 2002). Even in the final experiment under optimised conditions MAA concentrations obtained were only up to 61% higher than in the first induction experiment (cf. Table 4, Fig. 46A) and were still very low compared to values reached for instance in the red macroalgae (=seaweed) *Porphyra* sp. (~10 mg · g DW⁻¹ MAAs, Prof. Karsten personal communication).

In total, 10 MAAs were detected by HPLC analysis in samples obtained from the first induction survey (cf. Table 4) in which 22 samples were analysed out of 48 assays, showing distinctive strain specific differences. Three of the MAAs were not further identifiable and were therefore dedicated as M-328, M-329 and M-341. The attempt to isolate and characterise these MAAs at a later stage was not successful. The remaining seven identified MAAs such as asterina-330, shinorine and palythanol are common in cyanobacteria and are most discussed in literature as natural antioxidants (e.g. Wada et al. 2015). Furthermore, some cyanobacterial MAAs also contain sulfate esters or glycosidic linkages through the imine substituents (e.g. Sinha & Häder 2008) such as palythine-serine sulfate found in *Synechococcus* I and palythine-threonine glycoside detected in the present study in *Synechococcus* II.

Since UV broad band induction long-term experiments, including upscale trials, as conducted in the present survey have never been done before, it is difficult to compare the results with other studies. Only few reports regarding the active induction of sun protective compounds from cyanobacteria are available in the scientific literature, differing mainly from the present investigation in terms of analysis methods and experimental set ups. In this context the use of cut-off filters to induce specific MAAs (Garcia-Pichel & Castenholz 1993, Sinha et al. 2001, 2003, Rastogi & Incharoensakdi 2014) and scytonemin (Rastogi & Incharoensakdi 2014) is to mention, whereas in the study of Mushir & Fatma (2011) the type of UV source used in the experiments was not described. In these studies concentrations ranged between 1.02 A mg DW⁻¹ overall MAA content in *Gloeocapsa* C-90-Cal-G (Garcia-Pichel & Castenholz 1993), ~0.6-0.7 μmol (g · DW)⁻¹ for shinorine in *Nodularia* (Sinha et al.

2003), ~ 46 peak area/g \cdot DW⁻¹ $\times 10^4$ for palythine (Rastogi & Incharoensakdi 2014), ~ 8.8 peak area/g \cdot DW⁻¹ $\times 10^4$ for asterina (Rastogi & Incharoensakdi 2014) as well as 0.0046-0.0247 μg mg⁻¹ for scytonemin in *Anabaena ambigua* NCCU-16 and *Scytonema* NCCU-12, respectively (Mushir & Fatma 2011), and ~ 3.5 μg \cdot mg \cdot DW⁻¹ in *Lyngbya* sp. (Rastogi & Incharoensakdi 2014). All itemised concentrations given by Sinha et al. (2003) and Rastogi & Incharoensakdi (2014) were obtained after 72 h targeted UV exposure. In most cases MAAs and scytonemin were detected in filamentous cyanobacteria, whereas for the coccoid species *Synechocystis* and *Synechococcus* used in the present survey no data for direct comparison are available. Only Zhang et al. (2007) described the presence of three MAAs, namely mycosporine-aurine, M-343, dehydroxylusujirene, in *Synechocystis* sp. PCC 6803. This finding turned out to be highly controversial since Singh et al. (2010) stated after a targeted genome analysis that this peculiar strain was not able to synthesize MAAs even at trace levels. In addition, Singh et al. (2010) also found no ability to synthesize MAAs in *Synechococcus* PCC 6301. In contrast, D'Agostino et al. (2016) suggested according to their results that for example shinorine biosynthesis proceeded via an *Anabaena*-type mechanism and that the genes responsible for the production of other MAA analogues, including palythine-serine and glycosylated analogues, may be located elsewhere in the genome and were therefore not considered in the targeted genome analysis by Singh et al. (2010). Strain specific differences in terms of MAA presence and concentrations in cyanobacteria are common and were described by several authors (e.g. Garcia-Pichel & Castenholz 1993, Singh et al. 2008, Źyszka-Haberecht & Lipok 2019). For instance, Garcia-Pichel & Castenholz (1993) found for *Synechococcus* strain 0-89-H-Syn an absorbance maximum at 310 nm and a MAA content of 0.19 mg DW⁻¹, whereas in *Synechococcus* strain ATCC 27179 no MAAs were detected. Considering these findings, only whole genome analysis will shed light on the ability of strains to produce certain sun screening compounds and clarify evolutive developments.

Regarding sPS as photoprotective compound group in cyanobacteria, only in a few cases the compound was actively induced according to the literature (Matsunaga et al. 1996, Abd El Baky et al. 2013). In none of the studies UV exposure was tested. The concentrations given in the literature ranged from 43.69 mg \cdot g⁻¹ for sPS from *Spirulina platensis*, grown on medium containing 45 ppm N and extracted with hot water (Abd El Baky et al. 2013), to 116.0 mg (mg \cdot dry cells)⁻¹ day⁻¹ for sPS from *Aphanocapsa halophytia* MN-11, immobilized on light-diffusing optical fibres with a light intensity of 1380 cd sr m⁻² (Matsunaga et al. 1996). The results of the monosaccharide analysis presented by Abd El Baky et al. (2013) for *Spirulina platensis* showed that glucouronic acid was the predominant constituent in all extracts, followed by galactose and glucose, while rhamnose and arabinose were present as minor constituents. In contrast, the monosaccharide composition of the sPS from *Aphanocapsa halophytia* were not available (Matsunaga et al. 1996). Although the overall concentrations obtained for sPS in *Synechocystis* I and II as well as *Synechococcus* I and II were low compared to the values given above, the monosaccharide compositions found in the present survey are in accordance to those given by Panoff et al. (1988) and De Philippis et al. (1998).

5.2 The Induction of Components of the Antioxidative Defense System and Scavenging Activities

Induced accumulation of polyphenolics and flavonoids in the cyanobacterial strains *Synechocystis* I and II as well as *Synechococcus* I and II grown under different UV radiation sets and exposure lengths were investigated for correlations and enhanced antioxidant activity in the present study.

Cyanobacteria are known to possess stress-protective enzymatic and non-enzymatic antioxidative mechanisms to reduce the damages caused due to the reactive oxygen species (ROS) under physiological stresses (e.g. Kesheri et al. 2011). Adaptation and tolerance to abiotic stresses, especially to salt stress in cyanobacteria has widely been worked out in terms of the induction of distinct sets of genes whose products enable successful acclimation (Kanesaki et al. 2002), changes in physiological conditions like photosynthesis, protein, carbohydrate, lipids and fatty acid biosynthesis (Tang et al. 2007, Allakhverdiev & Murata 2008), biochemically active extrusion of toxic inorganic ions and accumulation of compatible solutes including sucrose, trehalose, glucosylglycerol and glycine betaine (Hagemann 2011). In contrast, studies focusing of the adaptation and tolerance of marine cyanobacteria to UV exposure are rather scarce. Values found in literature for total phenolic contents (TPC) and flavonoids (TFC), as peculiar polyphenolic metabolites, varying between $\sim 2700 \mu\text{g} \cdot \text{g FW}^{-1}$ TPC and $\sim 600 \mu\text{g} \cdot \text{g FW}^{-1}$ TFC in *Plectonema boryanum* exposed to 400 mM NaCl (Singh et al. 2014), $54.93 \pm 2.65 \text{ mg GAE g}^{-1} \text{ FW}$ (TPC) and $275.47 \pm 2.8 \mu\text{g QE g}^{-1} \text{ FW}$ (TFC) in *Synechocystis* sp. (Singh et al. 2017), $1.78 \pm 0.07 \text{ GAEs mg/g}$ (TPC) and $483.33 \pm 13.92 \text{ QEs mg/g}$ (TFC) in *Spirulina* sp. (Hossain et al. 2016). In none of the cases found during the literature recherche regarding TPC and TFC values UV exposure was tested.

Antioxidant activity of biological samples and/or natural compounds can be evaluated by various methods (e.g. Singh et al. 2017). Two free radicals commonly used to evaluate antiradical and antioxidant power of biological extracts or natural compounds in vitro are 2, 2-diphenyl-1-picrylhydrazyl (DPPH) and 2, 2-azinobis (3-ethylbenzothiazoline- 6-sulfonic acid) (ABTS). Free radical scavenging activity of the cyanobacterial extracts in the present survey was evaluated against one important radical, DPPH. DPPH method is widely used to determine antiradical and/or antioxidant power of biological extracts and/or purified compounds. It is relatively stable free radical that, upon reduction by an antioxidant loses its absorption (515 nm). Concentration-dependent assays for the determination of free radical scavenging activity using DPPH resulted in two categories of cyanobacterial samples, first with high activity while the second with low activity. Extracts of *Synechococcus* II exhibited high free radical scavenging activity in terms of DPPH activity in which more than 80% DPPH activity was recorded at the concentration of 5 mg ml^{-1} . Among assays exhibiting low DPPH activity were samples obtained in which less than 70% activity was achieved at 5 mg ml^{-1} and even at higher concentrations, the activity remained similar. Maximum DPPH activities were recorded in samples obtained during the final experiment in the final half ($t= 264\text{-}504 \text{ h}$, Fig. 44D). It has been shown that most phenolic antioxidants react slowly with DPPH, reaching a steady state in longer time (Bondet et al. 1997). The method also has limitations with the interference of the presence of anthocyanins that could lead to underestimation of the antioxidant activity of biological extract (Shalaby & Shanab 2013). Therefore, the requirement of high concentrations of polyphenolics-rich cyanobacterial extracts for obtaining the IC_{50} value of antioxidant activity using DPPH may be explained on the basis of slow reaction of phenolics with DPPH (Singh et al. 2017), leading thus the patterns observed during the final experiment.

Targeted metabolic profiling of cyanobacterial polyphenolic-rich extracts using HPLC has resulted in the characterization of five phenolic acids namely gallic, chlorogenic, caffeic, ferulic and vanillic acids and three flavonoids namely rutin, quercetin and kaempferol in various quantities (Singh et al. 2017). Specifically, in *Synechocystis* sp. the presence of gallic and chlorogenic acid as well as rutin, quercetin have been described (Singh et al. 2017), whereas for *Synechococcus* not data were found.

Phenolic acids and flavonoids from plant sources have been well-documented for their antioxidant, free-radical quenching and redox metal ion-chelating effects (Tutour 1990, Apati et al. 2003, Singh et al. 2009, 2014, Hossain et al. 2016) but cyanobacteria and microalgae are relatively new source for such compounds in recent years due to their potential benefits and ease of production (Guedes et al. 2013, Machu et al. 2015). Gallic, chlorogenic, caffeic and ferulic acids identified from plant sources have been known as strong antioxidants and free radical scavengers (Piazzon et al. 2012, Babić et al. 2015) but their presence in cyanobacteria is scarcely reported and this makes these organisms more potential. Being most primitive, these organisms are considered to evolve with various levels of environmental adaptations to overcome these stresses for their survival over the time (Tandeau-de-Marsac & Houmard 1993). This study implicates that the antioxidant properties of the cyanobacterial extracts can be thought of a reflection of intrinsic strategies of these organisms to reduce the damage caused due to ROS generated during environmental UV stresses. The presence of polyphenolics (phenolic acids and flavonoids) in cyanobacteria may also be considered as a part of the key functions responsible for the protection of these organisms from environmental stresses during the course of their evolution (Aydas et al. 2013, Singh et al. 2014).

All enzymatic components of the antioxidative defense system, represented by superoxide dismutase (SOD), catalase (CAT), ascorbate peroxidase (APX) and glutathione reductase (GR), were present in the four tested cyanobacteria, although with varying activities (cf. Table 6, Fig. 46). First antioxidant arsenal against nascent oxygen species is SOD which plays an important role in nullifying the toxic effect of superoxide ion by dismutating it to H_2O_2 . First time the protective role of cyanobacterial SOD in photooxidative damage was reported by Herbert et al. (1992) in *Anacystis nidulans* (*Synechococcus*). Subsequently, several workers have reported protective role of cyanobacterial SOD in response to various stresses (Rajendran et al. 2007, Saha et al. 2003). Three groups of CATs, (monofunctional heme-containing CATs, bifunctional heme-containing CAT-peroxidases, and nonheme-manganese CATs) have been reported from 20 cyanobacterial genomes (Latifi et al. 2009). It does not consume cellular reducing equivalents which makes this enzyme unique among H_2O_2 scavenging enzymes (Mallick & Mohn 2000). Enhanced CAT activity was reported in *Anabaena doliolum* in response to UV-B and Cu stresses (Malanga et al. 1999, Mallick & Rai 1999). Furthermore, APX catalyzes the reduction of H_2O_2 to H_2O utilizing the reducing power of ascorbate (Noctor & Foyer 1998). Quenching of Chl fluorescence induced by H_2O_2 was supported by the cells of *Synechocystis* 6803 containing-APX whereas it was completely found absent in the cells of *A. nidulans* devoid of APX (Miyake et al. 1990). In *Synechococcus* PCC 9742 (R2) cells, under oxidative stress, APX serves as the major enzyme involved in the removal of H_2O_2 (Mittler & Tel-or 1991). Enzymatic defense mechanisms of antioxidant enzymes such as CAT, SOD, and APX were studied in two *Nostoc* species when exposed to UV-B radiation (Richa & Sinha 2015). All the studied antioxidative enzymes showed a multifold induction upon UV-B exposure and *Nostoc* sp. strain HKAR-2, a hot-spring isolate showed higher antioxidative enzymatic activity as compared to the rice-field *Nostoc* sp. strain HKAR-6. Under UV stress, different cyanobacterial species show varying degree of induction in the level of antioxidative enzymes and this may govern the degree of survival in stressful conditions (Singh et al. 2013, 2017, Ahmed et al. 2017). Antarctic cyanobacterium *Nostoc commune* was found to possess two antioxidative enzymes, viz., CAT and SOD that jointly withstand the environmental stresses prevailing at its natural stressed habitat (Kesheri et al. 2014). In *Nostoc spongiaeforme* and *Phormidium corium* an increased activity of APX and SOD, respectively, was observed under high-intensity PAR treatment (Bhandari & Sharma 2006).

5.4 Processing of the Biomasses *versus* Compound Stability

The production of higher biomass amounts is usually linked to the utilization of different suitable harvest methods. The most applied methods comprise, besides others, centrifugation, flocculation, and gravitational sedimentation. While centrifugation was used in the present study for small biomass amounts as standard method during all experiments, the gravitational sedimentation was found to be far too lengthy for the tested cyanobacteria (over 5 days). Overall, three flocculation methods were tested in the present study. Chemical flocculation using iron (III) chloride (FeCl_3) and chitosan, and forced alkaline flocculation using sodium hydroxide (NaOH) (cf. 4.3.1.). Basically, flocculation is a complex process influenced by cell surface properties, cell concentration, pH of the environment, ionic strength, and type and dosage of flocculant (e.g. Sanyano et al. 2013). Flocculation as a unit operation is exploited in different industries such as brewing, waste and drinking water treatment and mining. While in these applications, liquid is often the end product, for harvesting microalgae and cyanobacteria it is the biomass and the compounds originating from these organisms which are the end products. In microalgal harvesting by flocculation, biomass contamination with a chemical flocculant is an important issue. In addition, chemical flocculants can cause harm to the final product (biomass for food or feed) or biomass processing (lipid extraction) (Vandamme et al. 2013).

Chemical flocculants may contain traces of toxic compounds, e.g., synthetic polyacrylamide polymers contain acrylamide, therefore flocculants based on natural biopolymers are a safer alternative (Vandamme et al. 2013). For instance, in order to interact with usually negatively charged microalgal cells, these biopolymers possess a positive surface charge. Such a positively charged biopolymer is chitosan (poly-(D)glucosamine), which is a very efficient flocculant but is relatively expensive (Chang & Lee 2012). Among flocculation methods, high pH induced (alkaline) flocculation of algae, mediated by inorganic salt precipitates, has the advantage of using cheap hydroxides (e.g., slaked lime) instead of chemical flocculants (Vandamme et al. 2012). Flocculation induced by both a natural increase in pH due to CO_2 depletion (Sukenik & Shelef 1984, Nguyen et al. 2014) and addition of magnesium/calcium/sodium hydroxide (Folkman & Wachs 1973) has long been reported and various mechanisms have been suggested. In the present study, samples obtained by flocculation with sodium hydroxide pH 10 showed the highest yields of sun protective compounds in comparison to the control and the other flocculants (cf. Fig. 38).

In principle, the flocculation in the present survey was successful, except for the marine cyanobacteria flocculated with chitosan (cf. Fig. 37). The effectiveness of chemical flocculation techniques often significantly decreases when they are applied to marine microalgae, due to the high ionic strength of seawater (Sukenik et al. 1988, Teixeira et al. 2012). This is due to the near elimination of electrostatic forces of charged particles/ions at high ionic strengths. In marine systems, the dose of flocculants required to flocculate marine microalgae has been found to be 5–10 times higher than that required for freshwater microalgae and the dose was found to increase linearly with salinity of the aqueous environment (Milledge & Heaven 2013). In the case of *Synechocystis*, Divakaran & Pillai (2002) reported that the high density of seawater obstructed rapid settling. Therefore, they diluted the raw suspension and brought the pH down to about 5 before adding chitosan to induce flocculation. The authors also found that, depending on the concentration of suspended alga, higher doses of flocculant were required to obtain maximum removal and that a maximum of 15 mg L^{-1} chitosan was sufficient to clarify all the suspensions examined. This method was not tested in the present study since

extremes of pH may cause cell damage or death, thus being unusable on a commercial scale (Milledge & Heaven 2013).

Basically, several cyanobacteria are known to be able to produce several MAAs in the presence of natural UV radiation (e.g. Katoch et al. 2016, D'Agostino et al. 2016). Interestingly, only one MAA was detected in each UV/time assay during the first induction trials (cf. Table 4), although the light equipment remained unchanged. In addition to this, the high number of contradictions between the assays regarding MAA positive and negative tested samples gave a further hint that the harvest, storage, and/or freeze-drying process needed to be adapted. While storage length and temperature were described as critical in the analysis of cyanobacterial MAAs by several authors (e.g. Hartman et al. 2017) and was also observed in the present survey, only one example does exist which points to relationships between the use of lyophilisation and lack of MAA diversity (Volkman & Gorbushina 2006). Most authors seemed to avoid this step and used fresh material for MAA analysis in cyanobacteria (e.g. Hartman et al. 2017). Therefore, the protocol in the present survey was adapted, omitting the freeze-drying step, although freeze drying was chosen in first place as safe procedure for storage and sample shipment to Prof. Karsten's laboratory. In the new protocol the samples for the MAA analysis were directly extracted after harvest using 100% methanol according to the method given by Sinha et al. (1999) and the storage length for dried material shortened to 24 h maximum.

5.5 Conventional Bubble Column PBR *versus* Internally Illuminated PBR

Bubble columns are widely used as multiphase reactors because of their simple construction and operation. They are used in chemical, metallurgical and biochemical processes (Ferreira et al. 2013), providing a competitive alternative in two- and three-phase processes with mass and heat transfer limitations, where efficient interphase contacting is needed (Nedeltchev et al. 2014). A bubble column is also a popular configuration for closed photobioreactors (PBRs) that has received considerable attention over the last decade (Pegallapati & Nirmalakhandan 2012, Bitog et al. 2014, Manjrekar et al. 2017, López-Rosales et al. 2017). The bubble column provides a number of advantages over other photobioreactor configurations such as simplicity in design and construction with no moving parts, ease of operation, small floor space requirements, excellent heat transfer characteristics and temperature control, and suitable interphase mass transfer at low energy input. Nonetheless, due to a lack of knowledge on the complex bubble-liquid hydrodynamics and its influence on transport process, cell growth, and scale up, bubble column photobioreactors are still not well understood. Hydrodynamics in bubble columns are determined by gas sparging at the bottom section. Gas injection is essential for microalgae culture processes, driving the flow and mixing, and indeed mass transfer and light penetration and distribution. However, bubble formation at the sparger, its upward movement, and rupture at the culture surface can produce significant shear forces in small regions that can potentially induce cell damage (López-Rosales et al. 2019).

In the present survey, two conventional bubble column PBRs with a diameter of 400 mm were used (cf. 3.2.4.1). The relatively high diameter of these PBRs was chosen to obtain stability as a stand-alone solution in the restricted space of the BioPol laboratory. During the experiments, this high diameter led to an increase of shading effects due to high biomass densities of the cyanobacteria and the increase of sparging to better mix the biomass would lead to an increase of cell damage. Therefore, a PBR with internal illumination was chosen because it provides more homogeneous intensity to the angular direction of the reactor. In the literature, the theoretical reactor analysis of IIPBR showed an

improvement over conventional bubble columns by doubling the biomass production per energy input, which was validated by experimental results on two algal strains (e.g. [Pegallapati et al. 2012](#)). In context to UV illumination this type of PBR was not tested yet and the main challenge was to overcome the heat of the high energy radiation. In the final experiment using this internal illuminated PBR, an air pump and a ventilator provided the inner space of the reactor with the UV/PAR lamp with cooling air, leading to the results presented in 4.4.2.

6. Conclusions and Future Perspectives

Cyanobacteria and microalgae are rich sources of various compounds including pigments, lectins, fibres, halogenated compounds, antioxidants, vitamins, polyketides, polysaccharides, MAAs, proteins, and essential lipids. Therefore, they are widely used due to their multifunctional applications in nutraceuticals as well as in pharmaceuticals. This study has emphasized that cyanobacteria are promising sources of structurally diverse biologically active compounds such as scytonemin, sulfated polysaccharides, MAAs, enzymes and polyphenolics which have the potential to replace artificial sunscreen compounds. Furthermore, this study has shown that an inducement of these compounds is possible, although still further optimizations and in deep analysis for example of the composition of phenolic compounds will be necessary. Specifically, there is a need to find answers to questions like whether the production rate of metabolites is sufficient to meet demands or if a “whole algae” approach can be realized to avoid losses of valuable metabolites? Whether these metabolites identified in the present study could have some additional beneficiary roles and if so, would be a biorefinery concept suitable? Whether changes made by bioengineering could be employed to enhance the production of these metabolites? Future work will no doubt reveal novel functions for secondary metabolites and the future research in this area will be very promising.

7. Acknowledgements

We are grateful to Linda Kristjánsdóttir and MSc. Daniel Liesner for their support in media production for the cultivation from 2017 to 2018 and 2016, respectively.

8. References

- Abd El Baky, H.; Hanaa El Baz, K.f.; EL-Latife, S. Induction of sulfated polysaccharides in *Spirulina platensis* as response to nitrogen concentration and its biological evaluation. *J. Aqua. Res. Develop.* **2014**, *5*, 1–8.
- Agar, N.S.; Halliday, G.M.; Barnetson, R.S.; Ananthaswamy, H.N.; Wheeler, M.; Jones, A.M. The basal layer in human squamous tumors harbors more UVA than UVB fingerprint. mutations: A role for UVA in human skin carcinogenesis. *Proc. Natl. Acad. Sci. USA* **2004**, *101*, 4954–4959.
- Agati, G.; Tattini, M. Multiple functional roles of flavonoids in photoprotection. *New Phytol.* **2010**, *186*, 786–793.
- Ahmed, H.; Singh, V.; Pandey, A.; Kannaujiya, V.K.; Rajneesh, P.; Sinha, R.P. Combined effects of UV radiation, PAR and 2,4-Dichlorophen oxyacetic acid on pigmentation, proteins and

- antioxidant enzymes in the cyanobacterium *Scytonema geitleri* HKAR-12. *JSM Environ. Sci. Ecol.* **2017**, 5 (3), 1048.
- Allakhverdiev, S.I.; Murata, N. Salt Stress Inhibits Photosystems II and I in Cyanobacteria. *Photosyn. Res.* **2008**, 98, 529–39.
- Andersen, R.A.; Jacobson, D.M.; Sexton, J.P. *Provasoli-Guillard Center for Culture of Marine Phytoplankton. Catalogue of Strains*. 98pp. West Boothbay Harbor, Maine, USA, **1991**.
- Apati, P.; Szentmihályi, K.; KristoSz, T.; Papp, I.; Vinkler, P.; Szoke, E.; Kery, A. Herbal remedies of Solidago, correlation of phytochemical characteristics and antioxidative properties. *J. Pharm. Biomed. Anal.* **2003**, 32, 1045–1053.
- Arad, S.; Levy-Ontman, O. Red microalgal cell-wall polysaccharides: biotechnological aspects. *Curr. Opin. Biotechnol.* **2010**, 21, 358–364.
- Arslan, M.; Temocin, Z.; Ylgitoglu, M. Removal of cadmium (II) from aqueous solutions using sporopollenin. *Fresenia Env. Bull.* **2004**, 13, 616–619.
- Atkinson, A.W.; Gunning, B.E.S.; John, P.C.L. Sporopollenin in the cell wall of *Chlorella* and other algae: ultrastructure, chemistry, and incorporation of ¹⁴C-acetate, studied in synchronous cultures. *Planta* **1972**, 107, 1–32.doi:10.1007/BF00398011.
- Aydas, S.B.; Ozturk, S.; Aslim, B. Phenylalanine ammonia lyase (PAL) enzyme activity and antioxidant properties of some cyanobacteria isolates. *Food Chem.* **2013**, 136, 164–169.
- Babić, O.; Kovač, D.; Rašeta, M.; *et al.* Evaluation of antioxidant activity and phenolic profile of filamentous terrestrial cyanobacterial strains isolated from forest ecosystem. *J. Appl. Phycol.* **2015**, 28, 2333–2342.
- Balskus, E.P.; Walsh, C.T. An enzymatic cyclopentyl[b]indole formation involved in scytonemin biosynthesis. *J. Am. Chem. Soc.* **2009**, 131, 14648–14649.
- Balskus, E.P.; Walsh, C.T. The genetic and molecular basis for sunscreen biosynthesis in cyanobacteria. *Science* **2010**, 329, 1653–1656.
- Balskus, E.P.; Case, R.J.; Walsh, C.T. The biosynthesis of cyanobacterial sunscreen scytonemin in intertidal microbial mat communities. *FEMS Microbiol. Ecol.* **2011**, 77, 322–332.
- Bhandari, R.; Sharma, P.K. High-light-induced changes on photosynthesis, pigments, sugars, lipids and antioxidant enzymes in freshwater (*Nostoc spongiaeforme*) and marine (*Phormidium corium*) cyanobacteria. *Photochem. Photobiol.* **2006**, 82, 702–710.
- Bitog, J.P.P.; Lee, I.B.; Oh, H.M.; Hong, S.W.; Seo, I.H.; Kwon, K.S. Optimised hydrodynamic parameters for the design of photobioreactors using computational fluid dynamics and experimental validation. *Biosyst. Eng.* **2014**, 122, 42–61.
- Bondet, V.; Brand-Williams, W.; Berset, C. Kinetics and mechanisms of antioxidant activity using the DPPH free radical method. *Lebensm. Wiss. Technol.* **1997**, 30, 609–615.
- Brady, P.V.; Pohl, P.I.; Hewson, J.C. A coordination chemistry model of algal autoflocculation. *Algal Res.* **2014**, 5, 226–230. <http://dx.doi.org/10.1016/j.algal.2014.02.004>.
- Bayerl, C.; Taake, S.; Moll, I.; Jung, E.G. Characterization of sunburn cells after exposure to ultraviolet light. *PhotoDermatol. Photoimmunol. Photomed.* **1995**, 11, 149–154.
- Beattie, P.E.; Dawe, R.S.; Ferguson, J.; Ibbotson, S.H. Dose-response and time-course characteristics of UV-A1 erythema. *Arch. Dermatol.* **2005**, 141, 1549–1555.

- Babitha, S.; Kim, E. K. *Effect of Marine Cosmeceuticals on the Pigmentation of Skin. Marine Cosmeceuticals: Trends and Prospects*. Boca Raton, FL: CRC Press, USA, **2011**.
- Booth, C.R.; Morrow, J.H. The penetration of UV into natural waters. *Photochem. Photobiol.* **1997**, *65*, 254–75
- Bradford, M.M. A rapid and sensitive method for the quantitation of microgram quantities of protein utilizing the principle of protein-dye binding. *Anal. Biochem.* **1976**, *72*, 248–254.
- Brand-Williams, W.; Cuvelier, M. E.; Berset, C. Use of a free radical method to evaluate antioxidant activity. *Lebensm. Wiss. Technol.* **1995**, *28*, 25-30.
- Bultel-Poncé, V.; Felix-Theodose, F.; Sarthou, C.; Ponge, J.F.; Bodo, B. New pigment from the terrestrial cyanobacterium *Scytonema* sp. collected on the Mitraka Inselberg, French Guyana. *J. Nat. Prod.* **2004**, *67*, 678-681.
- Carreto, J.I.; Carignan, M.O. Mycosporine-like amino acids: relevant secondary metabolites. Chemical and ecological aspects. *Mar. Drugs* **2011**, *9*, 387–446.
- Chang, Y.R.; Lee, D.J. Coagulation-Membrane Filtration of *Chlorella vulgaris* at Different Growth Phases. *Dry. Technol.* **2012**, *30*, 1317–1322.
- Chen, K.; Feng, H.; Zhang, M.; Wang, X. Nitric oxide alleviates oxidative damage in the green alga *Chlorella pyrenoidosa* caused by UV-B radiation. *Folia Microbiol.* **2003**, *48*, 389–393.
- Christen, V.; Zucchi, S.; Fent, K. Effects of the UV-filter 2-ethyl-hexyl-4-trimethoxycinnamate (EHMC) on expression of genes involved in hormonal pathways in fathead minnows (*Pimephales promelas*) and link to vitellogenin induction and histology. *Aquatic Toxicol.* **2011**, *102*, 167–176.
- Cleaver, J.E.; Crowley, E. UV damage, DNA repair and skin carcinogenesis. *Front. BioSci.* **2002**, *7*, d1024–d1043.
- Coelho, S.G.; Choi, W.; Brenner, M.; Miyamura, Y.; Yamaguchi, Y.; Wolber, R.; Smuda, C.; Batzer, J.; Kolbe, L.; Ito, S.; *et al.* Short- and long-term effects of UV radiation on the pigmentation of human skin. *J. Investig. Dermatol. Symp. Proc.* **2009**, *14*, 32–35.
- Concepcion, M.R.; Avalos, J.; Bonet, M.L.; Boronat, A.; Gomez-Gomez, L.; Hornero-Mendez, D.; Limon, M.C.; Meléndez-Martínez, A.J.; Olmedilla-Alonso, B.; Palou, A. A global perspective on carotenoids: Metabolism, biotechnology, and benefits for nutrition and health. *Prog. Lipid Res.* **2018**, *70*, 62–93.
- Cui, R.; Widlund, H.R.; Feige, E.; Lin, J.Y.; Wilensky, D.L.; Igras, V.E.; D’Orazio, J.; Fung, C.Y.; Schanbacher, C.F.; Granter, S.R.; *et al.* Central role of p53 in the Suntan response and pathologic hyperpigmentation. *Cell* **2007**, *128*, 853–864.
- D’Agostino, P.M.; Javalkote, V.S.; Mazmouz, R.; Pickford, R.; Puranik, P.R.; Neilan, B.A. Comparative Profiling and Discovery of Novel Glycosylated Mycosporine-Like Amino Acids in Two Strains of the Cyanobacterium *Scytonema* cf. *crispum*. *Appl. Environ. Microbiol.* **2016**, *82*(19), 5951–5959.
- Daniel, S.; Cornelia, S.; Fred, Z. UV-A sunscreen from red algae for protection against premature skin aging. *Cosmet. Toilet. Manuf. Worldw.* **2004**, *129*, 139–143.
- Davies K.J. Oxidative stress, antioxidant defenses, and damage removal, repair, and replacement systems. *IUBMB Life.* **2000**, *50*, 279–289.
- De Gruijl, F.R. UV-induced immunosuppression in the balance. *Photochem. PhotoBiol.* **2008**, *84*, 2–9.

- De Philippis, R.; Margheri, M.C.; Materassi, R.; Vincenzini, M. Potential of unicellular cyanobacteria from saline environments as exopolysaccharide producers. *Appl. Environ. Microbiol.* **1998**, *64*, 1130–1132.
- Dhindsa, R.H.; Plumb-Dhindsa, R.; Thorpe, T.A. Leaf senescence correlated with increased level of membrane permeability, lipid peroxidation and decreased level of SOD and CAT. *J. Exp. Bot.* **1981**, *32*, 93-101.
- Dickinson, H. G.; Bell, P. R. The identification of sporopollenin in sections of resin embedded tissues by controlled acetolysis. *Stain Technol.* **1973**, *48*, 17-22.
- Di Pietro, N.; Di Tomo, P.; Pandolfi, A. Carotenoids in cardiovascular disease prevention. *JSM Atheroscler.* **2016**, *1*, 1–13.
- Dodgson, K.S.; Price, R.G. A note on the determination of the ester sulphate content of sulphated polysaccharides. *Biochem. J.* 1962, *84*, 106–110.
- Donglikar, M.; Laxman Deore, S. Sunscreens: A review. *Pharmacogn. J.* **2016**, *8*, 171–179.
- D’Orazio, J.A.; Nobuhisa, T.; Cui, R.; Arya, M.; Spry, M.; Wakamatsu, K.; Igras, V.; Kunisada, T.; Granter, S.R.; Nishimura, E.K.; *et al.* Topical drug rescue strategy and skin protection based on the role of Mc1r in UV-induced tanning. *Nature* **2006**, *443*, 340–344.
- D’Orazio, J.; Jarrett, S.; Amaro-Ortiz, A.; Scott, T. UV radiation and the skin. *Int. J. Mol. Sci.* **2013**, *14*, 12222–12248.
- Dring, M.J.; Wagner, A.; Boeskov, J.; Lüning, K. Sensitivity of intertidal and subtidal red algae to UV-A and UV-B radiation, as monitored by chlorophyll fluorescence measurements: Influence of collection depth, and season, and length of irradiance. *Eur. J. Phycol.* **1996**, *31*, 293–302.
- Downs, C.A.; Kramarsky-Winter, E.; Fauth, J.E. *et al.* Toxicological effects of the sunscreen UV filter, benzophenone-2, on planula and in vitro cells of the coral, *Stylophora pistillata*. *Ecotoxicology* **2014**, *23*, 175–191.
- Downs, C.A.; Kramarsky-Winter, E.; Segal, R.; Fauth, J.; Knutson, S.; Bronstein, O.; Ciner, F.R.; Jeger, R.; Lichtenfeld, Y.; Woodley, C.M.; *et al.* Toxicopathological Effects of the Sunscreen UV Filter, Oxybenzone (Benzophenone-3), on Coral Planulae and Cultured Primary Cells and Its Environmental Contamination in Hawaii and the U.S. Virgin Islands. *Arch. Environ. Contam. Toxicol.* **2016**, *70*, 265–288.
- Dubinsky, O.; Simon, B.; Karamanos, Y.; Geresh, S.; Barak, Z.; Arad (Malis), S. Composition of the cell-wall polysaccharide produced by the unicellular red alga *Rhodella reticulata*. *Plant Physiol Biochem*, **1992**, *30*, 409–414.
- Eastman, J.T. Antarctic notothenioid fishes as subjects for research in evolutionary biology. *Antarct. Sci.* **2000**, *12*, 276–287.
- Eastman, J.T. The nature of the diversity of Antarctic fishes. *Pol. Biol.* **2005**, *28*, 94–107.
- Edwards, E.A.; Rawsthorne, S.; Mullineaux, P.M. Subcellular distribution of multiple forms of glutathione reductase in leaves of pea (*Pisum sativum* L.). *Planta* **1990**, *180*, 278–284.
- Faurschou, A.; Beyer, D.M.; Schmedes, A.; Bogh, M.K.; Philipsen, P.A.; Wulf, H.C. The relation between sunscreen layer thickness and vitamin D production after ultraviolet B exposure: A randomized clinical trial. *Brit. J. Dermatol.* **2012**, *167*, 391–395.
- Favre-Bonvin, J.; Arpin, N.; Brevard, C. Structure de la mycosporine (P 310). *Can. J. Chem.* **1976**, *54*, 1105–1113.

- Ferreira, A.; Cardoso, P.; Teixeira, J.A.; Rocha, F. PH influence on oxygen mass transfer coefficient in a bubble column. Individual characterization of kL and a. *Chem. Eng. Sci.* **2013**, *100*, 145–152.
- Fleming, E.D.; Castenholz, R.W. Effects of periodic desiccation on the synthesis of the UV-screening compound, scytonemin, in cyanobacteria. *Environ. Microbiol.* **2007**, *9*, 1448–1455.
- Fleming, E.D.; Castenholz, R.W. Effects of nitrogen source on the synthesis of the UV-screening compound, scytonemin, in the cyanobacterium *Nostoc punctiforme* PCC 73102. *FEMS Microbiol. Ecol.* **2008**, *63*, 301–308.
- Folkman, Y.; Wachs, A.M. Removal of algae from stabilization pond effluents by lime treatment. *Water Res.* **1973**, *7*, 419.
- Food and Drug Administration (FDA). FDA Rules Regulations for Sunscreen. **2012**. Available online: <https://smartshield.com/news/reviews/54-resources/127-new-fda-rules-regulations-for-sunscreen> (accessed on 1 March 2020).
- Foyer, C.H.; Halliwell B. The presence of glutathione and glutathione reductase in chloroplasts: a proposed role in ascorbic acid metabolism. *Planta* **1997**, *133*, 21–25.
- Garcia-Pichel, F.; Castenholz, R.W. Characterization and biological implications of scytonemin, a cyanobacterial sheath pigment. *J. Phycol.* **1991**, *27*, 395–409.
- Garcia-Pichel, F.; Castenholz, R.W. Occurrence of UV-Absorbing, Mycosporine-Like Compounds among Cyanobacterial Isolates and an Estimate of Their Screening Capacity. *Appl. Environ. Microbiol.* **1993**, *59*(1), 163–9.
- Gaspar, L.R.; Maia Campos, P.M.B.G. Evaluation of the photostability of different UV filter combinations in a sunscreen. *Int. J. Pharm.* **2006**, *307*, 123–128.
- Geresh, S.; (Malis) Arad, S.; Levy-Ontman, O.; Zhang, W.; Tekoah, Y.; Glaser, R. Isolation and characterization of poly- and oligosaccharides from the red microalga *Porphyridium* sp. *Carbohydr. Res.* **2009**, *344*, 343–349.
- Giacomoni, P.U. *Sun Protection in Man*; Elsevier: Amsterdam, The Netherlands, **2001**; Volume 3, pp. 495–519.
- Gill, S.S.; Tuteja, N. Reactive oxygen species and antioxidant machinery in abiotic stress tolerance in crop plants. *Plant Physiol. Biochem.* **2010**, *48*, 909–930.
- Goiris, K.; Muylaert, K.; Fraeye, I.; Foubert, I.; de Brabanter, J.; de Cooman, L. Antioxidant potential of microalgae in relation to their phenolic and carotenoid content. *J. Appl. Phycol.* **2012**, *24*, 1477–1486.
- Gómez, I.; Orostegui, M.; Huovinen, P. Morpho-functional patterns of photosynthesis in the South Pacific kelp *Lessonia nigrescens*: Effects of UV radiation on ¹⁴C fixation and primary photochemical reactions. *J. Phycol.* **2007**, *43*, 55–64.
- Gonzalez, A.D.; Pechko, A.H.; Kalafsky, R.E. Photostable Sunscreen Compositions and Methods of Stabilizing. US6440402B1, 27 August **2002**.
- Gorham, E.D.; Mohr, S.B.; Garland, C.F.; Chaplin, G.; Garland, F.C. Do sunscreens increase risk of melanoma in populations residing at higher latitudes? *Annals Epidemiol.* **2007**, *17*, 956–963.
- Guedes, A.C.; Giao, M.S.; Seabra, R.; Ferreira, A.C.; Tamagnini, P.; Moradas-Ferreira, P.; Malcata, F.X. Evaluation of the antioxidant activity of cell extracts from microalgae. *Mar. Drugs.* **2013**, *11*, 1256–1270.

- Guillard, R.R. Culture of phytoplankton for feeding marine invertebrates. In: Smith WL, Chanley MH (ed) Culture of marine invertebrate animals, Plenum Press, New York, USA, **1975**, pp. 26–60.
- Guillard, R.R.L.; Hargraves, P.E. *Stichochrysis immobilis* is a diatom, not a chrysophyte. *Phycologia* **1993**, *32*, 234–236.
- Guilford, W.J.; Schneider, D.M.; Labovitz, J.; Opella, S.J. High resolution solid state ¹³C NMR spectroscopy of sporopollenins from different plant taxa. *Plant Physiol.* **1988**, *86*, 134–136.
- Gunnison, D.; Alexander, M. Basis for the resistance of several algae to microbial decomposition. *Appl. Microbiol.* **1975**, *29*, 729–738.
- Hagemann, M. Molecular Biology of Cyanobacterial Salt Acclimation. *FEMS Microbio. Rev.* **2011**, *35*, 87–123.
- Halpern, A.C.; Kopp, L.J. Awareness, knowledge and attitudes to nonmelanoma skin cancer and actinic keratosis among the general public. *Int. J. Dermatol.* **2005**, *44*, 107–111.
- Hartmann, A.; Murauer, A.; Ganzera, M. Quantitative analysis of mycosporine-like amino acids in marine algae by capillary electrophoresis with diode-array detection. *J. Pharm. Biomed. Anal.* **2017**, *138*, 153–157.
- He, X.; Dai, J.; Wu, Q. Identification of sporopollenin as the outer layer of cell wall in microalga *Chlorella protothecoides*. *Front. Microbiol.* **2016**, *7*, 1047.
- Heo, S.-J.; Jeon, Y.-J. Protective effect of fucoxanthin isolated from *Sargassum siliquastrum* on UV-B induced cell damage. *J. Photochem. Photobiol. B* **2009**, *95*, 101–107.
- Herbert, D.; Phipps, P.J.; Strange, R.E. Chemical analysis of microbial cells. In: *Methods in microbiology* (Ed. by J.R. Norris & D.W. Ribbons), pp. 210–244. Vol. 5B. Academic Press, New York, USA, **1971**.
- Herbert, S.K.; Samson, G.; Fork, D.C.; Laudenbach, D.E. Characterization of damage to photosystems I and II in a cyanobacterium lacking detectable iron superoxide dismutase activity. *Proc. Natl. Acad. Sci. U. S. A.* **1992**, *89*, 8716–8720.
- Hodis, E.; Watson, I.R.; Kryukov, G.V.; Arold, S.T.; Imielinski, M.; Theurillat, J.P.; Nickerson, E.; Auclair, D.; Li, L.; Place, C.; *et al.* A landscape of driver mutations in melanoma. *Cell* **2012**, *150*, 251–263.
- Hoeijmakers, J.H. DNA damage, aging, and cancer. *N. Eng. J. Med.* **2009**, *361*, 1475–1485.
- Holick, M. Does sunscreen block the skin's ability to make vitamin D? If so, how can I get enough of this vitamin without raising my risk of skin cancer? *Health News* **2002**, *8*, 12.
- Holick, M.F. Vitamin D: A millenium perspective. *J. Cell. Biochem.* **2003**, *88*, 296–307.
- Hupel, M.; Lecointre, C.; Meudec, A.; Poupart, N.; Gall, E.A. Comparison of photoprotective responses to UV radiation in the brown seaweed *Pelvetia canaliculata* and the marine angiosperm *Salicornia ramosissima*. *J. Exp. Mar. Biol. Ecol.* **2011**, *401*, 36–47.
- Hossain, M.F.; Ratnayake, R.R.; Meerajini, K.; Kumara, K.L.W. Antioxidant properties in some selected cyanobacteria isolated from freshwater bodies of Sri Lanka. *Food Sci. Nutr.* **2016**, doi:10.1002/fsn3.340
- Ignat, I.; Volf, I.; Popa, V.I. A critical review of methods for characterisation of polyphenolic compounds in fruits and vegetables. *Food Chem.* **2011**, *126*, 1821–1835.

- Jahan S.; Yusoff, I.B.; Alias, Y.B.; Bakar, A.F. Reviews of the toxicity behavior of five potential engineered nanomaterials (ENMs) into the aquatic ecosystem. *Toxicol. Rep.* **2017**, *4*, 211–220.
- Jerez-Martel, I.; García-Poza, S.; Rodríguez-Martel, G.; Rico, M.; Afonso-Olivares, C.; Gómez-Pinchetti, J.L. Phenolic profile and antioxidant activity of crude extracts from microalgae and cyanobacteria strains. *J. Food Qual.* **2017**, <https://doi.org/10.1155/2017/2924508>.
- Kadarkar, A.L.; Chen, J.; Yang, J.; Chen, S.; Jameson, J.; Swope, V.B.; Cheng, T.; Kadakia, M.; Abdel-Malek, Z. Alpha-melanocyte-stimulating hormone suppresses oxidative stress through a p53-mediated signaling pathway in human melanocytes. *Mol. Cancer Res.* **2012**, *10*, 778–786.
- Kanesaki, Y.; Suzuki, I.; Allakhverdiev, S.I.; Mikami, K.; Murata, N. Salt Stress and Hyperosmotic Stress Regulate the Expression of Different Sets of Genes in *Synechocystis* sp. PCC 6803. *Biochem. Biophys. Res. Com.* **2002**, *290*, 339–348.
- Karentz, D. Chemical defenses of marine organisms against solar radiation exposure: UV-absorbing mycosporine-like amino acids and scytonemin. In *Marine Chemical Ecology*; McClintock, J.B., Baker, J., Eds.; CRC Press, Inc.: Boca Raton, FL, USA, **2001**; pp. 481–520, ISBN 978-0-8493-9064-7.
- Karentz, D.; McEue, F.S.; Land, M.C.; Dunlap, W.C. Survey of mycosporine like amino acid compounds in Antarctic marine organisms: Potential protection from ultraviolet exposure. *Mar. Biol.* **1991**, *108*, 157–166.
- Karsten, U.; Escoubeyrou, K.; Charles, F. The effect of re-dissolution solvents and HPLC columns on the analysis of mycosporine-like amino acids in the eulittoral macroalgae *Prasiola crispa* and *Porphyra umbilicalis*. *Helgol. Mar. Res.* **2009**, *63*, 231–238.
- Karsten, U.; Sawall, T.; Hanelt, D.; Bischof, K.; Figueroa, F.L.; Flores-Moya, A.; Wiencke, C. An inventory of UV-absorbing mycosporine-like amino acids in macroalgae from polar to warm-temperate regions. *Bot. Mar.* **1998**, *41*, 443–453.
- Katoch, M.; Mazmouz, R.; Chau, R.; Pearson, L.A.; Pickford, R.; Neilan, B.A. Heterologous production of cyanobacterial mycosporine-like amino acids mycosporine-Ornithine and mycosporine-Lysine in *Escherichia coli*. *Appl. Environ. Microbiol.* **2016**, *82*(20): 6167–6173.
- Katsumata T., Ishibashi T., Kyle D. A sub-chronic toxicity evaluation of a natural astaxanthin-rich carotenoid extract of *Paracoccus carotinifaciens* in rats. *Toxicol. Rep.* **2014**; *1*:582–588.
- Kerr, A.; Ferguson, J. Photoallergic contact dermatitis. *Photodermatol. Photoimmunol. Photomed.* **2010**, *26*, 56–65.
- Kesheri, M.; Richa, A.; Sinha, R.P. Antioxidants as Natural Arsenal against Multiple Stresses in Cyanobacteria. *Int. J. Phar. Bio Sci.* **2011**, *2*, B169–B187.
- Kim, K.C.; Piao, M.J.; Cho, S.J.; Lee, N.H.; Hyun, J.W. Phloroglucinol protects human keratinocytes from ultraviolet B radiation by attenuating oxidative stress. *Photodermatol. Photoimmunol. Photomed.* **2012**, *28*, 322–331.
- Kim, Y.-I.; Oh, W.-S.; Song, P.; Yun, S.; Kwon, Y.-S.; Lee, Y.; Ku, S.-K.; Song, C.-H.; Oh, T.-H. Anti-Photoaging Effects of Low Molecular-Weight Fucoïdan on Ultraviolet B-Irradiated Mice. *Mar. Drugs* **2018**, *16*, 286.
- Koes, R.; Verweij, W.; Quattrocchio, F. Flavonoids: a colorful model for the regulation and evolution of biochemical pathways. *Trends Plant Sci.* **2005**, *10*, 236–242.

- Komaristaya, V.P.; Gorbunin, O.S. Sporopollenin in the composition of cell walls of *Dunalliella salina* Teod. (Chlorophyta) zygotes. *Int J Algae* **2006**, *8*, 43–52.
- Kole, P.L.; Jadhav, H.R.; Thakurdesai, P.; Nagappa, A.N. Cosmetic potential of herbal extracts. *Nat. Prod. Radiance* **2005**, *4*, 315–321.
- Kováčik, J.; Klejdus, B.; Backor, M. Physiological responses of *Scenedesmus quadricauda* (Chlorophyceae) to UV-A and UV-C light. *Photochem. Photobiol.* **2010**, *86*, 612–616.
- Krol, E.S.; Kramer-Stickland, K.A.; Liebler, D.C. Photoprotective actions of topically applied vitamin E. *Drug Metab. Rev.* **2000**, *32*, 413–420.
- Kunisada, M.; Sakumi, K.; Tominaga, Y.; Budiyanto, A.; Ueda, M.; Ichihashi, M.; Nakabeppu, Y.; Nishigori, C. 8-Oxoguanine formation induced by chronic UVB exposure makes *Ogg1* knockout mice susceptible to skin carcinogenesis. *Cancer Res.* **2005**, *65*, 6006–6010.
- Latha, M.S.; Martis, J.; Shobha, V.; Shinde, R.S.; Banera, S.; Krishnankutty, B.; Bellary, S.; Varughese, S.; Rao, P.; Kumar, B.R.N. Sunscreening agents. *J. Clin. Aesthet. Dermatol.* **2013**, *6*, 16–26.
- Latifi, A.; Ruiz, M.; Zhang, C.-C. Oxidative stress in cyanobacteria. *FEMS Microbiol. Rev.* **2009**, *33*, 258–278.
- Lee, S.-H. New Technical Developments in Sun Care and Blue Light Defense; SUNJIN Beauty Science: Gyeonggi-do, Korea, **2018**, p. 134.
- Lesser, M.P. Oxidative stress in marine environments: Biochemistry and physiological ecology. *Annu. Rev. Physiol.* **2006**, *68*, 253–278.
- Lichtenthaler, H.K. Chlorophylls and carotenoids: Pigments of photosynthetic biomembranes. *Methods Enzymol.* **1987**, *148*, 350–382.
- Liu, Y.; Liu, M.; Zhang, X.; Chen, Q.; Chen, H.; Sun, L.; Liu, G. Protective effect of fucoxanthin isolated from *Laminaria japonica* against visible light-induced retinal damage both in vitro and in vivo. *J. Agric. Food Chem.* **2016**, *64*, 416–424.
- Llewellyn, C.A.; Airs, R.L. Distribution and abundance of MAAs in 33 species of microalgae across 13 classes. *Mar. Drugs* **2010**, *8*, 1273–1291.
- López-Rosales, L.; García-Camacho, F.; Sánchez-Mirón, A.; Contreras-Gómez, A.; Molina-Grima, E. Modeling shear-sensitive dinoflagellate microalgae growth in bubble column photobioreactors. *Bioresour. Technol.* **2017**, *245*, 250–257.
- López-Rosales, L.; Sánchez-Mirón, A.; et al. Characterization of bubble column photobioreactors for shear-sensitive microalgae culture. *Bioresour. Tech.* **2019**, *275*, 1–9.
- Lorenzen, C.J. Determination of chlorophyll and pheopigments: spectrophotometric equations. *Limnol. Oceanogr.* **1967**, *12*, 343–346.
- Lowe, N.J. An overview of ultraviolet radiation, sunscreens, and photo-induced dermatoses. *Dermatol. Clin.* **2006**, *24*, 9–17.
- Lupescu, N.; Arad (Malis), S.; Geresh, S.; Bernstein, M.; Glazer, R. Structure of some sulfated sugars isolated after acidhydrolysis of the extracellular polysaccharide of *Porphyridium* sp. a unicellular red alga. *Carbohydr Res.* **1991**, *210*, 349–352.
- Lushchak, V.I. Adaptive response to oxidative stress: bacteria, fungi, plants and animals. *Comp. Biochem. Physiol. C.* **2011**, *153*, 175–190.

- Machu, L.; Misurcova, L.; Ambrozova, J.V.; Orsavova, J.; Mlcek, J.; Sochor, J.; Jurikova, T. Phenolic acids and antioxidants in algal food products. *Molecules* **2015**, *20*, 1118–1133.
- Maier, T.; Korting, H.C. Sunscreens—which and what for? *Skin Pharmacol. Physiol.* **2005**, *18*, 253–262.
- Malanga, G.; Kozak, R.G.; Puntarulo, S. N-Acetylcysteine-dependent protection against UV-B damage in two photosynthetic organisms. *Plant Sci.* **1999**, *141*(2), 129–137.
- Malik, C.P. In: Singh MB (ed) Plant enzymology and histoenzymology. Kalyani Publishers, New Delhi, **1980**, pp 69–80
- Mallick, N.; Mohn, F.H. Reactive oxygen species: response of algal cells. *J. Plant Physiol.* **2000**, *157*, 183–193.
- Mallick, N.; Rai, L.C. Response of the antioxidant systems of the nitrogen fixing cyanobacterium *Anabaena doliolum* to copper. *J. Plant Physiol.* **1999**, *155*, 146–149.
- Malla, S.; Sommer, M.O.A. A sustainable route to produce the scytonemin precursor using *Escherichia coli*. *Green Chem.* **2014**, *16*, 3255–3265.
- Manjrekar, O.N.; Sun, Y.; He, L.; Tang, Y.J.; Dudukovic, M.P. Hydrodynamics and mass transfer coefficients in a bubble column photo-bioreactor. *Chem. Eng. Sci.* **2017**, *168*, 55–66.
- Marchant, H.J.; Davidson, A.T.; Kelly, G.J. UV-B protecting compounds in the marine alga *Phaeocystis pouchetii* from Antarctica. *Mar. Biol.* **1991**, *109*, 391–395.
- Markham, K.R. “Preface,” in *Flavonoids: Chemistry, Biochemistry and Applications*, eds O.M. Andersen and K.R. Markham, Boca Raton, FL: CRC Press, USA, **2006**.
- Mate, M.J.; Zamocky, M.; Nykyri, L.M.; Herzog, C.; Alzari, P.M.; Betzel, C.; Koller, F.; Fita, I. Structure of catalase-A from *Saccharomyces cerevisiae*. *J. Mol. Biol.* **1999**, *286*, 135–149.
- Matsui, M.S.; Muizzuddin, N.; Arad, S.; Marenus, K. Sulfated polysaccharides from red microalgae have anti-inflammatory properties in vitro and in vivo. *Appl. Biochem. Biotechnol.* **2003**, *104*, 13–22.
- Matsui, M.; Tanaka, K.; Higashiguchi, N.; Okawa, H.; Yamada, Y.; Tanaka, K.; Taira, S.; Aoyama, T.; Takanishi, M.; Natsume, C. Protective and therapeutic effects of fucoxanthin against sunburn caused by UV irradiation. *J. Pharmacol. Sci.* **2016**, *132*, 55–64.
- Matsunaga, T.; Sudo, H.; Takemasa, H.; Wachi, Y. Sulfated extracellular polysaccharide production by the halophilic cyanobacterium *Aphanocapsa halophytica* immobilized on light-diffusing optical fibres. *Appl. Microbiol. Biotechnol.* **1996**, *45*, 24–27.
- Meyskens, F.L., Jr.; Farmer, P.; Fruehauf, J.P. Redox regulation in human melanocytes and melanoma. *Pigment. Cell Res.* **2001**, *14*, 148–154.
- Milledge, J.; Heaven, S. A review of the harvesting of micro-algae for biofuel production. *Rev. Environ. Sci. Bio-Technol.* **2013**, *12*, 165–178.
- Mistry, N. Guidelines for formulating anti-pollution products. *Cosmetics* **2017**, *4*, 57.
- Misurcova, L.; Orsavova, J.; Ambrozova, J.V. “Algal polysaccharides and health,” in *Polysaccharides Bioactivity and Biotechnology*, eds K. G. Ramawat and J. M. Merillon (Cham: Springer International Publishing Switzerland), **2015**, 110–144.
- Mitra, D.; Fisher, D.E. Transcriptional regulation in melanoma. *Hematol. Oncol. Clin. N. Am.* **2009**, *23*, 447–465.

- Mittler, R.; Tel-or, E. Oxidative stress responses and shock protein in unicellular cyanobacterium *Synechococcus* PCC 7942 (R2). *Arch. Microbiol.* **1991**, *155*, 125–130.
- Miyake, C.; Michihata, F.; Asada, K. Scavenging of hydrogen peroxide in prokaryotic and eukaryotic algae: acquisition of ascorbate peroxidase during the evolution of cyanobacteria. *Plant Cell Physiol.* **1990**, *32*, 33–43.
- Moffitt, M.C.; Louie, G.V.; Bowman, M.E.; Pence, J.; Noel, J.P.; Moore, B.S. Discovery of two cyanobacterial phenylalanine ammonia lyases: kinetic and structural characterization. *Biochemistry* **2007**, *46*, 1004–1012. doi: 10.1021/bi061774g
- Mok, I.-K.; Lee, J.K.; Kim, J.H.; Pan, C.-H.; Kim, S.M. Fucoxanthin bioavailability from fucoxanthin-fortified milk: In vivo and in vitro study. *Food Chem.* **2018**, *258*, 79–86.
- Moon, H.J.; Park, K.S.; Ku, M.J.; Lee, M.S.; Jeong, S.H.; Imbs, T.I.; Zvyagintseva, T.N.; Ermakova, S.P.; Lee, Y.H. Effect of *Costaria costata* fucoïdan on expression of matrix metalloproteinase-1 promoter, mRNA, and protein. *J. Nat. Prod.* **2009**, *72*, 1731–1734.
- Morano, K.A.; Grant, C.M.; Moye-Rowley, W.S. The response to heat shock and oxidative stress in *Saccharomyces cerevisiae*. *Genetics* **2012**, *190*, 1157–1195.
- Moron, M.S.; Depierre, J.W.; Mannervik, B. Levels of glutathione, glutathione reductase and glutathione S-transferase activities in rat lung and liver. *Biochim. Biophys. Acta* **1979**, *528*, 67–78.
- Moyal, D. UVA protection labelling and in vitro testing methods. *Photochem. Photobiol. Sci.* **2010**, *9*, 516–523.
- Mushir, S.; Fatma, T. Monitoring stress responses in cyanobacterial scytonemin - screening and characterization. *Environ. Technol.* **2012**, *33*, 153–157.
- Mutanda, T. Introduction. In: Bux F, editor. Biotechnological applications of microalgae: biodiesel and value-added products. Boca Raton, Fla., CRC Press, **2013**, p 1–4.
- Nagai, T.; Reiji I, Hachiro I, Nobutaka S (2003) Preparation and antioxidant properties of water extract of propolis. *Food Chem* 80:29–33
- Nakano, Y.; Asada, K. Hydrogen peroxide is scavenged by ascorbate-specific peroxidase in spinach chloroplasts. *Plant Cell Physiol.* 1981, *22*, 867–880.
- Nantel, F.; Denis, D.; Gordon, R.; Northey, A.; Cirino, M.; Metters, K.M.; Chan, C.C. Distribution and regulation of cyclooxygenase 2 in carrageenan induced inflammation. *Br. J. Pharmacol.* **1999**, *128*, 853–859.
- Narayanan, D.L.; Saladi, R.N.; Fox, J.L. Ultraviolet radiation and skin cancer. *Int. J. Dermatol.* **2010**, *49*, 978–986.
- National Oceanic and Atmospheric Administration NOAA, USA, **2020** <https://oceanservice.noaa.gov/news/sunscreen-corals.html>
- Nedelchev, S.; Nigam, K.D.; Schumpe, A. Prediction of mass transfer coefficients in a slurry bubble column based on the geometrical characteristics of bubbles. *Chem. Eng. Sci.* **2014**, *106*, 119–125.
- Ngoc, L.T.N.; Tran, V.V.; Moon, J.-Y.; Chae, M.; Park, D.; Lee, Y.-C. Recent Trends of Sunscreen Cosmetic: An Update Review. *Cosmetics* **2019**, *6*, 64.

- Nguyen, T.D.P.; Frappart, M.; Jaouen, P.; Pruvost, J.; Bourseau, P. Harvesting *Chlorella vulgaris* by natural increase in pH: Effect of medium composition. *Environ. Technol.* **2014**, *35*, 1378–1388.
- Noctor, G.; Foyer, C.H. A re-evaluation of the ATP: NADPH budget during C3 photosynthesis. A contribution from nitrate assimilation and its associated respiratory activity. *J. Exp. Bot.* **1998**, *49*, 1895–1908.
- Núñez-Pons, L.; Avila, C.; Romano, G.; Verde, C.; Giordano, D. UV-Protective Compounds in Marine Organisms from the Southern Ocean. *Mar. Drugs* **2018**, *16*, 336.
- Oesterhelt, C.; Vogelbein, S.; Shrestha, R.P.; Stanke, M.; Weber, A.P. The genome of the thermo acidophilic red microalga *Galdieria sulphuraria* encodes a small family of secreted class III peroxidases that might be involved in cell wall modification. *Planta* **2008**, *227*, 353–362.
- Omidreza, F.; Antonio, L.; Rita, P.; Giancarlo, M.; Luciano, S. Evaluation of the antioxidant activity of flavonoids by ferric reducing antioxidant power Q assay and cyclic voltammetry. *Biochim. Biophys. Acta* **2005**, *1721*, 174–184.
- Oren, A.; Gunde-Cimerman, N. Mycosporines and mycosporine-like amino acids: UV protectants or multipurpose secondary metabolites? *FEMS Microbiol. Lett.* **2007**, *269*, 1–10.
- Osthoff, S.K.; Wiermann, R. Phenols as integrated compounds of sporopollenin from *Pinus* pollen. *J. Plant Physiol.* **1987**, *131*, 5–15.
- Osterwalder, U.; Herzog, B. Sun protection factors: Worldwide confusion. *Br. J. Dermatol.* **2009**, *161*, 13–24.
- Ozáez, I.; Martínez-Guitarte, J.L.; Morcillo, G. Effects of in vivo exposure to UV filters (4-MBC, OMC, BP-3, 4-HB, OC, OD-PABA) on endocrine signaling genes in the insect *Chironomus riparius*. *Sci. Total Env.* **2013**, *456*, 120–126.
- Palm, M.D.; O'Donoghue, M.N. Update on photoprotection. *Dermatol. Ther.* **2007**, *20*, 360–376.
- Pangestuti, R.; Siahaan, E.A.; Kim, S.K. Photoprotective substances derived from marine algae. *Mar. Drugs* **2018**, *16*, 399.
- Pangestuti, R.; Kim, S.-K. Biological activities and health benefit effects of natural pigments derived from marine algae. *J. Funct. Foods* **2011**, *3*, 255–266.
- Pangestuti, R.; Kim, S.-K. Marine-derived bioactive materials for neuroprotection. *Food Sci. Biotechnol.* **2013**, *22*, 1–12.
- Pangestuti, R.; Kim, S.-K. Biological activities of carrageenan. *Adv. Food Nutr. Res.* **2014**, *72*, 113–124.
- Panoff, J.; Priem, B.; Morvan, H. *et al.* Sulphated exopolysaccharides produced by two unicellular strains of cyanobacteria, *Synechocystis* PCC 6803 and 6714. *Arch. Microbiol.* **1988**, *150*, 558–563.
- Paris, C.; Lhiaubet-Vallet, V.; Jiménez, O.; Trullas, C.; Miranda, M.A. A blocked diketo form of avobenzene: Photostability, photosensitizing properties and triplet quenching by a triazine-derived UVB-filter. *Photochem. Photobiol.* **2019**, *85*, 178–184.
- Pathak, M.A. Sunscreens: Topical and systemic approaches for protection of human skin against harmful effects of solar radiation. *J. Am. Acad. Dermatol.* **1982**, *7*, 285–311.
- Pegallapati, A.K.; Nirmalakhandan, N. Modeling algal growth in bubble columns under sparging with CO₂-enriched air. *Bioresour. Technol.* **2012**, *124*, 137–145.

- Pegallapati, A.K.; Arudchelvam, Y.; Nirmalakhandan, N. Energy-efficient photobioreactor configuration for algal biomass production. *Bioresource Technol.* **2012**, *126*, 266–273.
- Peinado, N.K.; Abdala Díaz, R.T.; Figueroa, F.L.; Helbling, E.W. Ammonium and UV radiation stimulate the accumulation of mycosporine like amino acids in *Porphyra Columbina* (Rhodophyta) from Patagonia, Argentina. *J. Phycol.* **2004**, *40*, 248–259.
- Piao, M.J.; Zhang, R.; Lee, N.H.; Hyun, J.W. Protective effect of triphlorethol-A against ultraviolet B-mediated damage of human keratinocytes. *J. Photochem. Photobiol. B* **2012**, *106*, 74–80.
- Piao, M.J.; Ahn, M.J.; Kang, K.A.; Kim, K.C.; Zheng, J.; Yao, C.W.; Cha, J.W.; Hyun, C.L.; Kang, H.K.; Lee, N.H. Phloroglucinol inhibits ultraviolet B radiation-induced oxidative stress in the mouse skin. *Int. J. Radiat. Biol.* **2014**, *90*, 928–935.
- Piazzon, A.; Vrhovsek, U.; Masuero, D.; Mattivi, F.; Mandoj, F.; Nardini, M. Antioxidant activity of phenolic acids and their metabolites: synthesis and antioxidant properties of the sulfate derivatives of ferulic and caffeic acids and of the acyl glucuronide of ferulic acid. *J. Agri. Food Chem.* **2012**, *60*, 12312–12323.
- Pickett-Heaps, D.; Staehelin, L.A. The ultrastructure of *Scenedesmus* (Chlorophyceae). II. Cell division and colony formation. *J. Phycol.* **1975**, *11*, 186–202.
- Pikula, K.S.; Zakharenko, A.M.; Aruoja, V.; Golokhvast, K.S.; Tsatsakis, A.M. Oxidative stress and its biomarkers in microalgal ecotoxicology – A minireview. *Curr. Opin. Toxicol.* **2019**, *13*, 8–15.
- Polefka, T.G.; Meyer, T.A.; Agin, P.P.; Bianchini, R.J. Effects of solar radiation on the skin. *J. Cosmet. Dermatol.* **2012**, *11*, 134–143.
- Proteau, P.J.; Gerwick, W.H.; Garcia-Pichel, F.; Castenholz, R. The structure of scytonemin, an ultraviolet sunscreen pigment from the sheaths of cyanobacteria. *Experientia* **1993**, *49*, 825–829.
- Rajendran, U.M.; Kathirvel, E.; Anand, N. Desiccation-induced changes in antioxidant enzymes, fatty acids, and amino acids in the cyanobacterium *Tolypothrix scytonemoides*. *World J. Microbiol. Biotechnol.* **2007**, *23*, 251–257.
- Rajesh, P.; Rastogi, R.P.; Incharoensakdi, A. Characterization of UV-screening compounds, mycosporine-like amino acids, and scytonemin in the cyanobacterium *Lyngbya* sp. CU2555, *FEMS Microbiol. Ecol.* **2014**, *87*, 244–256.
- Rastogi, R.P.; Richa, Singh S.P.; Häder, D.-P.; Sinha, R.P. Mycosporine-like amino acids profile and their activity under PAR and UVR in a hot-spring cyanobacterium *Scytonema* sp. HKAR-3. *Aust. J. Bot.* **2010**, *58*, 286–293.
- Rastogi, R.P.; Sinha, R.P.; Incharoensakdi, A. Partial characterization, UV-induction and photoprotective function of sunscreen pigment, scytonemin from *Rivularia* sp. HKAR-4. *Chemosphere*, 2013, DOI: 10.1016/j.chemosphere.2013.06.057.
- Rath, J.; Mandal, S.; Adhikary, S.P. Salinity induced synthesis of UV-screening compound scytonemin in the cyanobacterium *Lyngbya aestuarii*. *J. Photochem. Photobiol. B* **2012**, *115*, 5–8.
- Reczek, C.R.; Chandel, N.S. ROS-dependent signal transduction. *Curr. Opin. Cell Biol.* **2015**, *33*, 8–13.
- Rice-Evans, C.A.; Miller, N.J.; Bolwell, P.G.; Bramley, P.M.; Pridham, J.B. The relative antioxidant activities of plant-derived polyphenolic flavonoids. *Free Radic. Res.* **1995**, *22*, 375–383.
- Richa; Sinha, R.P. Sensitivity of two *Nostoc* species harbouring diverse habitats to ultraviolet-B radiation. *Microbiology* **2015**, *84* (3), 398–407.

- Roe, J.H.; Keuther, C.A. The determination of ascorbic acid in whole blood urine through 2, 4-dinitro phenylhydrazine derivative of dehydro ascorbic acid. *J. Biol. Chem.* **1953**, *147*, 399–407.
- Rogers, A.D. Evolution and biodiversity of Antarctic organisms: A molecular perspective. *Philos. Trans. R. Soc. B* **2007**, *362*, 2191–2214.
- Rogers, H.W.; Weinstock, M.A.; Harris, A.R.; Hinckley, M.R.; Feldman, S.R.; Fleischer, A.B.; Coldiron, B.M. Incidence estimate of nonmelanoma skin cancer in the United States, 2006. *Arch. Dermatol.* **2010**, *146*, 283–287.
- Romero-Puertas, M.C.; Corpas, F.J.; Sandalio, L.M.; Leterrier, M.; Rodríguez-Serrano, M.; Del Río, L. A.; et al. Glutathione reductase from pea leaves: response to abiotic stress and characterization of the peroxisomal isozyme. *New Phytol.* **2006**, *170*, 43–52. doi: 10.1111/j.1469-8137.2006.01643.x
- Rosenberg, R. Eutrophication-related marine ecosystem studies in western Sweden. In: Marine eutrophication and population dynamics. Ed. by G. Colombo, I. Ferrari, U. Ceccherelli & R. Rossi. Olsen & Olsen, Fredensborg, **1992**, 17-20 (25th European Marine Biology Symposium).
- Rozema, J.; Broekman, R.A.; Blokker, P.; Meijkamp, B.B.; De Bakker, N.; Van De Staaij, J.; Van Beem A.; Arise, F.; Kars, S.M. UV-B absorbance and UV-B absorbing compounds (*para*-coumaric acid) in pollen and sporopollenin: the perspective to track historic UV-B levels. *J. Photochem. Photobiol. B Biol.* **2001**, *62*, 108-117.
- Saha, S.K.; Uma, L.; Subramanian, G. Nitrogen stress induced changes in the marine cyanobacterium *Oscillatoria willei* BDU 130511. *FEMS Microbiol. Ecol.* **2003**, *45*, 263–272.
- Sage, E.; Girard, P.M.; Francesconi, S. Unravelling UVA-induced mutagenesis. *Photochem. PhotoBiol. Sci.* **2012**, *11*, 74–80.
- Sambandan, D.R.; Ratner, D. Sunscreens: An overview and update. *J. Am. Acad. Dermatol.* **2011**, *64*, 748–758.
- Sander, C.S.; Chang, H.; Hamm, F.; Elsner, P.; Thiele, J.J. Role of oxidative stress and the antioxidant network in cutaneous carcinogenesis. *Int. J. Dermatol.* **2004**, *43*, 326–335.
- Sano S., Ueda M., Kitajima S., Takeda T., Shigeoka S., Kurano N., Miyachi S., Miyake C., Yokota A. Characterization of ascorbate peroxidases from unicellular red alga *Galdieria partita*. *Plant Cell Physiol.* **2001**, *42*, 433–440.
- Sanyano, N.; Chetpattananondh, P.; Chongkhong, S. Coagulation-flocculation of marine *Chlorella* sp for biodiesel production. *Bioresour. Technol.* **2013**, *147*, 471–476.
- Sarasin, A. The molecular pathways of ultraviolet-induced carcinogenesis. *Mutat. Res.* **1999**, *428*, 5–10.
- Sasso, S.; Pohnert, G.; Lohr, M.; Mittag, M.; Hertweck, C. Microalgae in the postgenomic era: a blooming reservoir for new natural products. *FEMS Microbiol. Rev.* **2012**, *36*, 761–785.
- Schade, N.; Esser, C.; Krutmann, J. Ultraviolet B radiation-induced immunosuppression: Molecular mechanisms and cellular alterations. *Photochem. PhotoBiol. Sci.* **2005**, *4*, 699–708.
- Schalka, S.; Reis, V.M.S.d. Sun protection factor: Meaning and controversies. *An. Bras. Dermatol.* **2011**, *86*, 507–515.
- Schieke, S.M.; Schroeder, P.; Krutmann, J. Cutaneous effects of infrared radiation: From clinical observations to molecular response mechanisms. *Photodermatol. Photoimmunol. Photomed.* **2003**, *19*, 228–234.

- Scholz, B.; Liebezeit, G. Chemical screening for bioactive substances in culture media of microalgae and cyanobacteria from marine and brackish water habitats: first results. *Pharmaceut Biol*, **2006**, *44* (7), 544-549.
- Schulz, I.; Mahler, H.C.; Boiteux, S.; Epe, B. Oxidative DNA base damage induced by singlet oxygen and photosensitization: Recognition by repair endonucleases and mutagenicity. *Mutat. Res.* **2000**, *461*, 145–156.
- Scott, T.L.; Christian, P.A.; Kesler, M.V.; Donohue, K.M.; Shelton, B.; Wakamatsu, K.; Ito, S.; D’Orazio, J. Pigment-independent cAMP-mediated epidermal thickening protects against cutaneous UV injury by keratinocyte proliferation. *Exp. Dermatol.* **2012**, *21*, 771–777.
- Serpone, N.; Dondi, D.; Albini, A. Inorganic and organic UV filters: Their role and efficacy in sunscreens and sun care products. *Inorganica Chim. Acta* **2007**, *360*, 794–802.
- Shalaby, E.A.; Shanab, S.M.M. Comparison of DPPH and ABTS assays for determining antioxidant potential of water and methanolic extracts of *Spirulina platensis*. *Ind. J. Geo-Mar. Sci.* **2013**, *42*, 556–564
- Shaw, G.; Yeadon, A. Chemical studies on the constitution of some pollen and spore membranes. *Grana Palynol.* **1964**, *5*, 247-252.
- Shen, L.; Ndayambaje, J.D.; Murwanashyaka, T.; Cui, W.; Manirafasha, E.; Chen, C.; Wang, Y.; Lu, Y. Assessment upon heterotrophic microalgae screened from wastewater microbiota for concurrent pollutants removal and biofuel production. *Bioresour. Technol.* **2017**, *245*, 386–393.
- Shick, J.M.; Dunlap, W.C. Mycosporine-like amino acids and related gadusols: Biosynthesis, accumulation, and UV-protective functions in aquatic organisms. *Annu. Rev. Physiol.* **2002**, *64*, 223–262.
- Siezen, R.J. Microbial sunscreens. *Microb. Biotechnol.* **2011**, *4*, 1–7.
- Siller, A.; Blaszkark, S.C.; Lazar, M. Update about the effects of the sunscreen ingredients oxybenzone and octinoxate on humans and the environment. *Plast. Surg. Nurs.* **2018**, *38*, 158–161.
- Singer, S.; Karrer, S.; Berneburg, M. Modern sun protection. *Curr. Opin. Pharmacol.* **2019**, *46*, 24–28.
- Singh, S.P.; Klisch, M.; Sinha, R.P.; Häder, D.-P. Effects of abiotic stressors on synthesis of the mycosporine-like amino acid shinorine in the cyanobacterium *Anabaena variabilis* PCC 7937. *Photochem. Photobiol.* **2008**, *84*, 1500–1505.
- Singh, B.N.; Singh, B.R.; Singh, R.L.; Prakash, D.; Singh, D.P.; Sarma, B.K.; Upadhyay, G.; Singh, H.B. Polyphenolics from various extracts/fraction of red onion (*Allium cepa*) peel with potential antioxidant and antimutagenic activities. *Food Chem. Toxicol.* **2009**, *47*, 1161–1167.
- Singh, S.P.; Klisch, M.; Sinha, R.P.; Häder, D.-P. Genome mining of mycosporine-like amino acid (MAA) synthesizing and non-synthesizing cyanobacteria: a bioinformatics study. *Genomics* **2010**, *95*, 120–128.
- Singh, G.; Babele, P.K.; Sinha, R.P.; Tyagi, M.B.; Kumar, A. Enzymatic and non-enzymatic defense mechanisms against ultraviolet-B radiation in two *Anabaena* species. *Process Biochem.* **2013**, *48*, 796–802.
- Singh, S.P.; Rastogi, R.P.; Häder, D.P.; Sinha, R.P. Temporal dynamics of ROS biogenesis under simulated solar radiation in the cyanobacterium *Anabaena variabilis* PCC 7937. *Protoplasma* **2014**, *251*(5), 1223–1230.

- Singh, D.K.; Richa; Kumar, D.; Chatterjee, A.; Rajneesh; Pathak, J.; Sinha, R.P. Response of the cyanobacterium *Fischerella* sp. strain HKAR-5 against combined stress UV-B radiation, PAR and pyrogallol. *JSM Environ. Sci. Ecol.* **2017**, *5*(3), 1049.
- Sinha, R.P.; Ambasht, N.K.; Sinha, J.P.; Klisch, M.; Häder, D.-P. UV-B induced synthesis of mycosporine-like amino acids in three strains of *Nodularia* (cyanobacteria). *J. Photochem. Photobiol. B Biol.* **2003**, *71*, 51–58.
- Sinha, R.P.; Häder, D.-P. UV-protectants in cyanobacteria. *Plant Sci.* **2008**, *174*, 278–289.
- Sinha, R.P.; Klisch, M.; Häder, D.-P. Induction of a mycosporine-like amino acid (MAA) in the rice-field cyanobacterium *Anabaena* sp. By UV irradiation. *J. Photochem. Photobiol. B: Biol.* **1999**, *52*, 59–64.
- Sinha, R.P.; Klisch, M.; Helbling, E.W.; Häder, D.-P. Induction of mycosporine-like amino acids (MAAs) in cyanobacteria by solar ultraviolet-B radiation. *J. Photochem. Photobiol. B Biol.* **2001**, *60*, 129–135.
- Sinha, R.P.; Klisch, M.; Gröniger, A.; Häder, D.P. Ultraviolet-absorbing/screening substances in cyanobacteria, phytoplankton and macroalgae. *J. Photochem. Photobiol. B Biol.* **1998**, *47*, 83–94.
- Sinha, R.P.; Singh, S.P.; Häder, D.P. Database on mycosporines and mycosporine-like amino acids (MAAs) in fungi, cyanobacteria, macroalgae, phytoplankton and animals. *J. Photochem. Photobiol. B Biol.* **2007**, *89*, 29–35.
- Sklar, L.R.; Almutawa, F.; Lim, H.W.; Hamzavi, I. Effects of ultraviolet radiation, visible light, and infrared radiation on erythema and pigmentation: A review. *Photochem. PhotoBiol. Sci.* **2013**, *12*, 54–64.
- Skobowiat, C.; Sayre, R.M.; Dowdy, J.C.; Slominski, A.T. Ultraviolet radiation regulates cortisol activity in a waveband-dependent manner in human skin *ex vivo*. *Br. J. Dermatol.* **2013**, *168*, 595–601.
- Slominski, A.; Wortsman, J.; Pisarchik, A.; Zbytek, B.; Linton, E.A.; Mazurkiewicz, J.E.; Wei, E.T. Cutaneous expression of corticotropin-releasing hormone (CRH), urocortin, and CRH receptors. *FASEB J.* **2001**, *15*, 1678–1693.
- Slominski, A.; Tobin, D.J.; Paus, R. Does p53 regulate skin pigmentation by controlling proopiomelanocortin gene transcription? *Pigment. Cell Res.* **2007a**, *20*, 307–308.
- Slominski, A.; Wortsman, J.; Tuckey, R.C.; Paus, R. Differential expression of HPA axis homolog in the skin. *Mol. Cell. Endocrinol.* **2007b**, *265–266*, 143–149.
- Slominski, A.; Zmijewski, M.A.; Pawelek, J. L-tyrosine and L-dihydroxyphenylalanine as hormone-like regulators of melanocyte functions. *Pigment. Cell Melanoma Res.* **2012**, *25*, 14–27.
- Smijs, T.G.; Pavel, S. Titanium dioxide and zinc oxide nanoparticles in sunscreens: Focus on their safety and effectiveness. *Nanotechnol. Sci. Appl.* **2011**, *4*, 95–112.
- Sorrels, C.M.; Proteau, P.J.; Gerwick, W.H. Organization, evolution, and expression analysis of the biosynthetic gene cluster for scytonemin, a cyanobacterial UV-absorbing pigment. *Appl. Environ. Microbiol.* **2009**, *75*, 4861–4869.
- Soule, T.; Stout, V.; Swingley, W.D.; Meeks, J.C.; Garcia-Pichel, F. Molecular genetics and genomic analysis of scytonemin biosynthesis in *Nostoc punctiforme* ATCC 29133. *J. Bact.* **2007**, *189*, 4465–4472.

- Stafford, H.A. Flavonoid evolution—an enzymatic approach. *Plant Physiol.* **1991**, *96*, 680–685.doi:10.1104/pp.96.3.680
- Stahl, W.; Sies, H. β -Carotene and other carotenoids in protection from sunlight. *Am. J. Clin. Nutr.* **2012**, *96*, 1179S–1184S.
- Stanier, R.Y.; Kunisawa, R.; Mandel, M.; Cohen-Bazire, G. Purification and properties of unicellular blue-green algae (Order *Chroococcales*). *Bacteriol. Rev.* **1971**, *35*, 171–205.
- Stevenson, C.S.; Capper, E.A.; Roshak, A.K.; Marquez, B.; Grace, K.; Gerwick, W.H.; *et al.* Scytonemin – a marine natural product inhibitor of kinases key in hyperproliferative inflammatory diseases. *Inflamm. Res.* **2002a**, *51*, 112–114.
- Stevenson, C.S.; Capper, E.A.; Roshak, A.K.; Marquez, B.; Eichman, C.; Jackson, J.R.; *et al.* The identification and characterization of the marine natural product scytonemin as a novel antiproliferative pharmacophore. *J. Pharmacol. Exp. Ther.* **2002b**, *303*, 858–866.
- Sukenik, A.; Shelef, G. Algal autoflocculation-Verification and proposed mechanism. *Biotechnol. Bioeng.* **1984**, *26*, 142–147.
- Sukenik, A.; Bilanovic, D.; Shelef, G. Flocculation of microalgae in brackish and sea waters. *Biomass* **1988**, *15*, 187–199.
- Takenaka, Y.; Miki, M.; Yasuda, H.; Mino, M. The effect of α -tocopherol as an antioxidant on the oxidation of membrane protein thiols induced by free radicals generated in different sites. *Arch. Biochem. Biophys.* **1991**, *285*, 344–351.
- Tandeau-de-Marsac, N.; Houmard, J. Adaptation of cyanobacteria to environmental stimuli: new steps towards molecular mechanisms. *FEMS Microbiol. Rev.* **1993**, *104*, 119–190.
- Tang, D.; Shi, S.; Li, D.; Hu, C.; Liu, Y. Physiological and Biochemical Responses of *Scytonema javanicum* (cyanobacterium) to Salt Stress. *J. Arid Envir.* **2007**, *71*, 312–320.
- Tannin-Spitz, T.; Bergman, M.; van-Moppes, D.; Grossman, S.; Arad (Malis), S. Antioxidant activity of the polysaccharide of the red microalga *Porphyridium* sp. *J. Appl. Phycol.* **2005**, *17*, 215–222.
- Teixeira, C.; Kirsten, F.V.; Teixeira, P.C.N. Evaluation of *Moringa oleifera* seed flour as a flocculating agent for potential biodiesel producer microalgae. *J. Appl. Phycol.* **2012**, *24*, 557–563.
- Terho, T.T.; Hartiala, K. Method for determination of the sulfate content of glucosaminoglycans. *Anal. Biochem.* **1971**, *41*, 471–476.
- Thevanayagam, H.; Mohamed, S.M.; Chu, W.-L. Assessment of UVB-photoprotective and antioxidative activities of carrageenan in keratinocytes. *J. Appl. Phycol.* **2014**, *26*, 1813–1821.
- Thurman, H. V. Introductory Oceanography. New Jersey, USA, **1997**, Prentice Hall College.
- Tripp, C.S.; Blomme, E.A.; Chinn, K.S.; Hardy, M.M.; LaCelle, P.; Pentland, A.P. Epidermal COX-2 induction following ultraviolet irradiation: Suggested mechanism for the role of COX-2 inhibition in photoprotection. *J. Investig. Dermatol.* **2003**, *121*, 853–861.
- Tutour, B.L. Antioxidative activities of algal extracts, synergistic effect with vitamin E. *Phytochem.* **1990**, *29*, 3759–3765.
- Tyrrell, R.M. Ultraviolet radiation and free radical damage to skin. *Biochem. Soc. Symp.* **1995**, *61*, 47–53.
- U.F.A.D. Administration, Sunscreen drug products for over-the-counter human use. In Final Monograph; Food and Drug Administration: Rockville, MD, USA, **2000**.

- Vandamme, D.; Beuckels, A.; Markou, G.; Foubert, I.; Muylaert, K. Reversible flocculation of microalgae using magnesium hydroxide. *BioEnergy Res.* **2015**, *8*, 716–725.
- Vandamme, D.; Foubert, I.; Fraeye, I.; Meesschaert, B.; Muylaert, K. Flocculation of *Chlorella vulgaris* induced by high pH: role of magnesium and calcium and practical implications. *Bioresour. Technol.* **2012**, *105*, 114–119.
- Vandamme, D.; Foubert, I.; Muylaert, K. Flocculation as a low-cost method for harvesting microalgae for bulk biomass production. *Trends Biotechnol.* **2013**, *31*, 233–239.
- Veal, E.A.; Day, A.M.; Morgan, B.A. Hydrogen peroxide sensing and signaling. *Mol. Cell.* **2007**, *26*, 1–14.
- Vergou, T.; Patzelt, A.; Richter, H.; Schanzer, S.; Zastrow, L.; Golz, K.; Doucet, O.; Antoniou, C.; Sterry, W.; Lademann, J. Transfer of ultraviolet photon energy into fluorescent light in the visible path represents a new and efficient protection mechanism of sunscreens. *J. Biomed. Opt.* **2011**, *16*, 105001.
- Vo, T.S.; Kim, S.-K.; Ryu, B.; Ngo, D.H.; Yoon, N.-Y.; Bach, L.G.; Hang, N.T.N.; Ngo, D.N. The Suppressive Activity of Fucofuroeckol-A Derived from Brown Algal *Ecklonia stolonifera* Okamura on UVB-Induced Mast Cell Degranulation. *Mar. Drugs* **2018**, *16*, 1.
- Volkman, M.; Gorbushina, A.A. A broadly applicable method for extraction and characterization of mycosporines and mycosporine-like amino acids of terrestrial, marine and freshwater origin. *FEMS Microbiol. Lett.* **2006**, *255*, 286–295.
- Wada, N.; Sakamoto, T.; Matsugo, S. Mycosporine-like amino acids and their derivatives as natural antioxidants. *Antioxidants* **2015**, *4*, 603–646.
- Wheeler, G.L.; Jones, M.A.; Smirnoff, N. The biosynthetic pathway of vitamin C in higher plants. *Nature* **1998**, *393*, 365–369.
- Witcover, J.; Yeh, S.; Sperling, D. Policy options to address global land use change from biofuels. *Energy Policy* **2013**, *56*, 63–74.
- Wang, S.Q.; Stanfield, J.W.; Osterwalder, U. In vitro assessments of UVA protection by popular sunscreens available in the United States. *J. Am. Acad. Dermatol.* **2008**, *59*, 934–942.
- Werner, D. Biologische Versuchobjekte. Kultivierung und Wachstum ausgewählter Versuchsorganismen in definierten Medien. 432pp. Fischer Verlag, Stuttgart, New York, **1982**.
- Winkel-Shirley, B. Flavonoid biosynthesis. A colorful model for genetics, biochemistry, cellbiology, and biotechnology. *Plant Physiol.* **2001a**, *126*, 485–493. doi: 10.1104/pp.126.2.485
- Winkel-Shirley, B. It takes a garden. How work on diverse plant species has contributed to an understanding of flavonoid metabolism. *Plant Physiol.* **2001b**, *127*, 1399–1404. doi:10.1104/pp.010675.
- Wyatt, N.B.; Gloe, L.M.; Brady, P.V.; Hewson, J.C.; Grillet, A.M.; Hankins, M.G.; Pohl, P. I. Critical conditions for ferric chloride-induced flocculation of freshwater algae. *Biotechnol. Bioeng.* **2012**, *109*, 493–501.
- Xiong, F.; Komenda, J.; Kopecky, J.; Nedbal, L. Strategies of ultraviolet-B protection in microscopic algae. *Physiol. Plant* **1997**, *100*, 378–388.
- Zhang, L.; Li, L.; Wu, Q. Protective effects of mycosporine-like amino acids of *Synechocystis* sp. PCC 6803 and their partial characterization. *J. Photochem. Photobiol. B Biol.* **2007**, *86*, 240–245.

Zhishen, J.; Mengcheng, T.; Jianming, W. The determination of flavonoid contents in mulberry and their scavenging effects on superoxide radicals. *Food Chem.* **1999**, *64*, 555-559.

Żyszka-Haberecht, B.; Niemczyk, E.; Lipok, J. Metabolic relation of cyanobacteria to aromatic compounds. *Appl. Microbiol. Biotechnol.* **2019**, *103*(3), 1167-1178.

8. Appendix

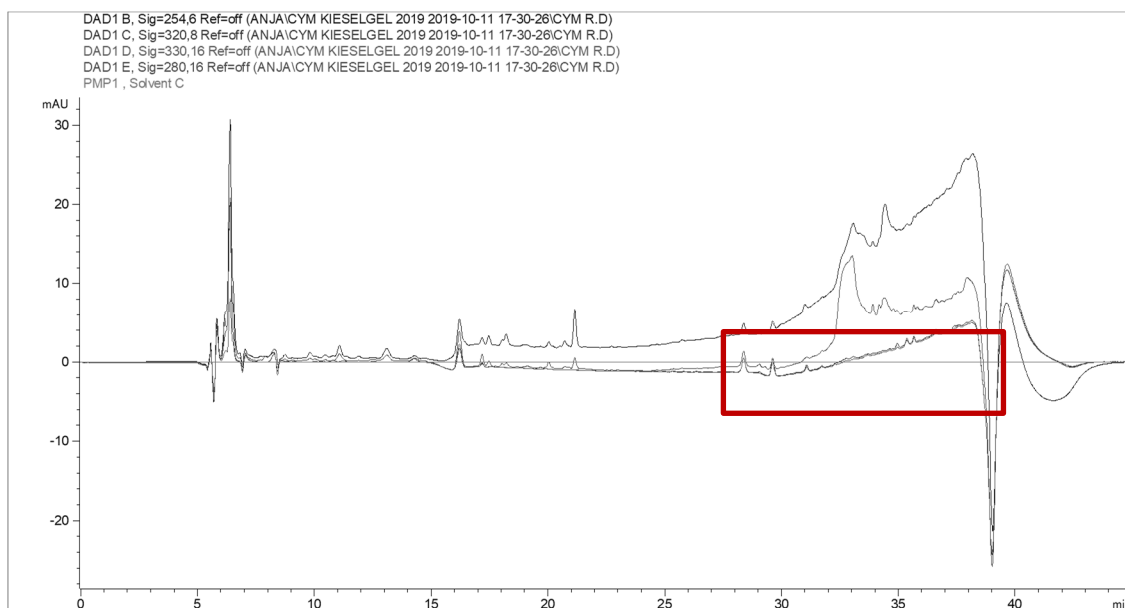


Figure A1. Screenshot of LC chromatogram (all wavelengths) from a sample obtained after the first induction experiments. The sample was extracted with MeOH 5x. In red rectangle MAA signals under 4 mAU.

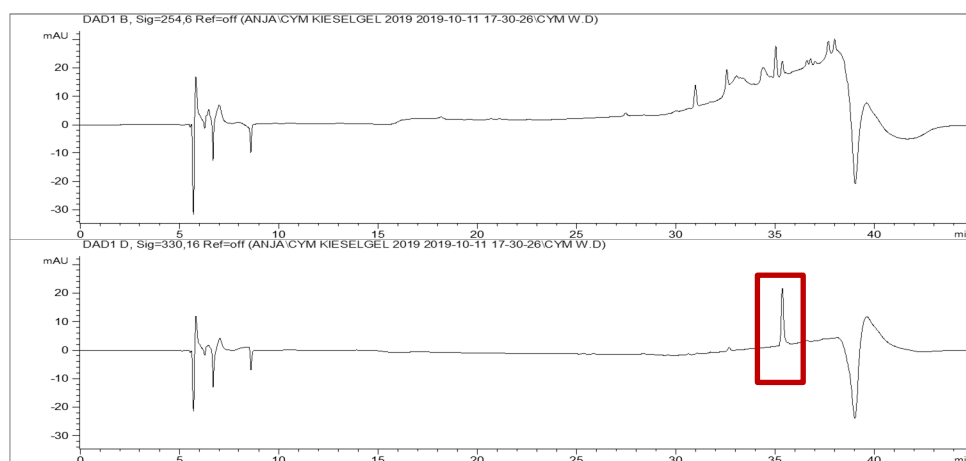


Figure A2. Screenshot of LC chromatogram from a sample from *Synechocystis* II obtained after the first induction experiments. Sample was extracted first with MeOH 5x, evaporated at 40 °C, redissolved again and extracted in 100 % H₂O (4x). In red rectangle a peak at 35.3 min with MAA-typical absorption maximum at 341 nm is depicted.

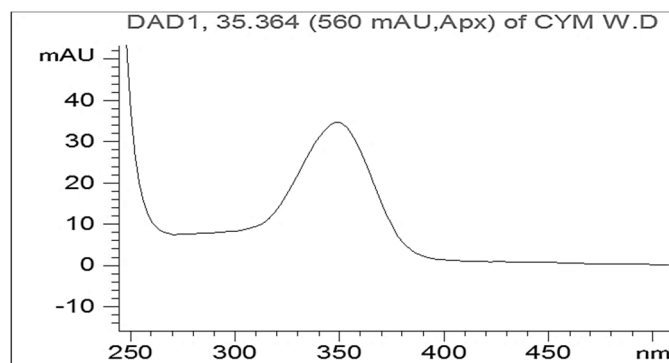


Figure A3. Absorption spectrum of M-341 from *Synechocystis* II after the first induction experiments.

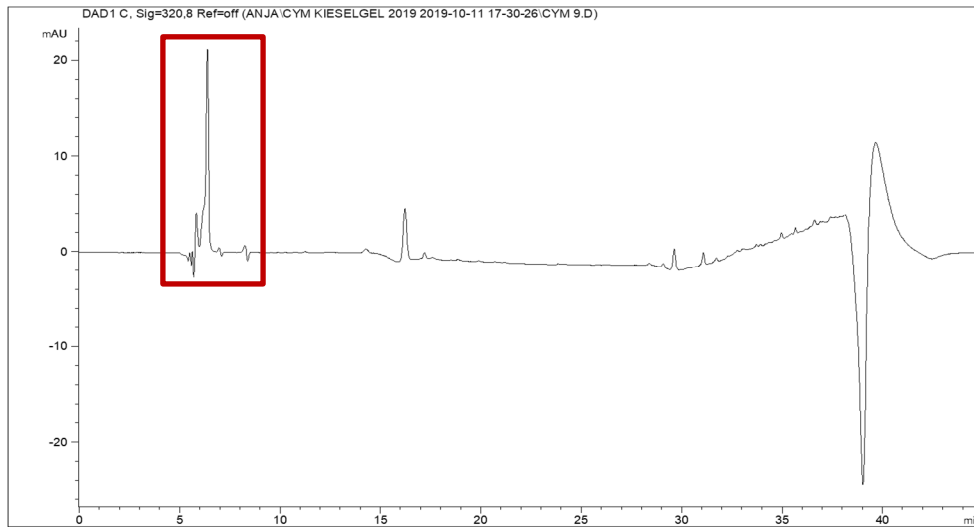


Figure A4. Screenshot of LC chromatogram from a sample from *Synechococcus* II after fractionation of the MeOH-extract over a silica gel column. Red rectangle: peak at 6.2 min MAA-typical absorption spectrum.

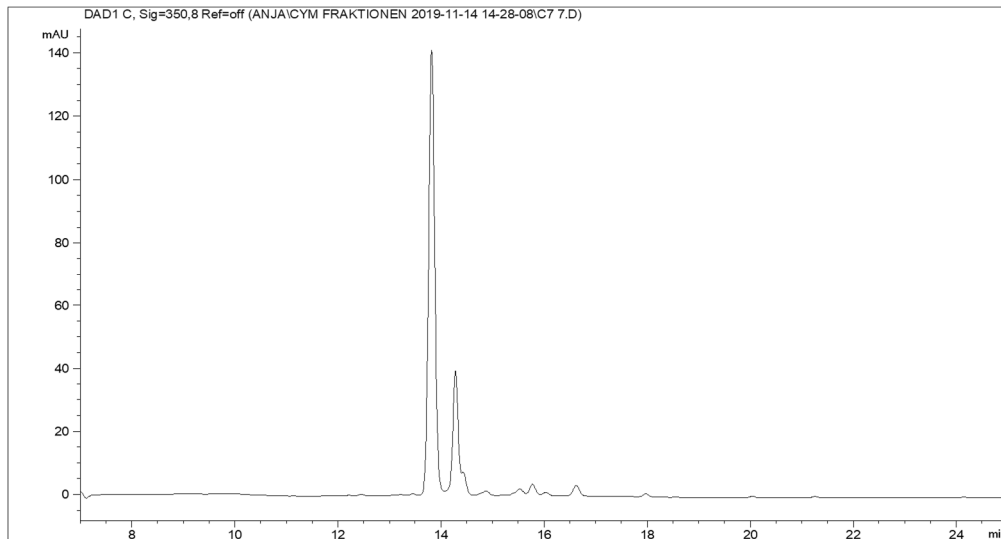


Figure A5. Scytonemin in fraction 7.